

University of Alberta

**The Role of High Molecular Weight Polyethylene Oxide in
Reducing Quartz Gangue Entrainment in Chalcopyrite Flotation
by Xanthate Collectors**

by

Jihua Gong

A thesis submitted to the Faculty of Graduate Studies and Research
in partial fulfillment of the requirements for the degree of

Doctor of Philosophy

in

Materials Engineering

Department of chemical & Materials Engineering

©Jihua Gong

Fall 2011

Edmonton, Alberta

Permission is hereby granted to the University of Alberta Libraries to reproduce single copies of this thesis and to lend or sell such copies for private, scholarly or scientific research purposes only. Where the thesis is converted to, or otherwise made available in digital form, the University of Alberta will advise potential users of the thesis of these terms.

The author reserves all other publication and other rights in association with the copyright in the thesis and, except as herein before provided, neither the thesis nor any substantial portion thereof may be printed or otherwise reproduced in any material form whatsoever without the author's prior written permission.

ABSTRACT

Fine particles pose two challenging problems to all mineral processors around the world today. The problems are the inefficient collection of hydrophobic particles (low recovery), and mechanical/hydraulic entrainment of hydrophilic gangue particles (low concentrate grade). Extensive research has been conducted to improve the flotation recovery of fine hydrophobic particles. However, much less effort was made to lower the mechanical/hydraulic entrainment of fine gangue mineral particles.

In this study, polyethylene oxide (PEO) was used to flocculate and depress fine quartz particles. Batch flotation results indicated that the addition of low dosages of PEO improved value mineral recovery and concentrate grade in the flotation of artificial mixtures of chalcopyrite/quartz and a commercial Au-Cu sulfide ore sample. It was found that PEO adsorbed on both minerals mainly through hydrogen bonding and caused non-selective flocculation of quartz and chalcopyrite, forming large hetero-aggregates. However, the addition of potassium amyl xanthate (KAX), a specific sulfide mineral collector, adsorbed on chalcopyrite through chemical interaction, replaced PEO and caused the chalcopyrite particles to break away from the hetero-aggregates, forming separate homo-aggregates of quartz and chalcopyrite. The flotation of the chalcopyrite and the depression of the quartz were thus both improved due to the larger sizes of the homo-aggregates compared to the discrete particles.

It was also observed that a completely solubilized PEO solution could not flocculate quartz, while a partially solubilized PEO solution was most effective. This was attributed to the better “bridging” functions of the undissolved PEO aggregates when it was partially solubilized. When the PEO was fully solubilized, the individual PEO molecules were probably too flexible and tended to flatten on the adsorbed solid surface and thus could not function as an effective bridging flocculant.

Furthermore, it was found that PEO could function as a “collector” for quartz due to its affinity to air-water interface and quartz, and it could increase quartz entrainment when used at high dosages. Selective flocculation and depression of the quartz gangue during chalcopyrite flotation could only be achieved at low PEO dosages. The implication of these observations on how to utilize the polyethylene oxide in industrial flotation was discussed.

ACKNOWLEDGEMENT

My deepest gratitude goes to my supervisors Dr. Qi Liu and Dr. Anthony A. Yeung for their all around guidance and encouragement during the course of my graduate study. Without their patience and tolerance, this work would not have been completed. Dr. Liu has set a good example for me not only academically but also morally. Dr. Yeung's solid knowledge in scientific theories has always inspired me to study more. It is very lucky for me to be their student. My gratitude extends to Dr. Philip.Y.K. Choi, my other supervisory committee member, for his helpful criticism and suggestions concerning this research.

I really appreciate Drs. Dimitre Karpuzov, Anqiang He and Shihong Xu (ACSES) for cryo-XPS measurement and the useful suggestions on data interpretation. My appreciation also goes to Dr. Allen Pratt for guidance on the interpretation of the XPS data.

The financial support from Natural Sciences and Engineering Research Council of Canada (NSERC), and COREM/Agnico-Eagle Mines Ltd (CRD grant) is gratefully acknowledged.

Special recognition and appreciation goes to Dr. Mingli Cao, who is like another mentor for me and has given me numerous valuable suggestions on my research and life. I would also like to thank my other group members Weibing Gan,

Zhewen Kang, Ying Jin, Weikang Liu, Ming Tang, Marc Parrent, Peng Huang, Xiao Ni, Huiran Wang and Lei Wang, for their friendship and encouragement.

Last but not least, I would like to thank to my family and special friends, Misuk Ryu and Sean D. Erickson, for being there when I needed support and encouragement.

TABLE OF CONTENTS

CHAPTER I INTRODUCTION	1
CHAPTER II LITERATURE REVIEW	4
2.1 FROTH FLOTATION	4
2.2 PROBLEMS ASSOCIATED WITH FINE PARTICLE FLOTATION.....	5
2.3 PREVIOUS RESEARCH TO IMPROVE FINE PARTICLE FLOTATION RATE	6
2.4 PREVIOUS RESEARCH ON FINE PARTICLE ENTRAINMENT.....	7
2.4.1 <i>Mechanism study: factors controlling entrainment</i>	7
2.4.2 <i>Techniques proposed to reduce fine particle entrainment</i>	8
2.5 GENERAL THEORY OF PARTICLE INTERACTIONS IN AN AQUEOUS SUSPENSION	10
2.5.1 <i>DLVO theory and coagulation</i>	10
2.5.2 <i>Hydrophobic forces and hydrophobic aggregation</i>	15
2.5.3 <i>Effect of polymers on suspension stability</i>	17
2.6 SELECTIVE COAGULATION AND SELECTIVE FLOCCULATION	20
2.7 POLYETHYLENE OXIDE (PEO).....	22
CHAPTER III OBJECTIVES AND SCOPE OF THIS RESEARCH	32
CHAPTER IV EFFECT OF PEO ON QUARTZ ENTRAINMENT DURING SULFIDE MINERAL FLOTATION.....	33
4.1 INTRODUCTION.....	33
4.2 EXPERIMENTAL	33
4.2.1 <i>Materials and chemicals</i>	33
4.2.2 <i>Batch flotation tests</i>	34
4.3 RESULTS AND DISCUSSION.....	35
4.3.1 <i>Batch flotation of pure quartz particles</i>	35
4.3.2 <i>Batch flotation of synthetic mineral mixture of quartz-chalcopyrite</i> ...	36
4.3.3 <i>Batch flotation of a Au-Cu ore from eastern Canada</i>	37
4.4 SUMMARY	38

**CHAPTER V FLOCCULATION OF QUARTZ AND CHALCOPYRITE BY
POLYETHYLENE OXIDE AND POTASSIUM AMYL XANTHATE51**

5.1 INTRODUCTION.....	51
5.2 EXPERIMENTAL.....	51
5.2.1 <i>Materials and chemicals</i>	51
5.2.2 <i>Flocculation/dispersion measurements</i>	52
5.2.3 <i>Microscope observation</i>	53
5.2.4 <i>SEM/EDS observations</i>	53
5.3 RESULTS.....	54
5.3.1 <i>Flocculation of 1:1 quartz-chalcopyrite mixtures</i>	54
5.3.2 <i>Flocculation of quartz and chalcopyrite single minerals</i>	56
5.3.3 <i>Flocculation of quartz-chalcopyrite mixtures with varying amounts of chalcopyrite</i>	58
5.4 DISCUSSION.....	59
5.5 SUMMARY.....	61

**CHAPTER VI ADSORPTION MECHANISM OF POLYETHYLENE
OXIDE (PEO) AND POTASSIUM AMYL XANTHATE (KAX).....73**

6.1 INTRODUCTION.....	73
6.2 EXPERIMENTAL.....	74
6.2.1 <i>Materials and chemicals</i>	74
6.2.2 <i>Zeta potential measurements</i>	74
6.2.3 <i>Adsorption tests</i>	74
6.2.4 <i>Flocculation/dispersion measurements</i>	76
6.2.5 <i>Cryo-XPS analysis</i>	76
6.3 RESULTS AND DISCUSSION.....	77
6.3.1 <i>Effect of PEO and KAX on the zeta-potential of quartz and chalcopyrite</i>	77
6.3.2 <i>Adsorption of PEO on quartz and chalcopyrite</i>	78
6.3.3 <i>Interaction of quartz with PEO</i>	78
6.3.4 <i>Interaction of chalcopyrite with PEO, and with KAX</i>	87

6.4 SUMMARY	94
CHAPTER VII EFFECT OF PEO DISSOLUTION STATES ON PEO- INDUCED FLOCCULATION.....	116
7.1 INTRODUCTION.....	116
7.2 EXPERIMENTAL	116
7.2.1 <i>Materials and chemicals</i>	116
7.2.2 <i>Sedimentation tests</i>	116
7.2.3 <i>Viscosity measurement</i>	117
7.2.4 <i>Visual observation</i>	117
7.3 RESULTS	118
7.3.1 <i>Effect of PEO dissolution time on the sedimentation of quartz</i>	118
7.3.2 <i>Effect of storage temperature of the PEO solutions on the sedimentation of quartz</i>	119
7.3.3 <i>Effect of preparation method of PEO solution on the sedimentation of quartz</i>	120
7.4 DISCUSSION	122
7.5 SUMMARY	125
CHAPTER VIII FROTHING PROPERTY AND DOSAGE CONTROL OF PEO	137
8.1 INTRODUCTION.....	137
8.2 EXPERIMENTAL	137
8.2.1 <i>Materials and chemicals</i>	137
8.2.2 <i>Small-scale flotation test</i>	137
8.2.3 <i>Frothing tests</i>	138
8.2.4 <i>Dynamic pendant drop tests</i>	138
8.3 RESULTS	139
8.3.1 <i>Small scale flotation tests on quartz particles</i>	139
8.3.2 <i>Frothing property of PEO in flotation</i>	140
8.3.3 <i>Effect PEO on air/water interfacial tension</i>	140

8.4 DISCUSSION	141
8.5 SUMMARY	142
CHAPTER IX CONCLUSIONS AND RECOMMENDATIONS.....	151
9.1 GENERAL FINDINGS	151
9.2 CLAIMS OF ORIGINALITY	153
9.3 LIMITATIONS OF THE RESULTS.....	154
9.4 RECOMMENDATIONS FOR FUTURE RESEARCH.....	155
BIBLIOGRAPHY	156

LIST OF TABLES

Table 6.1 Binding energy of Si 2p peaks in the four quartz suspension samples, using C 1s 284.65 eV as calibration standard	84
Table 6.2 Binding energy of O 1s peaks of quartz suspension samples at pH 9 ..	85
Table 6.3 Binding energy of O 1s peaks of quartz suspension samples at pH 2. .	86
Table 6.4 Binding energy of O 1s peaks of chalcopyrite suspension samples	91
Table 6.5 Binding energy of S 2p peaks of chalcopyrite suspension samples	92

LIST OF FIGURES

Figure 2.1 Schematic diagram of the flotation process in a froth flotation cell....	27
Figure 2.2 Schematic diagram of an electrical double layer around a charged spherical particle.....	28
Figure 2.3 Schematic energy versus separation distance profiles of DLVO interaction.	29
Figure 2.4 Schematic illustration of destabilization/stabilization by polymers....	30
Figure 2.5 Electrostatic patch model of polymer adsorption leading to flocculation.	31
Figure 4.1 Denver laboratory flotation machine.....	39
Figure 4.2 Wemco laboratory flotation machine.	40
Figure 4.3 Quartz recovery as a function of water recovery in the batch flotation of pure quartz at various PEO dosages.....	41
Figure 4.4 Degree of quartz entrainment as a function of PEO dosage in the batch flotation of pure quartz.	42
Figure 4.5 Cumulative recovery of water and quartz as a function of PEO dosage in the batch flotation of pure quartz.	43
Figure 4.6 Comparison of quartz recovery as a function of water recovery in the batch flotation of pure quartz and synthetic quartz/chalcopyrite mixture without the use of PEO.....	44
Figure 4.7 Quartz and chalcopyrite recovery as a function of water recovery in the batch flotation of synthetic quartz/chalcopyrite mixture at several PEO dosages.	45
Figure 4.8 Recovery-grade relationship of the batch flotation of synthetic chalcopyrite-quartz mixtures.	46
Figure 4.9 Cu recovery as a function of water recovery in the batch flotation of a commercial Au-Cu sulfide ore at several PEO dosages.....	47
Figure 4.10 Quartz recovery as a function of water recovery in the batch flotation of a commercial Au-Cu sulfide ore at several PEO dosages.	48

Figure 4.11 Recovery-grade relationship of Cu in the batch flotation of a commercial Au-Cu sulfide ore.....	49
Figure 4.12 Recovery-grade relationship of Au in the batch flotation of a commercial Au-Cu sulfide ore.....	50
Figure 5.1 Photometric Dispersion Analyzer (PDA 2000).....	62
Figure 5.2 Microscope apparatus for visual observation.....	63
Figure 5.3 Effect of KAX and PEO on the flocculation/dispersion of 1:1 quartz-chalcopyrite mixtures.	64
Figure 5.4 (a) SEM image of a typical PEO floc of quartz-chalcopyrite; (b) EDS spectrum of point (1): chalcopyrite; (c) EDS spectrum of point (2): quartz.	65
Figure 5.5 Effect of KAX on the quartz-chalcopyrite flocs induced by PEO	66
Figure 5.6 Effect of KAX and PEO on the flocculation/dispersion of quartz.	67
Figure 5.7 Effect of KAX and PEO on the flocculation/dispersion of chalcopyrite.	68
Figure 5.8 Effect of PEO and KAX on the flocculation/dispersion of quartz-chalcopyrite mixtures with different chalcopyrite content (a) 10% chalcopyrite (b) 30% chalcopyrite.	69
Figure 5.9 Effect of PEO and KAX on the flocculation/dispersion of quartz-chalcopyrite mixtures with different chalcopyrite contents.	70
Figure 5.10 SEM images of suspension samples taken 15 minutes after the addition of PEO.	71
Figure 5.11 Illustration of the breakage of quartz/chalcopyrite hetero-aggregate and the formation of homo-aggregate of quartz and chalcopyrite.....	72
Figure 6.1 Calibration curve for PEO concentration determination	96
Figure 6.2 Effect of KAX and PEO on the zeta potentials of chalcopyrite and quartz.	97
Figure 6.3 Adsorption kinetics of PEO on quartz and chalcopyrite particles.....	98
Figure 6.4 Adsorption isotherm of PEO on quartz and chalcopyrite particles	99
Figure 6.5 Effect of pH on quartz flocculation by PEO.	100
Figure 6.6 Relative surface density of three surface species on quartz surface..	101

Figure 6.7 Schematic diagram of the conformation of PEO chains adsorbed on quartz surface.	102
Figure 6.8 The change of pH of PEO solution as the function of the amount of PEO dissolved.	103
Figure 6.9 XPS spectra for C 1s region of the four quartz suspension samples.	104
Figure 6.10 XPS spectra for Si 2p region of the four quartz suspension samples.	105
Figure 6.11 XPS spectra for O 1s region of the quartz suspension samples at pH=9.	106
Figure 6.12 XPS spectra for O 1s region of the quartz suspension samples at pH=2.	107
Figure 6.13 XPS spectra for O 1s region of the PEO solution at pH=9.	108
Figure 6.14 Effect of pH on chalcopyrite flocculation by PEO.	109
Figure 6.15 XPS spectra for C 1s region of the chalcopyrite suspension samples.	110
Figure 6.16 XPS spectra for S2p region of KAX solution.	111
Figure 6.17 XPS spectra for Fe 2p region of the chalcopyrite suspension samples.	112
Figure 6.18 XPS spectra for Cu 2p region of the chalcopyrite suspension samples.	113
Figure 6.19 XPS spectra for O 1s region of the chalcopyrite suspension samples.	114
Figure 6.20 XPS spectra for S 2p region of the chalcopyrite suspension samples.	115
Figure 7.1 Effect of dissolution time of PEO suspension on quartz flocculation.	127
Figure 7.2 Images of swollen granules of PEO in water.	128
Figure 7.3 Illustration of PEO granule dissolution process at low concentrations.	129
Figure 7.4 Effect of storage temperature of stock PEO solution on quartz flocculation.	130

Figure 7.5 Comparison of entanglement sizes using Ostwald viscometer.	131
Figure 7.6 Effect of preparation method on flocculation efficiency of PEO solution.	132
Figure 7.7 Illustration of PEO particle dissolution-dilution process at high concentrations.	133
Figure 7.8 Image of a mass of 0.5% PEO solution injected in distilled water. ..	134
Figure 7.9 Comparison of PEO entanglement sizes prepared with different methods.	135
Figure 7.10 Illustration of destruction of PEO-induced flocs.	136
Figure 8.1 Small scale flotation setup using a columnar flotation tube.	143
Figure 8.2 A 1-m tall frothing column for frothing property test.	144
Figure 8.3 Pendant drop apparatus for interfacial tension measurement.	145
Figure 8.4 Linear relationship between quartz recovery and water recovery.	146
Figure 8.5 Effect of PEO dosage on the degree of entrainment of quartz.	1477
Figure 8.6 Frothing power of PEO.	1488
Figure 8.7 Interfacial tension vs. step-up area for a solution with 18mg/L DF250.	14949
Figure 8.8 Interfacial tension vs. Step-up area for a solution with 18 mg/L DF250 and 25 mg/L PEO.	1500

Chapter I Introduction

With the depletion of high grade and easy-to-process ores, froth flotation process is facing severe problems caused by fine and ultrafine particles, which are generated by ultrafine grinding that is required to liberate value minerals from low grade and highly disseminated ores. The problems are two folds. Firstly, the fine and ultrafine value minerals are lost to the tailings as the low inertia of the fine particles cause infrequent and inefficient particle-bubble collision, leading to low recovery. Secondly, the grade of the flotation concentrate is lowered by the mechanical entrainment of the fine and ultrafine gangue minerals into the froth product. The efficiency of the flotation separation diminishes as a result of those two problems.

As has been shown by several researchers in the 1970s and early 1980s (Thorne et al., 1976; Trahar, 1981; Warren, 1984), mechanical entrainment becomes significant generally for particles smaller than about 30 μm , and it is proportional to the recovery of water into the froth products. However, the problem of mechanical entrainment of fine and ultrafine hydrophilic particles has been largely sidelined as research effort has been mainly focused on improving the flotation recovery of fine and ultrafine hydrophobic particles. Such research effort led to many publications and several techniques to improve the recovery of fine and ultrafine hydrophobic particles. The reason for the lack of research on reducing mechanical entrainment is not clear. However, although the developed techniques and processes can improve the recovery of fine hydrophobic particles, almost in all such processes the fine and ultrafine hydrophilic (gangue) particles are kept highly dispersed. This makes mechanical entrainment worse. In fact, the severe entrainment of fine and ultrafine hydrophilic particles into the flotation froth product is one of the reasons why the developed recovery-enhancing fine and ultrafine particle flotation processes have not found widespread applications in commercial flotation circuits.

Since fine and ultrafine hydrophilic particles are carried into froth product because of their small mass and particle size, one method to reduce mechanical entrainment is to increase the sizes of these particles. This concept has been verified by the recent work of Liu et al. (Liu et al., 2006) who showed that, in the flotation of several oxide minerals including iron oxide, hydroxyapatite, and quartz, the use of high molecular weight selective polymeric flotation depressants could flocculate the fine and ultrafine particles as well as render them hydrophilic, thus lowering both the flotation and mechanical entrainment of the minerals that are to be depressed.

In the current dissertation research, the concept of using high molecular weight polymeric depressants to induce both selective depression and flocculation was applied to commercial sulfide ore flotation. Sulfide ores are the major sources of base metals such as copper, lead, zinc, nickel, etc., and froth flotation - since its invention more than a hundred years ago - is the major technology used to process these ores and extract the base metals. With the depletion of high grade and easy-to-process ores, the minerals industry has to deal with increasingly lower grade and more finely disseminated ores. For such sulfide ores, grinding to smaller than 400 mesh (38 μm) is often required, which produce a large proportion of particles less than 10 μm , thereby compromising flotation kinetics and flotation selectivity. For instance, it has been reported that in the flotation of a lead sulfide (galena, PbS) ore, the concentrate grade dropped from 70% Pb at a grind size of 100 μm to 25% Pb at a grind size of 20 μm (Thorne et al., 1976).

One of the main objectives of this research is to find suitable polymeric depressants to process low grade and finely disseminated sulfide ores for gangue rejection. As quartz is the most common gangue mineral present in most sulfide ores, the research is focused on reducing quartz entrainment during the flotation of sulfide minerals, particularly copper sulfide minerals such as chalcopyrite (CuFeS_2). Polyethylene oxide (PEO) of high molecular weight has been chosen for this research as it has been reported to be a good flocculant for quartz.

In the dissertation that follows, Chapter II provides background information on the froth flotation technology, specifically a review of previous work on fine and ultrafine particle flotation, a brief description of polymer flocculation and the properties and applications of polyethylene oxide (PEO). Chapter III describes the scope of this research. Chapter IV presents and discusses the batch flotation results when PEO was used in chalcopyrite and commercial Au-Cu sulfide ore flotation, using xanthate as a sulfide mineral collector. Chapter V presents the flocculation/dispersion results of using PEO and xanthate in the quartz-chalcopyrite system and discusses the reasons for the selective flocculation. Chapter VI examines the adsorption mechanisms of PEO and xanthate on chalcopyrite and quartz. Chapter VII presents and discusses the effects of PEO solution properties and solution preparation methods on its flocculation behavior. The effects of PEO on froth stability and hence its potential negative effect on quartz entrainment are discussed in Chapter VIII. The thesis ends with Chapter IX which summarizes the major findings of this dissertation research and the recommendations for future work.

Chapter II Literature Review

2.1 Froth flotation

Mineral processing concerns the separation and enrichment of commercially valuable minerals from their raw ores, the products of which are either used directly or processed further to extract the contained metals. The separation processes take advantage of the differences in the physical properties of the minerals and those of the ores that contain them. These physical properties can include density, particle size and shape, electrical and magnetic properties, and surface wettability.

The froth flotation process utilizes the surface wettability of minerals, which, unlike other physical properties, can be readily modified with chemical reagents. Therefore, the flotation process has been developed to treat almost all types of minerals and ores, including sulfides, oxides, salt-type and non-metallic ores, and is the most important and widely used mineral processing technique. In a typical froth flotation process, the raw ore is first ground to liberate the value minerals from gangue minerals and forms an aqueous suspension. Chemical reagents are then added to make the value mineral particles hydrophobic and the gangue (waste) particles hydrophilic (in the so-called reverse flotation process, it is the gangue minerals that are made hydrophobic). Small air bubbles that are subsequently generated in or injected into the system collect the hydrophobic particles into a stable froth layer that forms on top of the suspension, thus separating them from the hydrophilic particles that remain suspended in the flotation pulp. This process is illustrated in Figure 2.1.

The reagents employed in flotation are usually classified as collectors, frothers and regulators or modifiers. Collectors are reagents that react with mineral surfaces and render them hydrophobic to attach to air bubbles. Frothers are surface active reagents that can provide a froth layer stable enough to transport

the mineral-bubble aggregates to the flotation concentrate. Regulators or modifiers can be further classified into pH modifiers which control the pH of flotation pulp, activators which assist in the adsorption of collectors on surface, and depressants which render certain minerals, typically gangue minerals, hydrophilic so that they do not float.

The versatility of the froth flotation process lies in the selection of different flotation reagents. To this day, the selection of flotation reagents is still an art than science. Nevertheless, the development of new flotation reagents under the guidance of scientific principles has always been a driving force for the advancement of froth flotation.

2.2 Problems associated with fine particle flotation

With the depletion of high grade ores that are more easily processed, the minerals industry has had to deal with ores of an increasingly lower grade and more complex dissemination. As a result, the flotation process needs to treat fine and ultrafine particles because the liberation of minerals from the low grade and highly disseminated ores typically requires ultrafine grinding which generates large amount of fine and ultrafine particles. In froth flotation terminology, the fine and ultrafine particles typically refer to those particles that are less than 20 μm and 10 μm , respectively. These particles possess small mass and high specific surface area, and cause two major problems in froth flotation: the slow flotation rate of hydrophobic particles and the mechanical entrainment of hydrophilic particles (Trahar and Warren, 1976; Trahar, 1981). The slow flotation rate leads to the low recovery of the hydrophobic particles. As a result, value minerals are lost as fine particles to the tailings. It was estimated that one third of the phosphate, one sixth of the copper, and one tenth of the iron mined in the U.S., half of the tin explored in Bolivia and one fifth of the tungsten mined in the world are discarded into the tailings ponds as slimes due to the issue (Subrahmanyam and Forssberg, 1990). The problem associated with mechanical entrainment is that

it is non-selective with no distinction between hydrophobic and hydrophilic particles. The grade of the flotation concentrate is lowered when fine and ultrafine gangue particles entrain into the froth product. Low value mineral recovery and low concentrate grade caused by fine and ultrafine particles shows us that froth flotation was never meant to deal with particles of this size and is not a good separation process for the fine and ultrafine particles.

2.3 Previous research to improve fine particle flotation rate

The problem of low recovery of fine hydrophobic particles has attracted much research worldwide, which has resulted in a large number of publications in the open literature and several techniques to improve the recovery of these particles. Fuerstenau (1980), Singh et al., (1997), Sivamohan (1990), and Subrahmanyam and Forssberg (1990) have reviewed the techniques developed. The main reason for the low recovery is the inefficient collision between the fine and ultrafine particles with the gas bubbles due to the small masses and sizes of the particles. Therefore most techniques proposed are therefore aimed at improving the collision efficiency either by increasing the collision probability, and/or subsequent adhesion following the collision. These techniques include flocculation (Wareen, 1975; Song et al., 2001), spherical agglomeration (Cebeci, 2003; Sonmez and Cebeci, 2003), carrier flotation (Rubio and Hoberg, 1993), dissolved air flotation (Rodrigues and Rubio, 2007), micro-bubble flotation (Ahmed and Jameson, 1985; Neethling and Cilliers, 2001), split conditioning and combined flotation (Singh et al., 1997), use of chemisorbing flotation collector (Fuerstenau et al., 1970), etc. These techniques improve the recovery of fine hydrophobic particles to different degrees. However, in all processes the fine gangue particles are kept highly dispersed, which cause severe mechanical entrainment and lowers the grade of the concentrate produced. In fact, the low concentrate grade is likely the reason why these proposed processes have not found widespread applications in commercial flotation circuits. As Trahar (1981) pointed out, “It should be emphasized that unless entrainment can be reduced it is

difficult to be optimistic about the ultimate applicability of conventional flotation as the sole concentrating method to systems in which fine particles predominate.”

2.4 Previous research on fine particle entrainment

2.4.1 Mechanism study: factors controlling entrainment

Smith and Warren (Smith and Warren, 1989) proposed a bubble swarm theory to explain the entrainment of fine particles in flotation. According to them, the bubble swarm rises through the flotation pulp and crowds near the froth-pulp interface. At this point, the water trapped in the swarm starts to flow downwards, but due to the restricted paths for drainage through the bubble swarm, some water is pushed over the froth-pulp interface into the froth phase. So are the particles.

Research has been carried out to examine the various factors that affect the entrainment, and a general consensus is that fine particle entrainment is proportional to water recovery. In fact, a linear relationship is usually observed between fine particle entrainment and water recovery when particles are fine enough (Jowett, 1966; Trahar, 1981). This relationship can be described by the following equation:

$$R_g = e_g R_{water} \quad (1)$$

Where R_g is the recovery of fine gangue of a given size in a given time, e_g a constant for a given particle size and specific gravity, and R_{water} is the recovery of water for the same time period. Obviously, if a plot of the recovery of gangue versus the recovery of water yields a straight line, e_g will be the slope of the line. In this case, e_g is called “Degree of Entrainment” (Warren, 1985).

It has been found that some factors, such as air flow rate and froth lamella thickness, i.e., the thickness of the intervening water film between bubbles, which were reported to affect particle entrainment, essentially did so by affecting the

water recovery (Hemmings, 1980). In fact, their effects on water recovery are self-evident: an increase in air flow rate or froth lamella thickness would lead to an increase in water recovery and hence particle entrainment.

Fine particle entrainment is a result of the competition between particle carry-over into the froth phase by water and particle drainage back to the flotation pulp. Factors affecting particle drainage were also examined. These include froth height, particle density and particle size (Waksmundzki et al., 1972; Cutting, 1989; Szatkowski, 1987). It was reported that entrainment decreases with increasing froth height since a deep froth layer would allow more drainage, decreases with increasing particle density due to weight-induced drainage, and decreases with increasing particle size due to volume-induced drainage.

The foregoing review shows that the degree of entrainment depends on many factors, including particle size, water recovery, and froth properties. But among all factors, particle size is most important since if particles are sufficiently large, they will not be lifted high enough to enter the froth phase under normal operation conditions in flotation, and even if they do, they can easily drain back to the flotation pulp. In fact, entrainment is not a problem for coarse particles.

2.4.2 Techniques proposed to reduce fine particle entrainment

Lowering the solid density in pulp is often employed to reduce fine particle entrainment in mineral processing plant, especially during cleaner flotation. Apart from it, most of the techniques proposed so far are based on how to encourage particle drainage across the froth zone. One common practice is froth washing by spraying water onto the froth (Kaya, 1996; Banisi et al., 2003). Froth washing is an essential part of column flotation (Finch et al., 1989) but its effectiveness on conventional mechanical flotation cells is still doubtful because wash water might not drain fast enough to the pulp in conventional mechanical flotation cells. In this

case the wash water would increase the froth lamella thickness, thus increase froth stability, hinder particle drainage and increase entrainment.

Mulleneers et al. (2002) modified mechanical flotation cells by adding a countercurrent sedimentation zone, which is expected to prevent entrainment. This design is akin to flotation columns to some degree and could lead to low value recovery in a mechanical flotation machine.

Cheng et al. (1999) added an oscillating separator to a conventional flotation cell. It is thought to reduce mechanical entrainment by 1) breaking up the bubble-particle aggregates and thus releasing entrapped particles; 2) deforming the intervening water films between air bubbles and promoting the detachment of particles; 3) producing a greater horizontal fluid flow to buffer against the upward fluid flow thereby to reduce the carry-over of particles into the froth phase.

Liu et al. (2006) recently proposed to lower the fine particle entrainment by using polymeric depressants with sufficient molecular weight so that they could cause selective flocculation of the fine hydrophilic particles. The technique targets at increasing particle size, which is the essential factor controlling entrainment. Compared to other methods reported above, this method entails the use of chemical reagents and does not require any modification to existing process equipment. It therefore appears to be the most convenient and economical way to be adopted in conventional mechanical flotation cells.

The formation of selective particle aggregates (coagula and flocs) in a complicated mineral and ore suspension is governed by fundamental colloidal and surface forces. The feasibility of using the polymeric depressants depends on a thorough understanding of these forces operating on the mineral particles across an aqueous medium. These interaction forces are briefly reviewed in the following.

2.5 General theory of particle interactions in an aqueous suspension

2.5.1 DLVO theory and coagulation

In the classical DLVO (Derjaguin-Landau-Verwey-Overbeek) theory, the total interaction energies between two colloidal particles are considered to be the sum of the van der Waals attractive energy and the repulsive double layer interaction energy. Therefore, depending on the magnitude of the van der Waals energy and the electrical double layer interaction energy, the overall interaction can be attractive or repulsive, leading to coagulation or dispersion of the colloidal system, respectively.

Van der Waals forces

The van der Waals forces account for a group of relatively weak interactions between all molecules and atoms, compared to those due to covalent bonds or the electrostatic interaction. Van der Waals forces are typically attractive and are comprised of three distinct forces:

- 1) Keesom orientation forces: electrostatic interaction between two permanent molecular dipoles.
- 2) Debye induction forces: electrostatic interaction between a permanent dipole on one molecule and an induced dipole on another.
- 3) London dispersion forces: electromagnetic interaction between two instantaneous dipoles due to the instantaneous positions of electrons about the nuclear protons.

A macroscopic body such as a particle is made up of numerous molecules so that van der Waals forces also operate between macroscopic objects. Assuming these inter-molecular forces can be added by a pairwise summation, Hamaker (Hamaker, 1937) derived a simple expression for the interaction energy between two spheres:

$$V_A = -\frac{A_{12}R_1R_2}{6d(R_1 + R_2)} \quad (1)$$

Where V_A is the inter-particle van der Waals interaction energy; A_{12} the Hamaker constant for the material 1 and 2, of which the spheres are made of; d the inter-particle distance and R_1, R_2 the radius for the spheres respectively.

For equal spheres, it can be simply put as:

$$V_A = -\frac{A_{11}R}{12d} \quad (2)$$

Even though these equations ignore the influence of neighboring atoms on the interaction between any pair of atoms, they work well at close approach.

Electrical Double Layer forces

When submerged in aqueous solutions, most particles acquire charges. There are various reasons for this, including isomorphous substitution of the lattice metal ions by other metal ions of different valence, preferential dissolution, selective ionization of surface groups and chemisorption of ionic species from solution. Due to the net charges on particle surface, the ion distribution in the vicinity of the particle is different from the bulk solution, giving rise to an electrical double layer. The structure of the electrical double layer, schematically shown in Figure 2.2, is comprised of a Stern layer where the counter ions are tightly bounded with the particle surface, and a diffuse layer where the counter ions are distributed more broadly and can diffuse with a certain degree of freedom. When the particle moves relative to the solution, the tightly-held Stern layer moves with the particle generating a "shear surface".

When two charged particles approach each other to within certain distance, their diffuse layers start to overlap and the higher concentration of the counter ions in

the diffuse layers causes an osmotic pressure, which prevents further approaching of the particles. Effectively, this generates a repulsive force. For oppositely charged particles, however, the two approaching diffuse layers will attract each other since they carry higher concentrations of oppositely charged counter ions.

The origin of the electric double layer interaction is entropic (osmotic), not electrostatic. Therefore it is the Stern potential at the boundary between the Stern layer and diffuse layer rather than the particle surface potential (Nernst potential) that is more relevant to the interaction. Stern potential cannot be measured with direct experimental method but the electrokinetic or zeta potential is believed to be a good substitute (Lyklema, 1977), which can be easily determined by the particle electrophoresis technique. Zeta potential can be modified in two ways:

- 1) Adding indifferent electrolytes, which raises the ionic strength, compresses the electric double layer, and causes a steeper potential drop across the Stern layer and a lower zeta potential.
- 2) Adding specifically adsorbing counter ions, which adsorb on the particle surface through specific interactions such as chemical reactions. These specifically adsorbing ions are considered to be residing in the Stern layer. In some cases, such ions can even reverse the sign of zeta potential.

The osmotic pressure can be calculated by assuming either that the surface potentials of the particles do not change during the double layer overlapping or that the surface charge densities do not change. Even though neither assumption reflects the reality, they can give an approximation of the interaction energy for charged particles. A simple expression, Linear Superposition Approximation, represents a useful compromise between the two extremes. For two identical spheres with a radius R, the interaction energy due to the overlapping of the diffuse layer is (Gregory, 1989):

$$V_E = 32\pi\epsilon_0\epsilon_r(kT/ze)^2\gamma^2\exp(-\kappa l) \quad (3)$$

When the surface potential (or zeta-potential) is quite small, it can be simplified to

$$V_E = 2\pi\epsilon_o\epsilon_r R\zeta^2 \exp(-\kappa d) \quad (4)$$

Where ϵ_o is the permittivity of vacuum ($8.85 \times 10^{-12} \text{ C}^2/\text{N}\cdot\text{m}^2$); ϵ_r the relative permittivity of the medium (for water at 25°C , ϵ_r is 78); d the distance between the two spheres; ζ the zeta-potential in V; k the Boltzmann constant ($1.38 \times 10^{-23} \text{ J/K}$); T the absolute temperature; z the valence of counter ions; e the magnitude of electron charge ($1.602 \times 10^{-19} \text{ C}$); $\gamma = \tanh(ze\zeta / 4kT)$; κ the inverse of Debye length. The range of the interaction depends on the extent of diffuse layer which is typically 3 or 4 times of the Debye length, $1/\kappa$. The Debye length can be calculated from the following equation (Hunter, 2001, page 320):

$$\frac{1}{\kappa} = \left(\frac{\epsilon_o\epsilon_r kT}{\sum_i (z_i e)^2 c_i} \right)^{\frac{1}{2}} \quad (\text{m}) \quad (5)$$

Where the meaning of ϵ_o , ϵ_r , T , z and e are described as before; c_i is the electrolyte concentration (number of electrolytic ions per unit volume).

As can be seen, the Debye length, $1/\kappa$, and thus the thickness of the diffuse layer, only varies with temperature and bulk electrolyte concentration in water. A higher temperature makes the diffuse layer thicker, whereas a higher electrolyte concentration makes the diffuse layer thinner.

Combined Interaction

The total interaction energy for two identical spherical particles can be calculated by combining equations (2) and (3):

$$V_T = 32\pi\epsilon_o\epsilon_r (kT/ze)^2 \gamma^2 \exp(-\kappa d) - AR/12d \quad (6)$$

Therefore, depending on the magnitude of the van der Waals energy and the electrical double layer energy, the overall interaction can be attractive or repulsive, leading to coagulation or dispersion, respectively. Furthermore, since the van der Waals energy and the double layer energy follow different decay functions with distance, the former a power law and the latter exponential, the total interaction energy curves may show peaks or valleys as illustrated in Figure 2.3. Figure 2.3(a) represents the particles with high surface potential. When two particles start approaching each other, the van der Waals energy (V_A) outweighs the double layer energy (V_E) at a large distance, giving rise to "Secondary Minimum" in the total interaction energy and the particles may form loose aggregates. When the particles get closer, V_E rises faster than V_A , resulting in an energy barrier which needs to be overcome in order for the particles to aggregate. When the particles do not have sufficient energy to overcome the energy barrier, they form stable colloidal dispersions. However, if the particles acquire sufficient kinetic energy from an external source, such as from hydrodynamic forces exerted by intensive agitation, the energy barrier can be overcome, and the particles form tightly-held aggregates by the steeply dropping interaction energy with decreasing distance. This very low energy states at a close distance is called the "Primary Minimum". If the particles do not have sufficient kinetic energy, they may still be held together by the secondary energy well. However, such loose aggregates can be easily broken. If the particle surface potential is low, V_A might outweigh V_E over the entire range of the separation distance and the energy barrier disappears as shown in Figure 2.3(b). Particles would aggregate instantly upon collision.

For a specific particle suspension, V_A is more or less fixed. The only method to reduce the energy barrier and induce coagulation is to reduce V_E . According to equation (4), this can be achieved by adding electrolytes, which increases κ , compresses the diffuse layer and reduces V_E . When the electrolyte is added, it can reach a point where a spontaneous coagulation occurs in the suspension. Such minimum electrolyte concentration is called the critical coagulation concentration

(c.c.c.). In some cases, the added electrolytes can specifically adsorb on the particle surface and cause a significant drop in surface potential and even inverse the sign of surface charges, which would also result in particle coagulation. Those added electrolytes are called coagulants. In minerals industry, the most commonly used coagulants are iron and aluminum salts, which are used in solid/liquid separation processes (Richardson and Connelly, 1988). Their coagulation effectiveness is attributed to their hydrolysis in aqueous solution. Three mechanisms have been proposed to explain such coagulation:

- 1) Charge neutralization. The hydroxyl complexes of those cations, FeOH^{2+} , $\text{Fe}(\text{OH})_2^+$, AlOH^{2+} , $\text{Al}(\text{OH})_2^+$, etc., would adsorb on particle surfaces, leading to electric double layer compression and even surface charge neutralization, which causes particle coagulation (Fuerstenau et al., 1985).
- 2) Sweep coagulation. At sufficiently high dosages, the metal hydroxides would form as colloidal precipitates initially and grow into large flocs. The suspended particles can be trapped into the flocs and settle down with them from the suspension (Packham, 1965).
- 3) Bridging coagulation. The metal hydroxide precipitates may bridge particles – causing coagulation – through electrostatic interaction, chemical interaction, or hydrogen bonding (Healy and Jellett, 1967; Krishnan and Iwasaki, 1986).

2.5.2 Hydrophobic forces and hydrophobic aggregation

When hydrophobic particles are suspended in water, an attractive interaction arises among those particles, known as hydrophobic interaction. Despite of extensive studies of the hydrophobic forces, the origin of this long-range attraction is still a subject of considerable debate. It has been suggested that the force originates from the ordering of water on the particle surface (Rabinovich and Derjaguin, 1988). When the surface is hydrophobic, water molecules at the

surface cannot form strong bonds with the surface and they form “icebergs” close to the surface, so that the ordering of water structure is enhanced, resulting in a lower entropy and hence an increase in interaction energy. Therefore, when two hydrophobic surfaces approach, they tend to merge so that the number of water molecules involved in “iceberg” structure is smaller after the merger. Other proposed mechanisms include an unusual polarization of water close to hydrophobic surfaces (Attard, 1989), the cavitation in the vicinity of hydrophobic surfaces (Yushchenko et al., 1983) and the formation of nano-bubbles at hydrophobic surfaces (Ducker et al., 1994).

It has been reported that the hydrophobic force between two macroscopic surfaces is much stronger than the van der Waals attraction and of long range of 0-10 nm (Israelachvili and Pashley, 1984; Claesson and Christenson, 1988). The magnitude and long range of the hydrophobic force is of special importance in flotation system since hydrophobic particles are always present. It has been exploited to improve fine hydrophobic particle flotation, such as floc-flotation. The principle of this technique is that the desired mineral particles are rendered hydrophobic by the addition of collectors and modifiers and then brought together through hydrophobic forces under intensive agitation. The shear field is necessary because it provides the required mechanical energy for particles to overcome the energy barrier and approach closely so that hydrophobic forces can take effect and hold the particles together, as first suggested by Warren (Warren, 1975). In fact, Warren coined the phrase “shear-flocculation” to describe the hydrophobic aggregation process. However, there is an optimum agitation speed, beyond which the flocs are broken up. In order to improve the flocculation, non-polar oil is often added. In addition to enhancing the hydrophobicity of particles, the non-polar oil also increases the strength of the flocs through oil bridge formation (Schubert, 1984).

Another technique that makes use of hydrophobic forces is oil agglomeration where much higher oil dosage, 10% or greater, is used depending on feed solids.

In this process, a nonpolar oil and the aqueous solid suspension are mixed mechanically at a high pulp density (i.e., high solids content). Particles first form loose open flocs through oil bridges, and the suspension fluid, often water, is then squeezed out and replaced by the oil under agitation. When the floc surface is covered with sufficient oil, it grows very fast and forms large and firm spherical oil-particle aggregates (Bemer and Zuiderweg, 1980) . Due to the high strength and large sizes, the aggregates can be separated from the dispersed particles by screening or other particle size separation techniques.

2.5.3 Effect of polymers on suspension stability

In addition to the inter-particle forces discussed in the preceding sections, polymers can alter the stability of a mineral suspension as well. The added polymers may or may not be adsorbed on the mineral surface, resulting in different effects on the mineral suspensions.

2.5.3.1 Adsorbing polymers: bridging flocculation and steric stabilization

If the added polymers adsorb on the mineral surface, the mineral suspension may be stabilized or destabilized, depending on the polymer molecular weight, dosage and its affinity for water.

With a sufficiently high molecular weight and at a low dosage, the polymer can adsorb on more than one particle, “bridging” them together (Figure 2.4). This bridging mechanism was postulated by Ruehrwein and Ward in 1952 (Ruehrwein and Ward, 1952) and has been widely accepted. Since the particles are linked together by the polymer chains, which are orders of magnitude larger than a few nanometers, the inter-particle forces discussed previously may have little effect since their effective range is much shorter.

With an increase in the polymer dosage, it may occur that the mineral particle surfaces have been completely covered by the polymers, leaving no “unoccupied

adsorption sites”. In this case, the bridging flocculation will not occur. Instead, the particles will repel each other as the overlapping or interpenetration of the adsorbed polymer chains is prevented due to osmotic forces. Therefore, the suspension will be “sterically stabilized” (Figure 2.4). Steric stabilization also often happens when a low molecular weight polymer is used. In such case, the polymer molecule chains are too short to cause bridging flocculation, and their adsorption only leads to dispersion due to steric effects.

It is worth noting that the steric stabilization only occurs when using polymers that have a strong affinity for water. If the polymer chains are not strongly attracted to water (i.e., if they are hydrophobic), then the polymer will cause “hydrophobic aggregation” due to the hydrophobic bonding forces of the polymer chains (Laskowski, 2002).

When the adsorbed polymers are charged, they can act as counterions, neutralizing the particle charges and resulting in destabilization of a mineral suspension. But bridging effects may still predominate, especially for high molecular weight polymers. They can also cause the destabilization through “electrostatic patch” coagulation, schematically shown in Figure 2.5 (Gregory, 1973). When the charged polymer adsorbs on an oppositely charged particle, it may cause a local charge reversal due to its higher charge density than the particle surface, giving rise to “patches” of excess charge. A particle with oppositely charged “patches” can attract another particle through the electrostatic interaction between the “patches” and bare areas on the other particle. However, this phenomenon has not yet been exploited in mineral flotation system.

In addition to coagulation, flocculation is another commonly used method for solid/liquid separation in mineral processing (Richardson and Connelly, 1988). The reagents used for flocculation are normally called flocculants. Due to their large molecular chain length, relatively small amount of such polymeric flocculants is generally required in flocculation process, making it very efficient.

Another advantage of the polymer flocculants is their versatility. The polymer flocculants vary widely in structure, molecular weight, charge, and functional groups, which make it possible to tailor-make the polymers to suite different applications in different mineral flotation systems.

Many polymers used as flocculants are natural polymers in origin, such as starch, gums, cellulose, etc., and their derivatives. However, in recent years, synthetic polymers have shown better performance and found more applications in mineral industry. This is probably because their structure and chemistry can be designed for a specific application. These synthetic polymers are normally classified into anionic, cationic and nonionic polymers, according to their polar groups. Natural polymers can also be charged either naturally or after chemical treatment.

Anionic polymers typically contain anionic groups such as $-\text{COOH}$, $-\text{SO}_3\text{H}$, $-\text{PO}_3\text{H}_2$. Those containing $-\text{COOH}$ are the most common and most important, for example, carboxymethyl cellulose (CMC), polyacrylic acid, etc.

Cationic polymers contain positively charged groups such as $-\text{NH}_2$, $-\text{NH}$ or $-\text{N}$. For example, chitosan is a natural cationic polymer, with $-\text{NH}_2$ in the molecular chain. There are some sulfonium-based or phosphonium-based cationic polymers but their applications are very limited. Because the majority of minerals are negatively charged in an alkaline flotation pulp, charge neutralization might have a large impact in many cases where cationic polymers are used.

Nonionic polymers contain no ionized group and are relatively more scarce than anionic or cationic polymers. Many natural polymers belong to this group, such as starch, tannin and guar gum. Two of the most common synthetic nonionic polymers used in the mineral industry are polyethylene oxide (PEO) and polyarylamide (PAM). PEO will be described in more detailed in the next section. A truly nonionic PAM does not exist because it tends to be hydrolyzed during the polymerization of acrylamide, rendering them slightly anionic (Vorchheimer,

1981). Most synthetic flocculants in the minerals industry are based on PAM, for example, PAM that is copolymerized with salts of acrylic acid (anionic PAM), and PAM that is copolymerized with unsaturated amines (cationic PAM).

2.5.3.2 Non-adsorption polymers: depletion effects

If the added polymer does not adsorb on the solid surfaces, at sufficiently high dosages the polymers can cause “depletion effects” which can either be “depletion flocculation”, or “depletion stabilization”. Since the polymer chains do not adsorb on the solid surface, when the two solid surfaces approach each other, the polymers are expelled from the region between the surfaces. With more polymers outside than inside the region between the surfaces, the osmotic pressure pushes the two particles together (or removes the liquid from the region between the two surfaces). This leads to depletion flocculation (Figure 2.4) (Asakura and Oosawa, 1958; Sieglaff, 1959). However, when polymer concentration is higher, the polymer chains may not be able to diffuse fast enough out of the region between the two approaching particles and hence are compressed into a smaller volume. This would reduce the configurational entropy of the polymer chains and increase the free energy. As a result, a repulsive force rises between the surfaces and leads to depletion stabilization (Feigin and Napper, 1980).

Depletion effects are rare in mineral flotation systems as the added polymers usually adsorb on mineral surfaces. Even if they do not, the dosage used are usually not high enough to cause the depletion effects.

2.6 Selective coagulation and selective flocculation

So far, coagulants and flocculants are mainly used for solid/liquid separation in mineral processing, where all suspended solids are to be aggregated and separated from water. However, with the emergence of the problems associated with fine particle flotation, researchers and plant operators start to turn to selective coagulation or selective flocculation, i.e., only the desired minerals are aggregated

and settled or floated, while other minerals remain dispersed such that selective separation can be achieved.

A number of reports on selective coagulation and selective flocculation can be found from open literature, for example, the selective coagulation of chromite from serpentine by adjusting particle zeta potential (Akdemir and Hicyilmaz, 1998); the selective coagulation of chalcopyrite from pyrite using acidithiobacillus group bacteria (Akdemir and Hicyilmaz, 1998); the selective flocculation of tribasic calcium phosphate from its mixtures with quartz using polyacrylic acid (Pradip and Moudgil, 1991); the selective flocculation of dolomite from apatite using polyacrylic acid (Mathur et al., 1996); the selective flocculation of hematite from quartz using hydrolyzed polyacrylamide (Jin et al., 1987), and so on. However, most of the investigations were conducted on synthetic mixtures of mineral particles, and the industrial application is very limited. The successful case reported so far might only be the Tilden Mine, where starch selectively flocculates iron oxide minerals from the iron ore and gangue minerals are then floated away (Villar and Dawe, 1975; Colombo, 1986).

Selective flocculation can be difficult to achieve due to the following reasons:

- 1) The interaction between organic polymers and minerals, mostly hydrogen bonding, is not as selective as that of inorganic reagents, such as collectors (Somasundaran, 1980).
- 2) The ores are much more complex and normally consist of as many as 20 different types of minerals. Furthermore, the comminution operation makes the particle surface chemistry even more complex (Lin et al., 1975; Somasundaran and El-Shall, 1983).

Selective coagulation can also be difficult to achieve. According to Pugh and Kitchener (Pugh and Kitchene, 1971), the prerequisites for selective coagulation are:

- 1) The surface potentials of particle 1 and particle 2 should be the same sign to prevent their hetero-coagulation.
- 2) The coagulation rate of particles 1-1 should be much faster than that of 1-2 and 2-2.

Ideally, selective coagulation can be achieved by adjusting either the van der Waals forces, and/or the electric double layer forces. However, it is not possible to adjust the van der Waals forces for a fixed system as the Hamaker constants and particle sizes are all fixed. Therefore, it is only possible to adjust the electric double layer interactions. But to meet the above prerequisites, the surface potential of particle 1 should be of small magnitude to achieve fast coagulation rate, while the surface potential of particle 2 should be high to prevent fast coagulation but not too high – otherwise it can induce hetero-coagulation with particle 1. Such requirements are too sensitive to be met.

2.7 Polyethylene oxide (PEO)

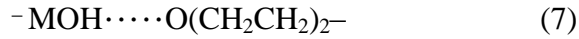
Polyethylene oxide, with a general chemical formula $\text{HO}-(\text{CH}_2\text{CH}_2\text{O})_n-\text{H}$, is a thermoplastic polymer. At room temperature and pressure it is in crystalline form but soluble in water. Its molecular weights range from as low as a few hundred to several million. Products with low molecular weights are commonly referred to as poly(ethylene glycol) (PEG) and those with high molecular weight are known as polyethylene oxide or as polyoxyethylene. PEO solids have a monoclinic crystalline structure with lattice parameters $a = 8.16 \text{ \AA}$, $b = 12.99 \text{ \AA}$, $c = 19.3 \text{ \AA}$ and $\beta = 126^\circ 5'$ and the molecular chains have a helical conformation with two turns in a unit length of c-axis (Tadokoro et al., 1964). In molten state, such conformation disappears but PEO retains the helical conformation when it is dissolved in aqueous solutions (Matsuura and Miyazawa, 1968; Liu and Parsons, 1969; Rabolt et al., 1974). It was suggested that the perfect fitting of PEO molecular chains into water tetrahedral structure accounts for the retaining of the helical conformation and good solubility of PEO in water (Kjellander and Florin,

1981). PEO is completely soluble in water at room temperature in all proportions. The aqueous solution of a high molecular weight PEO appears stringy and shows elastic character at concentrations of less than 1 wt%, and becomes a non tacky, reversible and elastic gel at concentration of up to 20 wt%. At even higher concentrations, the solution turns into a hard, tough, and water-plasticized polymer solution. The solubility of PEO is inversely related to temperature (Bailey et al., 1958; Blueston et al., 1974). Near the boiling point of water, PEO precipitates and the solution becomes cloudy.

In addition to its extraordinary water solubility, PEO also possesses other desirable properties such as low toxicity, blood compatibility, thermoplasticity, drag reduction, complexation with organic acids, etc. Therefore, PEO has found widespread applications in many fields (Back and Schmitt, 2000). In this work, the flocculation property of the high molecular weight PEO was utilized. As a flocculant, PEO has been used in conjunction with cofactors as retention system in the paper industry since the middle of 1980s (Braun and Ehms, 1984; Yeung and Pelton, 1996; Kratochvil et al., 1999; Laivins et al., 2001). In the minerals industry, PEO is not a commonly used flocculant but it has attracted more and more interest in recent years as it has demonstrated better flocculation performance than conventional polymers/flocculants (e.g., polyacrylamide) (Koksal et al., 1990; Sworska et al., 2000; Mpofu et al., 2004). For example, in the 1980s, the US Bureau of Mines developed a dewatering technique, involving flocculation by high-molecular weight PEO, which facilitates disposal of phosphatic clay wastes (Smelley and Scheiner, 1980). At the same time, research on the flocculation mechanisms of PEO is also very active. It is generally accepted that, like other long molecular chain flocculants, PEO flocculates particles through bridging, with individual molecular chains adsorbing onto several particles simultaneously (Swenson et al., 1998; Smalley et al., 2001).

The adsorption of PEO on particle surfaces has been proposed to occur through one or more of the following interactions:

- 1) Hydrogen-bonding between the ether oxygen of PEO and the hydroxyl groups on solid surface. The two lone pairs of electrons in the outer orbital of the ether oxygen act as electron donors while the hydroxyl groups as electron acceptors to form the hydrogen bond.



It is also proposed that the isolated hydroxyl groups on silica surface, i.e., silanol groups, are better sites to form hydrogen bonds with PEO than other surface hydroxyl groups (Rubio and Kitchener, 1976). Mathur and Moudgil further suggested that the hydrogen bonds can be thought of as an acid-base interaction so that the interaction strength depends on the acidity of the hydroxyl group (since it is an electron acceptor, or Lewis acid). The acidity of the hydroxyl groups in turn depends on the electronegativity of the surface metal atom, i.e., the capability of the metal atom to donate electron pairs to the attached oxygen in the hydroxyl groups. When the metal atom is less electronegative (or more electropositive), a stronger ionic bond will form between the metal atom and the oxygen, which means that the electron pairs are concentrated more towards the oxygen. As a result, the proton (H^+) in the hydroxyl group is more tightly bound to the oxygen, i.e., the hydroxyl groups are less acidic, and they will interact with the ether oxygen in PEO less strongly. For example, the affinity of a few oxides towards PEO are: $\text{SiO}_2 > \text{Al}_2\text{O}_3 > \text{MgO}$ (Mathur et al., 2000) while the electronegativity sequence is $\text{Si} (1.9) > \text{Al} (1.61) > \text{Mg} (1.31)$.

- 2) Hydrophobic interaction due to the hydrophobicity of the ethylene group - $\text{CH}_2\text{-CH}_2\text{-}$ of PEO. Rubio (1981) observed that PEO flocculated the hydrophobic particles such as talc, graphite and chalcopyrite better than the hydrophilic ones such as rutile, quartz, copper, and silica. He also reported that when the hydrophilic minerals are made hydrophobic, the flocculation caused by the PEO could be promoted. Based on such

observations he proposed that hydrophobic interaction was responsible for PEO adsorption (Rubio, 1981).

- 3) Complexation with phenolic resins, polyarylic acids and polymethacrylic acids through hydrogen bonding. This has been proposed in paper making processes where PEO is used as a retention aid for cofactor (Kratochvil et al., 1999; Lu and Pelton, 2005).

The adsorption of polymer molecular chains on the surfaces of a solid can be divided into three steps: (i) mass transfer to the solid surfaces by diffusion or convection; (ii) attachment to the surface; (iii) chain re-configuration. It was found that in the case of PEO adsorption on silica, the adsorption rate was determined by mass transfer up to 75% of the maximum adsorption density, and saturation was reached within 40 seconds under good flow conditions (Dijt et al., 1990). This means that the two latter steps are rapid, which is probably due to the strong affinity of silica towards PEO.

As mentioned earlier, polymer flocculation takes place when individual polymer molecular chains attach to several particles simultaneously. Therefore those dangling loops and tails, i.e., molecular chain conformation on solid surfaces, play a significant role in polymer flocculation. The hydrodynamic thickness (δ_h) of the adsorbed layer is a commonly measured parameter to study the conformation of the adsorbed polymer chains. Kawaguchi et al. (1984) measured the hydrodynamic thickness of PEO chains adsorbed onto cellulose ester at saturation and observed that it was half the radius of gyration of a free PEO chain in solution, which indicates a flattened conformation of the adsorbed PEO chains. Kawaguchi et al. (1984) also compared the hydrodynamic thickness of PEO chains adsorbed on different solid surfaces and concluded that the stronger interaction between PEO and solid results in more flattened conformation of adsorbed PEO chains (Kawaguchi et al., 1984). Such flattened conformation would have a marked effect on PEO's flocculation performance.

PEO is able to effectively flocculate many minerals but its flocculation efficiency is difficult to control and is subject to many variables, such as molecular weight, concentration, shear history, temperature, polymer solution storage time and its injection method (Killmann et al., 1986; Brine et al., 1992b; Gibbs and Pelton, 1999; Bednar et al., 2004). This is probably one of the reasons that PEO is not widely used in industry. Kratochvil et al. (Kratochvil et al., 1999) attributed good PEO-induced flocculation to the presence of entanglements of PEO molecular chains. In freshly dissolved PEO solutions, PEO molecular chains are present in the form of entanglements such that good flocculation can be achieved. Any factor which causes disentanglement, such as aging, dilution or high intensity stirring and long stirring time during PEO dissolution, leads to deteriorated flocculation performance. This entanglement hypothesis indeed shed some light on the effects of PEO solution preparation methods on PEO-induced flocculation. Van de Ven et al. (2004) attributed the worsened flocculation performance to a reduction of entanglement sizes to below the thickness of the electrical double layer surrounding the particles. However, according to their earlier paper on PEO solution properties (Polverari and vandeVen, 1996), the thermodynamically stable clusters, which are thought to be the smallest entanglements, were as large as 450 nm. The thickness of the electrical double layer is normally about 10-20 nm even in a very dilute electrolyte (Hiemenz and Rajagopalan, 1997). Therefore, it is not likely that the sizes of the entanglements would be smaller than the thickness of the electrical double layer even considering flattening of the PEO entanglements after their adsorption on the solid surfaces. Clearly, more studies are needed to understand the mechanisms of flocculation induced by PEO.

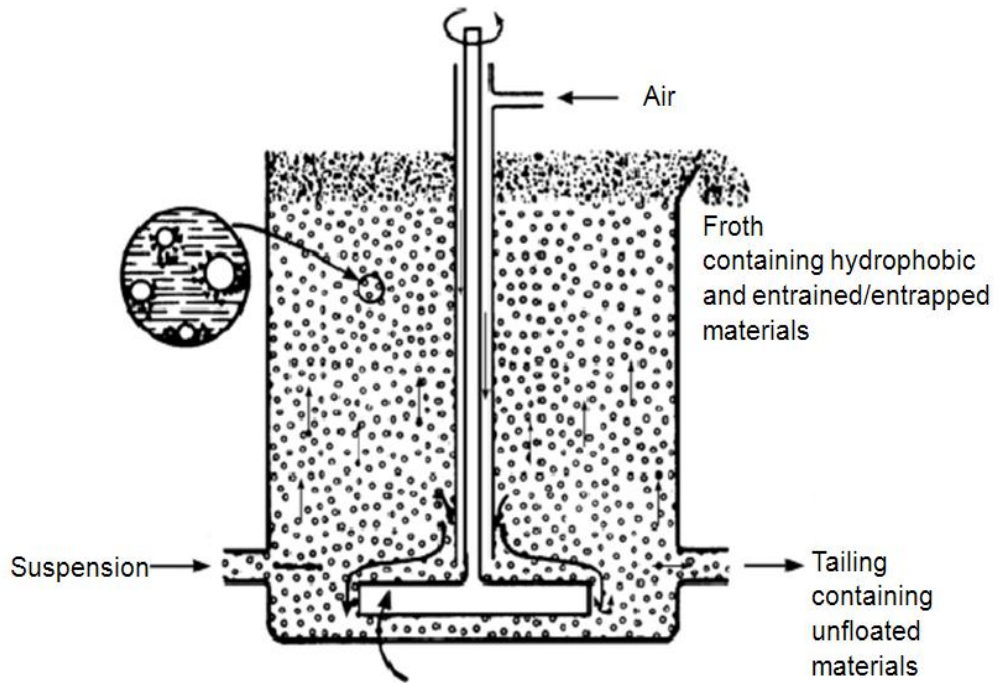


Figure 2.1 Schematic diagram of the flotation process in a froth flotation cell.
(Jiang et al., 2006)

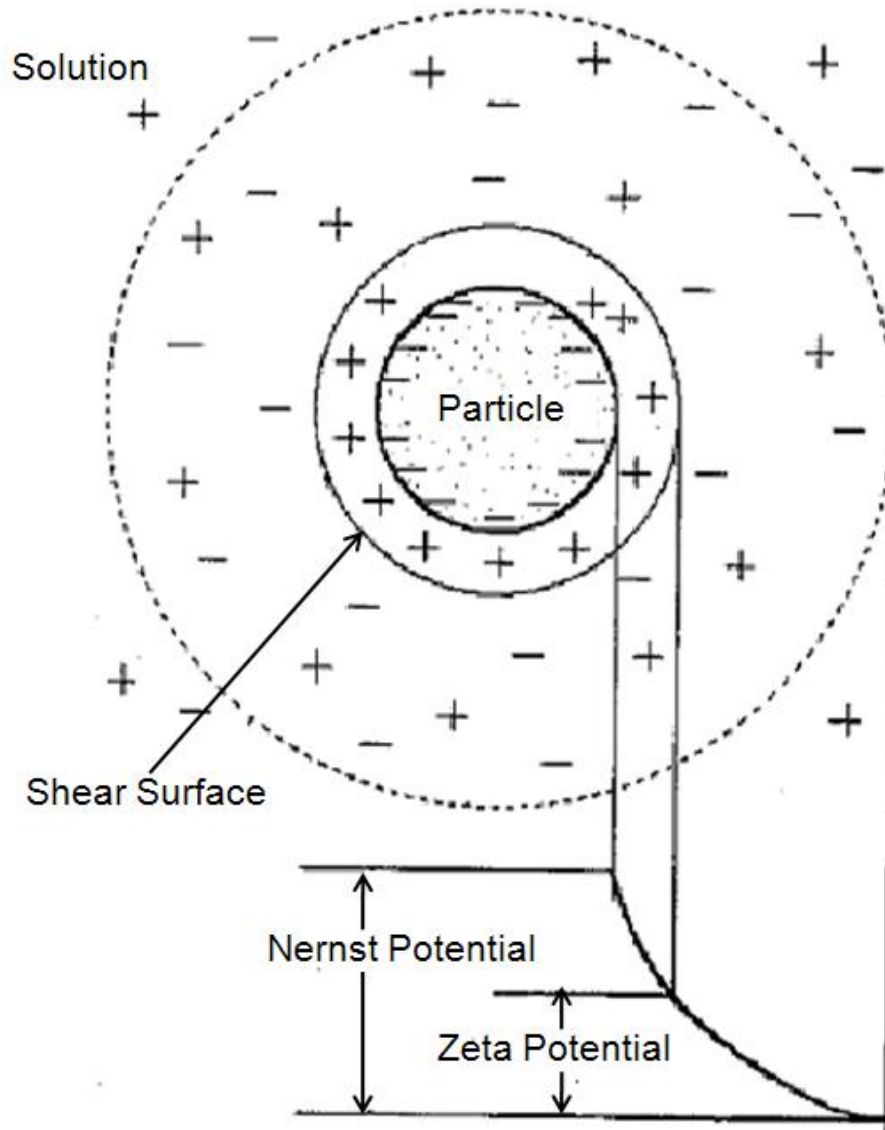


Figure 2.2 Schematic diagram of an electrical double layer around a charged spherical particle.

(from Nguyen and Schulze, 2004, page 325, with modification)

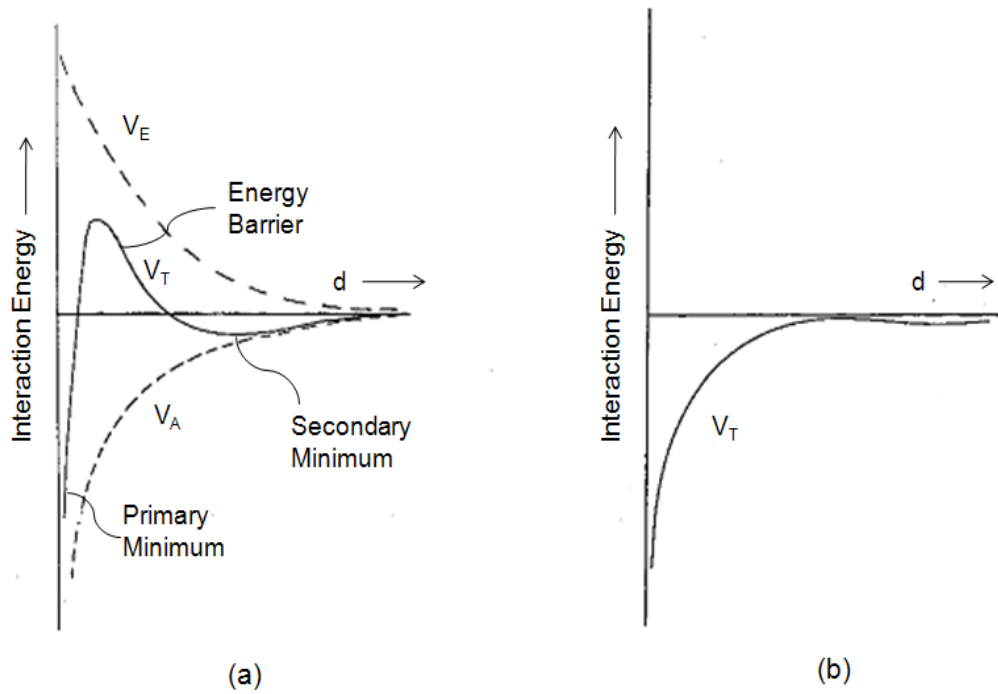


Figure 2.3 Schematic energy versus separation distance profiles of DLVO interaction.

V_E , electrical repulsion, V_T , total energy, V_A , van der Waals attraction.

(Gregory, 1989)

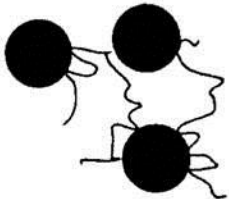
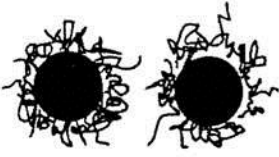
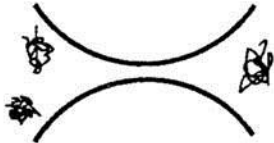
	Attraction	Repulsion
Adsorbing polymer	<p>Bridging flocculation</p> 	<p>Steric stabilization</p> 
Nonadsorbing polymer	 <p>Depletion flocculation</p>	 <p>Depletion stabilization</p>

Figure 2.4 Schematic illustration of destabilization/stabilization by polymers.
 (Nguyen and Schulze, 2004, page 375, with modification)

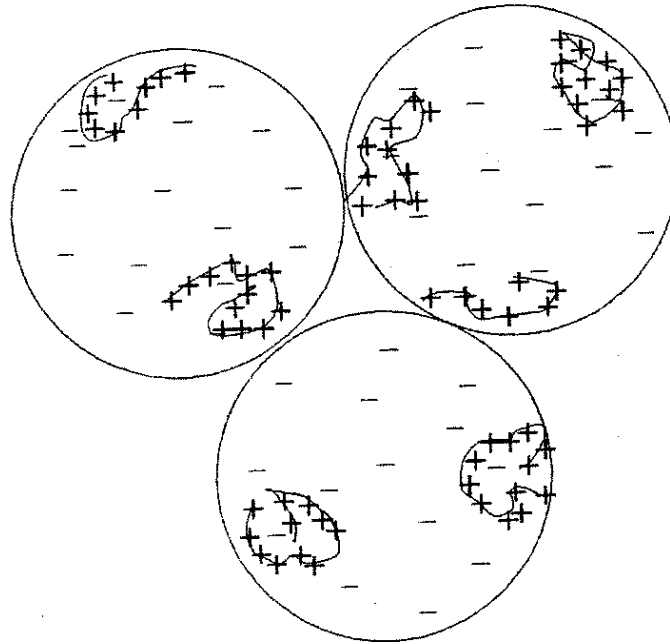


Figure 2.5 Electrostatic patch model of polymer adsorption leading to flocculation.

(Gregory, 1973)

Chapter III Objectives and Scope of This Research

This research project addresses the problem of non-sulfide gangue entrainment in the flotation of fine and ultrafine sulfide minerals. More specifically, the fine and ultrafine non-sulfide gangue minerals, particularly quartz, will be selectively flocculated and depressed by a suitable polymer such as polyethylene oxide (PEO), while the sulfide mineral (chalcopyrite) is floated by a thiol collector such as xanthate.

The effectiveness of the polymeric depressants such as polyethylene oxide will be studied by small-scale and batch flotation tests on both high purity single minerals, mineral mixtures and commercial sulfide ore samples, as well as aggregation/dispersion measurements of the mineral suspensions and studies of the interaction mechanisms of the polyethylene oxide and mineral surfaces. Sulfide mineral recovery and concentrate grade will be the primary criteria to be used to assess the effectiveness of the polymeric depressants.

The mechanisms by which the polymeric depressants (polyethylene oxide) function in the sulfide mineral flotation system will also be studied. These include the adsorption mechanisms of the polyethylene oxide on the mineral surface, the effect of polymer solution preparation methods on its flocculation performance, and the possible side effects of the polyethylene oxide in the investigated sulfide flotation system.

Chapter IV Effect of PEO on Quartz Entrainment during Sulfide Mineral Flotation

4.1 Introduction

As discussed in the literature review, polyethylene oxide (PEO) is able to flocculate quartz particles. And this is the reason why PEO is chosen as the flocculant for quartz particles in this research. It is expected to reduce quartz entrainment in sulfide mineral flotation. In order to test its effect on reducing quartz entrainment, PEO was applied to a series of batch flotation on pure quartz particles, synthetic quartz-chalcopyrite mixtures and a commercial Au-Cu sulfide ore sample. The flotation results are presented in this chapter.

4.2 Experimental

4.2.1 Materials and chemicals

A quartz single mineral sample was obtained from Iron Ore Company of Canada. X-ray fluorescence (XRF) analysis indicated that it contains 99.9% SiO₂. A chalcopyrite single mineral sample, originated from Durango, Mexico, was purchased from Ward's Natural Sciences. Inductively coupled plasma mass spectrometric (ICP-MS) analysis showed that it contains 31.8% Cu, 27.9% Fe and 39.4% S, representing a purity of 91.8% CuFeS₂. The quartz and chalcopyrite single mineral samples were separately crushed to collect the -3.2+0.6 mm particles to use in batch grind-flotation tests, where they were ground together.

A commercial Au-Cu sulfide ore sample was taken from one of the member mining companies of COREM, Quebec, Canada, from the SAG mill discharge point. The sample has a prevailing particle size of about 1 mm, and contains chalcopyrite as the value mineral. Au was associated with the chalcopyrite. The ore sample assayed 0.37 g/t Au, 0.07% Cu, 4.82% Fe and 32.2% Si. The collected

sample was air-dried, riffled into 1 kg batches and stored in a freezer in individual sealed plastic bags.

Two polyethylene oxide (PEO) reagents, with molecular weights of 1 million and 8 million, respectively, were obtained from Polysciences, Inc. Fresh stock solutions of PEO was prepared at a concentration of either 0.5% or 1% daily to eliminate the effect of solution aging (Kratochvil et al., 1999). Potassium amyl xanthate (KAX) and sodium isopropyl xanthate (NaIPX) were used as collectors for the sulfide minerals and were obtained from Charles Tennant & Company Ltd and Cytec Industries, respectively. Both xanthate reagents were purified by following the procedure described by Dewitt and Roper (DeWitt and Roper, 1932). Dowfroth 250 (DF250) and F-150 were obtained from Charles Tennant & Company and used as frothers.

Other common chemical reagents used in the experiment, such as sodium hydroxide and hydrochloric acid, etc., were purchased from Fisher Scientific. They were used directly without further purification.

4.2.2 Batch flotation tests

Batch flotation tests on quartz single mineral and synthetic mixtures of chalcopyrite and quartz were conducted in COREM labs, using a Denver laboratory flotation machine in a 1.25 L cell as shown in Figure 4.1. Prior to flotation, 100 g of quartz or a mixture of 100 g quartz and 20 g chalcopyrite were ground with 150 mL of demineralized water in a zircon pebble mill to 80% passing 20 μm . Mill discharge was transferred to the 1.25 L flotation cell and conditioned with PEO (molecular weight = 1 million, various dosages), NaIPX (60 g/t) and DF250 (100 g/t) for 2 minutes with each reagent addition at 1200 rpm of agitation. Lime (CaO) was used to adjust pulp pH to 11 in the grinding mill and to 9 in the flotation cell. The flotation froth was scraped every 10 seconds and four rougher concentrates were collected at 0.5, 2, 4 and 8 min, and analyzed

separately. Another 50 g/t DF250 was added before the fourth collection to compensate the scraped frother. Most of the reagents used in the flotation were prepared as solutions, PEO as 0.05%, NaIPX as 0.1% and DF250 as 0.5% solutions.

Batch flotation tests on the Au-Cu sulfide ore sample were conducted in a laboratory Wemco flotation machine with a 2 L flotation cell at the University of Alberta, as shown in Figure 4.2. Prior to flotation, 1 kg of the ore sample was ground with 700 mL of Edmonton tap water in a mild steel ball mill to 80% passing 75 μm . The ground slurry was transferred to the 2 L flotation cell, conditioned for 3 minutes with lime addition to a pH of 10, another 3 minutes with PEO (molecular weight = 8 million) (if used), and finally with KAX for 3 minutes. This was followed by two stages of flotation (2 minutes for the first stage and 3 minutes for the second stage). Frother was added before both flotation stages. In the base flotation test where no PEO was used, 3 mL 0.1% F-150 solution was added before both stages. In the other five flotation tests where PEO was added, only one used F-150 as the frother and others used PEO as a frother. But the amount used is the same, 3 mL for the first stage and 2 mL for the second stage. PEO solution was prepared at the same concentration (0.1%) as F-150.

4.3 Results and discussion

4.3.1 Batch flotation of pure quartz particles

Batch flotation tests were first carried out on pure quartz. In these tests, 100 grams of quartz particles were ground to 80% passing 20 μm in a laboratory zircon pebble mill and floated in a 1.25 L flotation cell with the addition of 60 g/t NaIPX, 150 g/t of a frother (DF250) and varying dosages of PEO (molecular weight = 1 million) at about 6 wt% solids. Since no collector for quartz was used, quartz recovery in these tests was considered purely a result of entrainment. Figure 4.3 shows the relationship between quartz recovery and water recovery at different PEO dosages. As can be seen, when no PEO was used, quartz recovery increases

linearly with water recovery, consistent with the observations of other researchers (Trahar, 1981). As discussed in the literature review, the slope of the line, variously called the degree of entrainment or entrainment factor, e_g (Bailey et al., 1958), can be used to indicate the severity of entrainment. When no PEO was used, the degree of entrainment for quartz was 0.7. After adding PEO, the linear relationship remained for low dosages of PEO (less than 100 g/t). However, at high PEO dosages, i.e., 500, 1,000 and 1,500 g/t, the linear relationship only held at low water recoveries of up to about 25%. Furthermore, the degree of entrainment of quartz was reduced at lower PEO dosages and increased at higher PEO dosages. The degree of entrainment was plotted against PEO dosage in Figure 4.4 to show this trend more clearly. It also indicates that there is an optimum dosage for PEO in reducing quartz entrainment. In Figure 4.5 where the cumulative recovery of both water and quartz was plotted as the function of PEO dosage, it can be seen that not only was the quartz recovery affected by the addition of PEO, but also the water recovery. As expected, the reduction of quartz entrainment was likely due to the bridging flocculation of quartz by PEO. But the detrimental effect of PEO at higher dosages and the effect on water recovery are somewhat unexpected. Further study has been carried out and the results are presented in chapter 8.

4.3.2 Batch flotation of synthetic mineral mixture of quartz-chalcopyrite

In order to examine if the addition of PEO can reduce quartz entrainment in the presence of chalcopyrite, batch flotation tests were performed on synthetic quartz-chalcopyrite mineral mixtures (100 g quartz + 20 g chalcopyrite), which were ground together to 80% passing 20 μm . Flotation of the ground slurry was carried out at about 6 wt% solids, using different dosages of PEO (molecular weight = 1 million), and 60 g/t NaIPX which served as a collector for the chalcopyrite. A base flotation test was first carried out where no PEO was added. Figure 4.6 presents the results and shows that quartz entrainment was not affected by the presence of chalcopyrite, with a degree of entrainment e_g of 0.72. Figure 4.7

shows the recovery of chalcopyrite and quartz at various PEO dosages. As can be seen, the quartz entrainment was reduced while the chalcopyrite recovery was improved after adding PEO. The flotation results of the quartz-chalcopyrite mixtures are also presented in the typical recovery-grade plot in Figure 4.8, which shows the beneficial effect of PEO more clearly. It can be seen that the recovery-grade curves moved upward as PEO dosage was increased from 0 to 100 g/t (9.6 mg/L), indicating that the use of PEO resulted in a higher chalcopyrite recovery and higher concentrate grade in the floated concentrate.

4.3.3 Batch flotation of a Au-Cu ore from eastern Canada

Based on the success of the batch flotation on synthetic mixtures of quartz and chalcopyrite, PEO with a molecular weight of 8 million was used to treat a commercial Au-Cu sulfide ore. The ore sample was ground in a mild steel ball mill at 70% solids to 80% passing 75 μm . Two rougher concentrates were collected at a flotation time of 2 min and 3 min, respectively. Six flotation tests were carried out at various PEO dosages. During flotation, it was found that PEO could function as a frother. It is understandable given that PEO is comprised of hydrophobic ethylene (-CH₂CH₂-) group and hydrophilic ether oxygen (-O-). In order to examine the frothing function of PEO, another 5 g/t PEO was added as a frother in four sets of flotation tests instead of the regular frother F-150, after the slurry was conditioned with certain amount of PEO. It turned out that PEO was an excellent frother. Figure 4.9 shows the recovery of Cu from the ore sample as a function of water recovery into froth product. As can be seen, Cu recovery was improved in all flotation tests no matter whether the frother F-150 was used or not. In the meantime, quartz entrainment was reduced after the addition of PEO, as can be seen from Figure 4.10, which shows that the degree of entrainment of quartz was lowered in all cases, except at a total dosage of 50 g/t PEO.

Since Au was associated with the chalcopyrite in the commercial Au-Cu sulfide ore sample, the recovery-grade plots of both value elements were presented in

Figure 4.11 and Figure 4.12, respectively. Both figures clearly show that the use of PEO improved the flotation since the curves moved towards the upper right corner of the quadrant, indicating an increase in both value recovery and grade in the floated concentrate.

Assay results showed that the addition of 10 g/t PEO in the rougher and 5 g/t PEO in the cleaner significantly improved the flotation performance of the Au-Cu ore sample. At a fixed Si content in the flotation concentrate of 22%, the Cu recovery could increase from about 55% (without PEO) to about 70% (with PEO), and the Au recovery could increase from about 68% (without PEO) to about 90% (with PEO).

4.4 Summary

All the batch flotation results, including pure quartz, synthetic quartz-chalcopyrite mixtures and especially a commercial Au-Cu sulfide ore sample, indicated that the use of polyethylene oxide (PEO) could lower quartz entrainment and improve flotation concentrate quality. And it is expected that quartz entrainment was reduced through the flocculation of fine quartz particle induced by PEO. More work has been done to verify this hypothesis and the results are presented in the next chapter.



Figure 4.1 Denver laboratory flotation machine.



Figure 4.2 Wemco laboratory flotation machine.

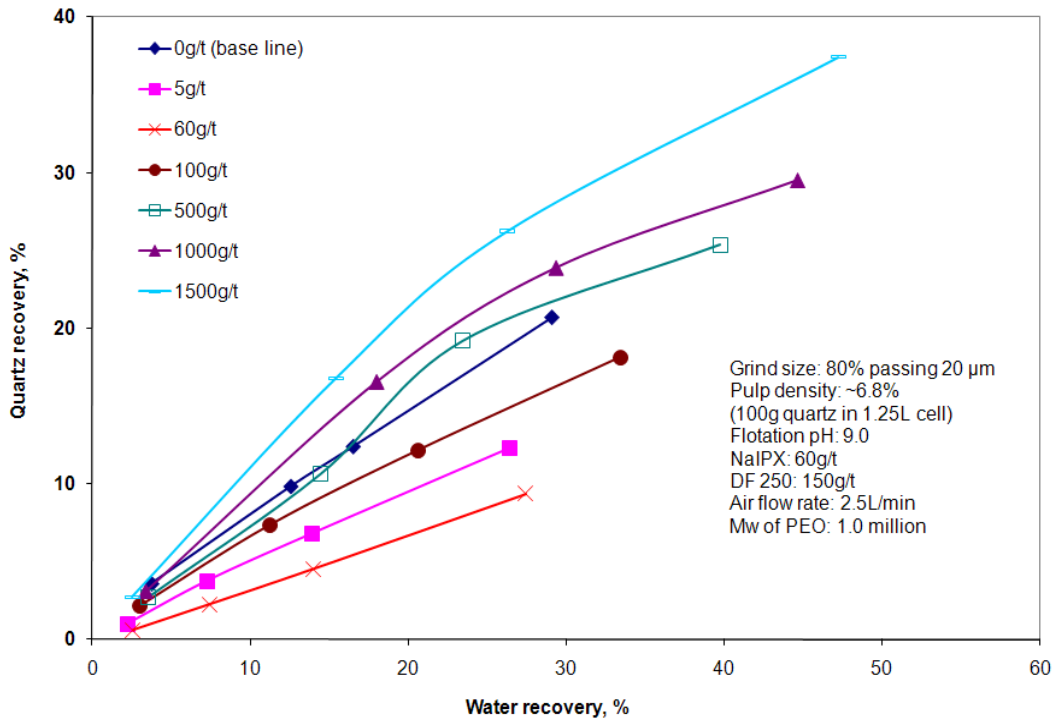


Figure 4.3 Quartz recovery as a function of water recovery in the batch flotation of pure quartz at various PEO dosages.

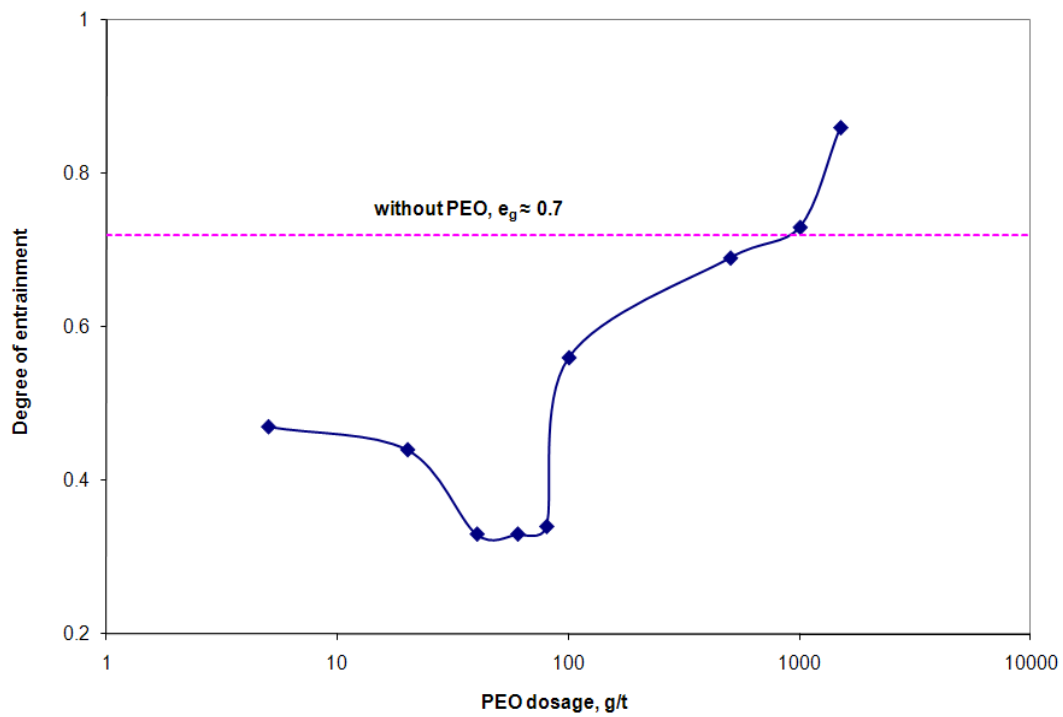


Figure 4.4 Degree of quartz entrainment as a function of PEO dosage in the batch flotation of pure quartz.

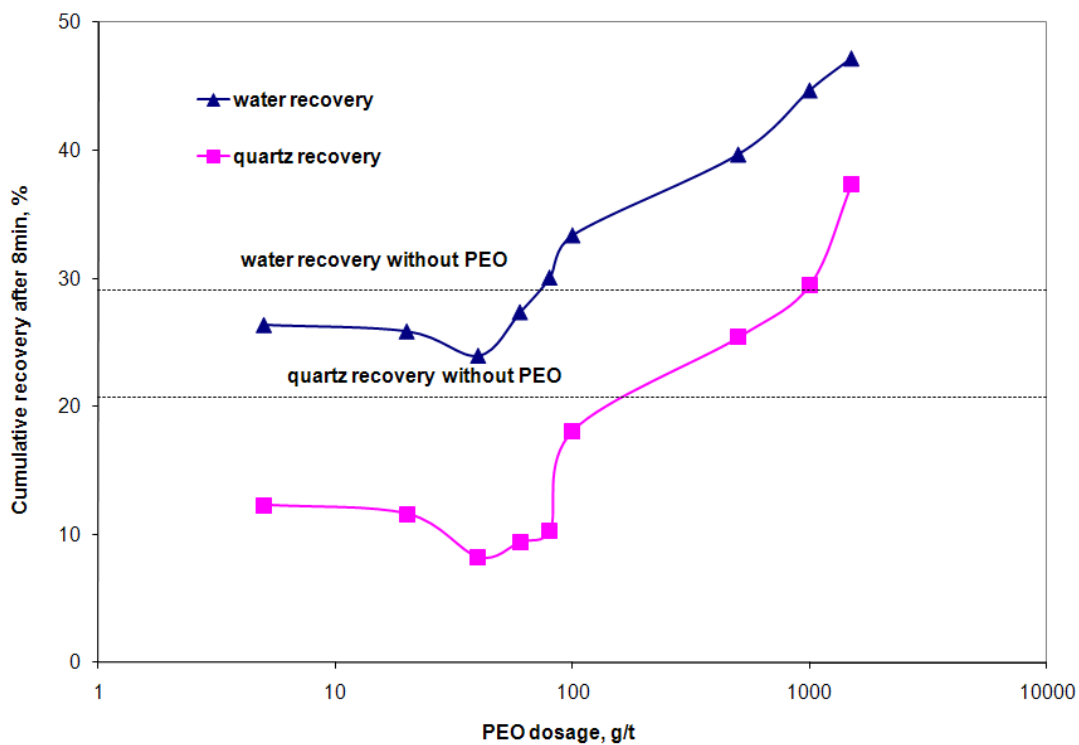


Figure 4.5 Cumulative recovery of water and quartz as a function of PEO dosage in the batch flotation of pure quartz.

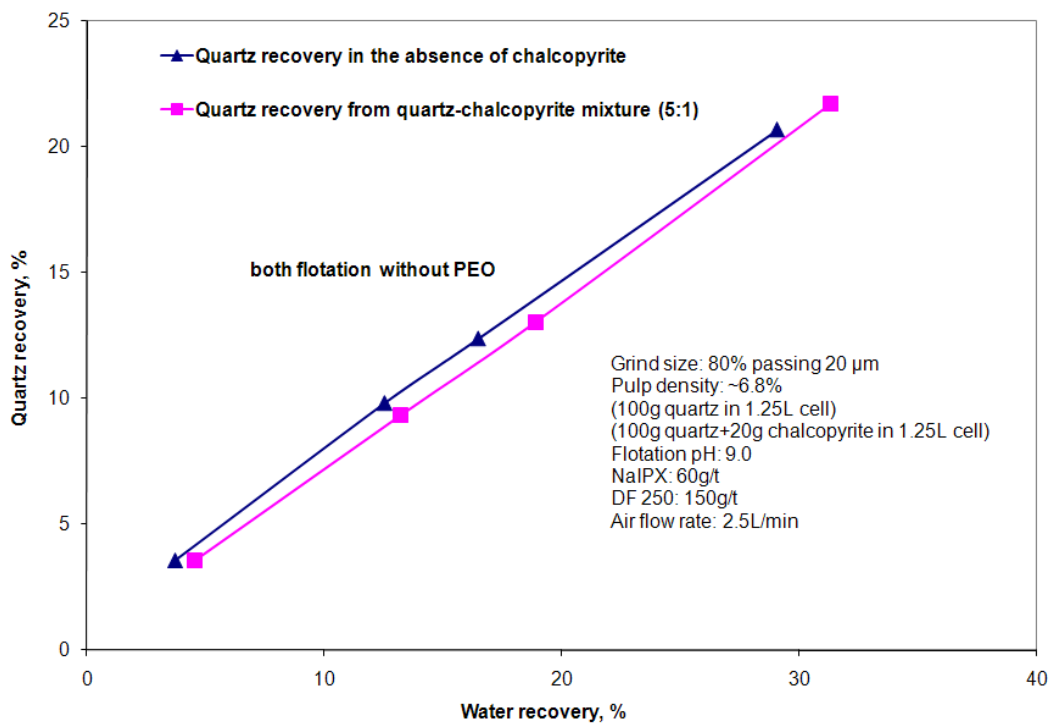


Figure 4.6 Comparison of quartz recovery as a function of water recovery in the batch flotation of pure quartz and synthetic quartz/chalcocopyrite mixture without the use of PEO.

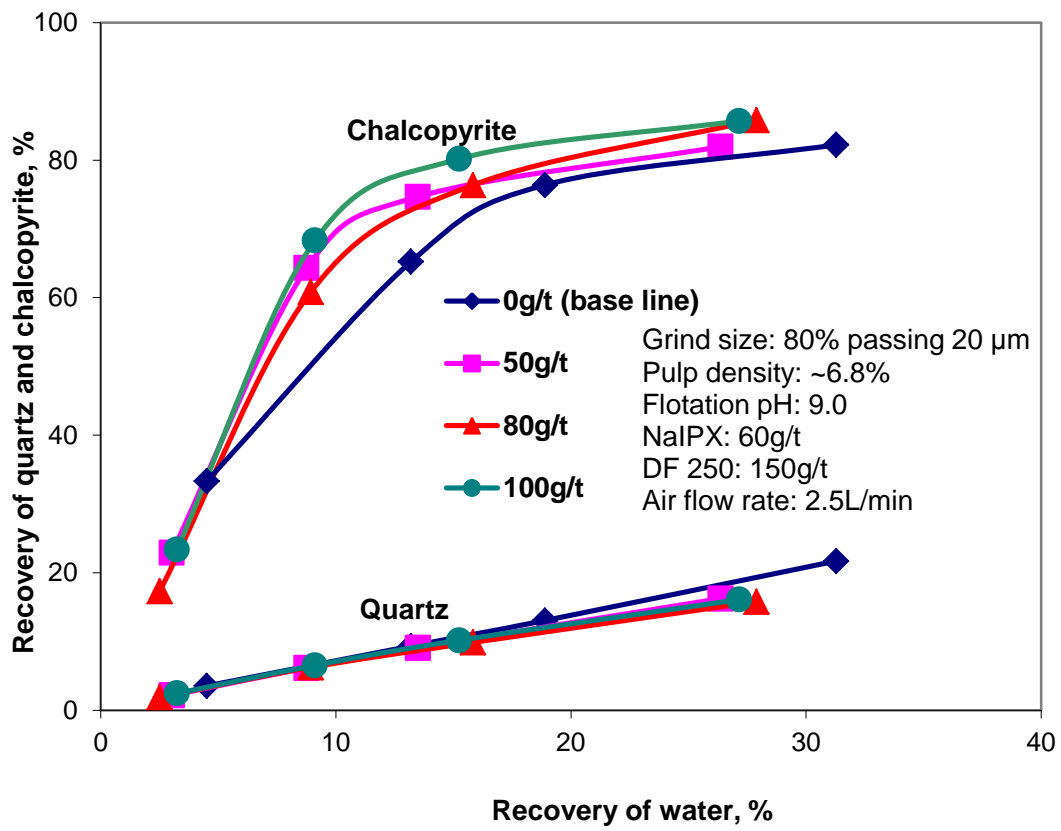


Figure 4.7 Quartz and chalcopyrite recovery as a function of water recovery in the batch flotation of synthetic quartz/chalcopyrite mixture at several PEO dosages.

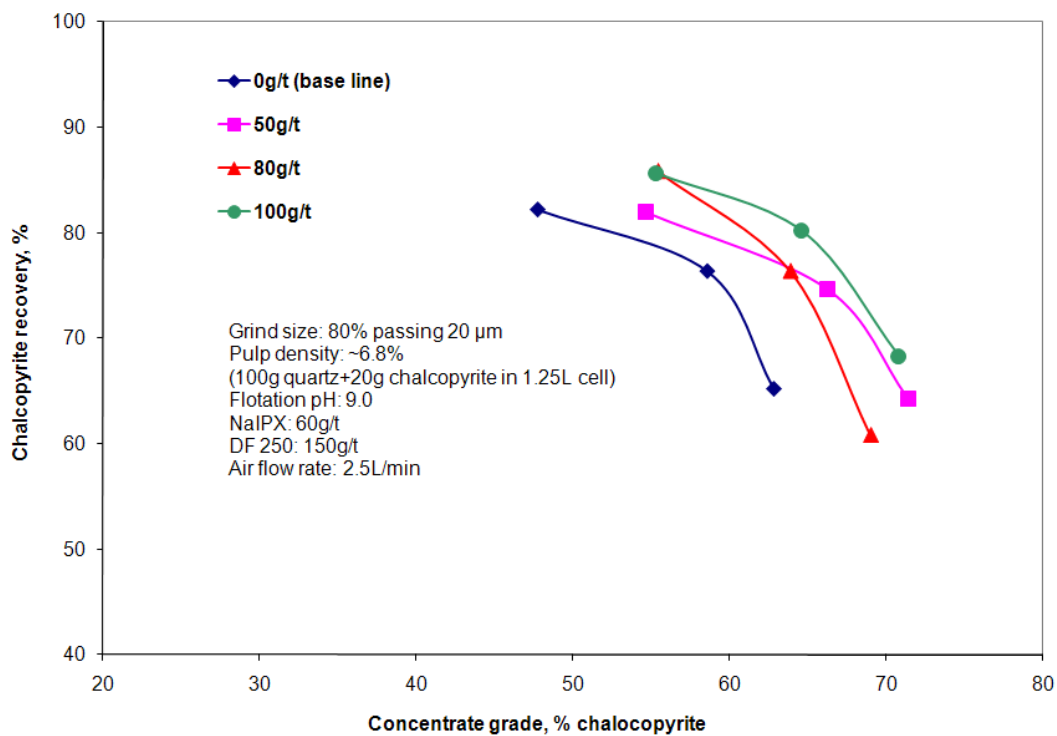


Figure 4.8 Recovery-grade relationship of the batch flotation of synthetic chalcopyrite-quartz mixtures.

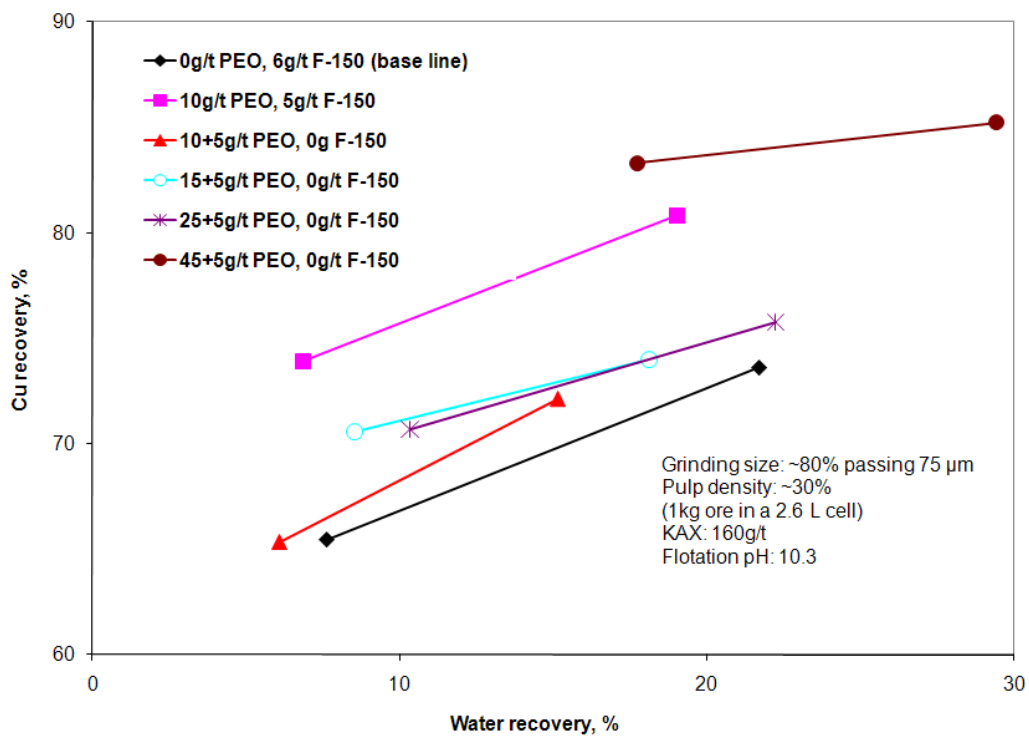


Figure 4.9 Cu recovery as a function of water recovery in the batch flotation of a commercial Au-Cu sulfide ore at several PEO dosages.

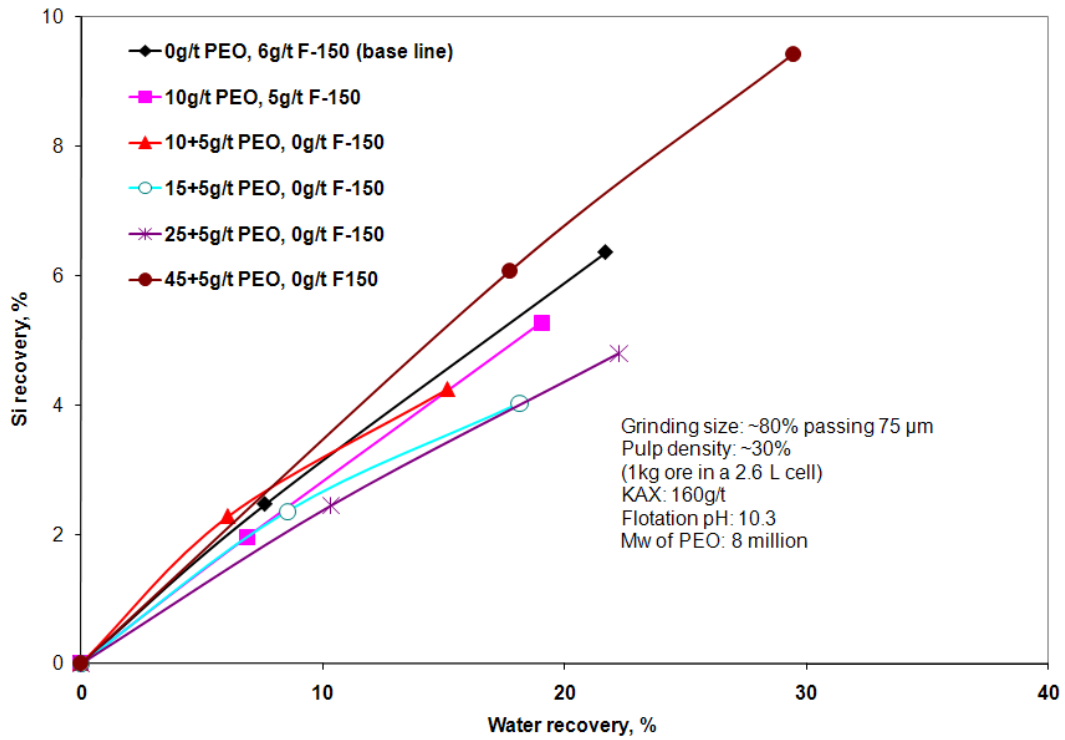


Figure 4.10 Quartz recovery as a function of water recovery in the batch flotation of a commercial Au-Cu sulfide ore at several PEO dosages.

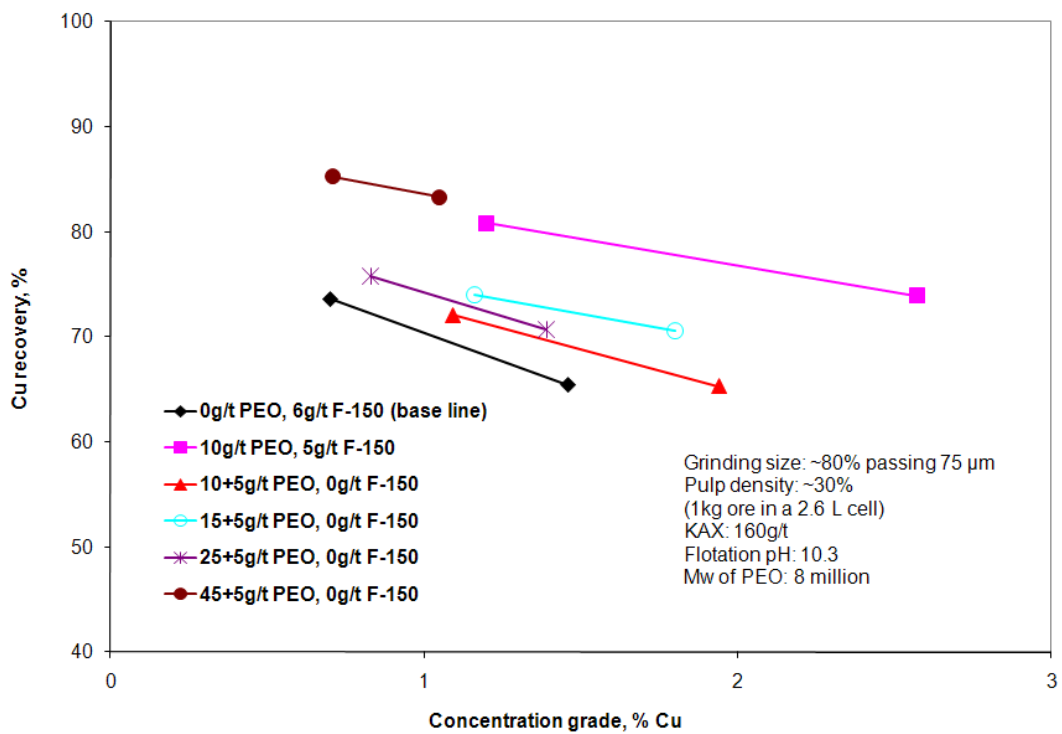


Figure 4.11 Recovery-grade relationship of Cu in the batch flotation of a commercial Au-Cu sulfide ore.

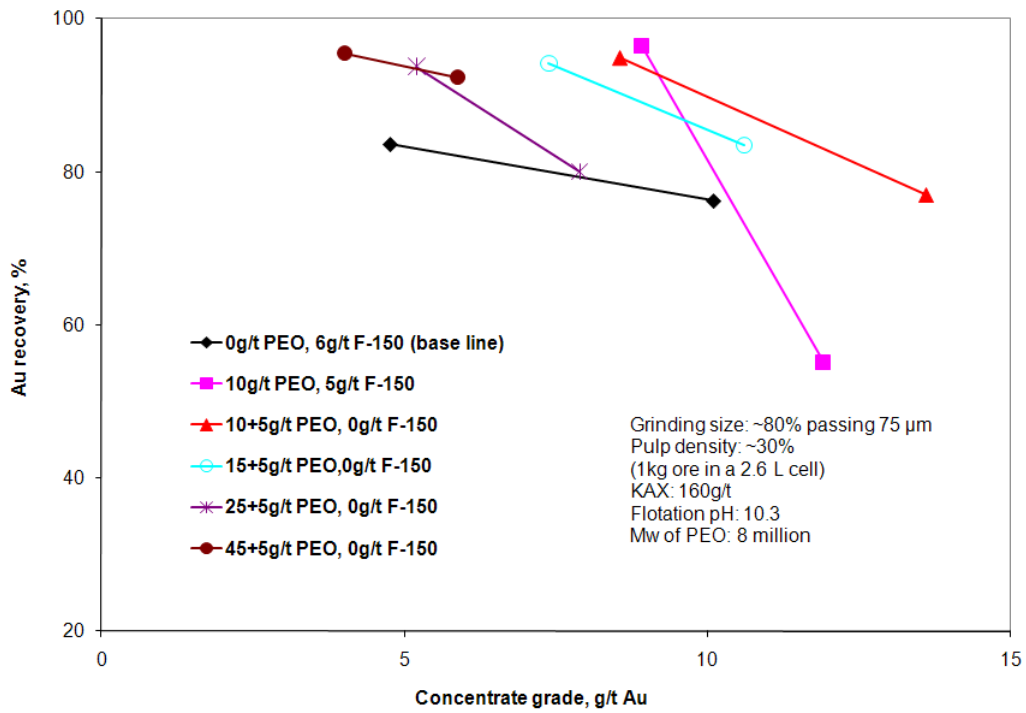


Figure 4.12 Recovery-grade relationship of Au in the batch flotation of a commercial Au-Cu sulfide ore.

Chapter V Flocculation of Quartz and Chalcopyrite by Polyethylene Oxide and Potassium Amyl Xanthate

5.1 Introduction

The previous chapter has shown that polyethylene oxide (PEO) can lower quartz entrainment in batch flotation of synthetic quartz-chalcopyrite mixtures and a commercial Au-Cu sulfide ore sample. And it is thought to be achieved through the flocculation of quartz particles induced by PEO. This correlates well with the concept mentioned in the literature review that fine gangue particles entrainment can be reduced by enlarging their sizes. In order to confirm the correlation, the flocculation behavior of quartz-chalcopyrite mixtures in the presence of PEO was studied using a Photometric Dispersion Analyzer (PDA 2000). Since potassium amyl xanthate (KAX) is the collector used in the flotation, its effect on the flocculation was studied as well.

5.2 Experimental

5.2.1 Materials and chemicals

A quartz single mineral sample, originated from Hot Springs, Arkansas, USA, was purchased from Ward's Natural Sciences. A chalcopyrite single mineral sample, originated from Durango, Mexico, was purchased from Ward's Natural Sciences. The quartz and chalcopyrite single mineral samples were separately crushed to collect the -3.2+0.6 mm particles, which were dry ground in a mechanized agate mortar and pestle grinder manufactured by Fritsch GmbH. The ground mineral particles were screened and the -20 μm size fraction was collected.

The chemicals used in flocculation tests were the same as in batch flotation (Chapter 4) and were described in section 4.2.1, except that sodium hydroxide was used to adjust pH of the particle suspension instead of lime.

5.2.2 Flocculation/dispersion measurements

The degree of flocculation or dispersion of mineral suspension was measured by a Photometric Dispersion Analyzer (PDA 2000) manufactured by Rank Brothers Inc, as shown in Figure 5.1. Photometric dispersion analysis is a sensitive technique developed to monitor the aggregation state of particle suspensions by Gregory and Nelson (1986). Compared to the traditional settling tests, it has the advantage of providing information about the change in the aggregation or dispersion state of the suspended particles, such as initial aggregation, floc growth, floc breakage and re-aggregation, etc., in real-time. It has been widely used by many researchers (Gregory and Carlson, 2003; Hopkins and Ducoste, 2003; Jin et al., 2007).

Its principle has been described in detail by (Ching et al., 1994; Gregory and Nelson, 1985). The PDA measures the intensity of light transmitted through a flowing suspension by a photodiode. For a well-agitated suspension, there is a small fluctuation in the intensity of the transmitted light due to the random variation in the composition of the slurry flowing through the path of the light beam. Therefore, the output of the light intensity can be divided into two components, a large mean value (DC) and a small fluctuating value (AC). The DC value corresponds to the average transmitted light intensity and depends on the turbidity of the flowing suspension. Compared to the DC value, the AC value is very small and can be amplified by a desired factor. The root mean square (RMS) of the AC value is then derived and divided by the DC value. The result is reported as a “Ratio” reading. The Ratio value is very sensitive to the concentration and size of the suspended particles. When aggregation occurs, the Ratio value increases. Conversely, when the suspension becomes more dispersed, the Ratio reading decreases. Therefore, the relative change in “Ratio” value is a sensitive indicator of the aggregation or dispersion state of the suspension.

In each test, certain amount of minerals (-20 μm) and water were agitated using a magnetic stirrer in a 250 mL beaker and circulated through the flow cell of the

PDA 2000 using a peristaltic pump. The stirring bar was 51 mm long and the stirring speed was fixed at 330 rpm. The Ratio output as the function of time was recorded by a computer connected to the PDA 2000. In such a way, the flocculation/dispersion state of the suspension was monitored in real time.

5.2.3 Microscope observation

The aggregation states of the particle suspensions were also observed using an optical microscope (Axiovert 100; Carl Zeiss Canada), which was connected to a video system (CCD camera and a monitor) so that microphotographs of the particle suspensions could be taken (Figure 5.2). Particle suspensions were prepared and conditioned with reagents the same way as in the above flocculation tests, except that the amount of reagents was different. A small amount of suspension was taken out at certain points along the flocculation procedure and placed in a Petri dish which held some distilled water such that the suspension could be diluted and single floc or particle could be observed.

5.2.4 SEM/EDS observations

A JEOL 6301F SEM scanning electron microscope (SEM) coupled with an energy dispersive X-ray spectrometer (EDS) was used to examine the quartz-chalcopyrite flocs. This instrument is equipped with a PGT (Princeton Gamma-Tech) IMIX digital imaging system, a solid state silicon backscattered electron detector and a liquid nitrogen cooled silicon (lithium) detector for energy dispersive X-ray analysis. Since all the constituent elements in chalcopyrite (Cu, Fe and S) have higher atomic weights than those in quartz (Si and O), chalcopyrite particles can scatter more electrons and hence appear much brighter than quartz particles in SEM images, especially back-scattered electron images. EDS also showed that the brighter spots are mostly comprised of Cu, Fe and S, indicating that they are CuFeS_2 while the majority of the gray spots are Si and O, i.e., SiO_2 .

To prepare a SEM sample, chalcopyrite and quartz were mixed in 250 mL beakers into a 10% solids suspension, at a ratio of 10% chalcopyrite and 90% quartz. The suspension was agitated using a magnetic stirrer and the pH was adjusted to 9. Two parallel tests were conducted: one with only PEO addition, and the other with KAX addition 3 minutes after PEO. Small slurry samples were taken from the beakers at 1 minute and 15 minutes after PEO addition (the 15 minute samples may have also been treated by KAX). All slurry samples were diluted 20 times with distilled water and small amount of the diluted suspension (two or three drops) was then deposited on the SEM sample stand such that the flocs would be well separated and would not overlap with each other after being dried in air. The dried samples were coated with chromium for conductivity before placed into the SEM sample chamber.

5.3 Results

5.3.1 Flocculation of 1:1 quartz-chalcopyrite mixtures

The first set of PDA measurements was carried out on suspensions of chalcopyrite and quartz mixtures (50 wt% quartz and 50 wt% chalcopyrite). The suspension was prepared at 1 wt% solids and pH 9, and was agitated with a magnetic stir bar (51 mm long) at 330 rpm while being circulated through the PDA 2000 photometric dispersion analyzer. Three tests were conducted. In the first test, only PEO (molecular weight = 8 million) was added (to a final concentration of 10 mg/L). In the next two tests, KAX (300 mg/L) was added 3 minutes before or after the addition of PEO, while the Ratio output was continuously monitored. The results are presented in Figure 5.3, where the points of PEO and KAX additions were noted.

As can be seen from Figure 5.3, in all tests, the addition of PEO caused an immediate increase in the Ratio value by about 5 times, indicating that the particles were flocculated by PEO. A typical SEM image of the suspension,

shown in Figure 5.4, confirms the presence of large flocs and it also shows that chalcopyrite and quartz particles formed hetero-flocs.

Figure 5.3 shows that after reaching a maximum value, the Ratio reading in all three tests started to drop quickly. This means that the flocs were not strong and they were easy to break by the mechanical forces such as magnetic stirring and the peristaltic pumping. The rate at which the Ratio value drops can be taken as an indication of the breakage rate of the flocs. Since the initial part of the dropping segment of the curve appeared to be linear, the slope of that segment was calculated to indicate the dropping rate of the Ratio reading.

The upper curve in Figure 5.3 represents the case where only PEO was added and its slope in the initial dropping segment is -0.49 min^{-1} . The middle curve represents the test where KAX was added 3 minutes after PEO. In this case the slope increases to -0.66 min^{-1} , indicating a faster floc breakage with the addition of KAX. When KAX was added 3 minutes before PEO, the Ratio reading increased from 1 to about 2.2 immediately following the KAX addition. This increase was most likely caused by the aggregation of the chalcopyrite due to its surface hydrophobicity induced by the adsorption of KAX. Subsequent addition of PEO 3 minutes later resulted in a further increase of the Ratio reading from about 2.2 to about 5, followed by a sharp drop. In fact, the slope of the dropping segment of the Ratio curve in this case was the highest (-0.95 min^{-1}).

The above PDA measurement results reveal that PEO caused unselective hetero-aggregation of the quartz and chalcopyrite particles. The flocs were not strong and tend to break as a result of magnetic stirring and peristaltic pumping. The addition of KAX accelerated the breakage of these hetero-aggregates, especially when KAX was added ahead of PEO.

Microscopic pictures show the effect of KAX on the flocs more directly. Figure 5.5 represents the images of flocs taken from four parallel flocculation tests that

were conducted in four 250 mL beakers. PEO was added to induce flocculation in all tests but various amount of KAX was added three minutes after PEO addition. The flocs were taken out from the beakers 9 minutes after PEO was added. As can be seen in Figure 5.5a where no KAX was added, the flocs are still large while in the other images where KAX was added, the flocs appeared smaller as the amount of KAX increased. In Figure 5.5d where 6 g/L KAX was added, the particles were almost fully dispersed again.

5.3.2 Flocculation of quartz and chalcopyrite single minerals

To examine the role that KAX played in the quartz-chalcopyrite mixture system, its effect on quartz and chalcopyrite single mineral flocculation was studied. The test procedures were the same as above except that only quartz or chalcopyrite was used in each test. Figure 5.6 shows the results of pure quartz particle suspension at about 5 wt% solids (i.e., about 5 times more concentrated than the quartz-chalcopyrite mixture tests) at pH 9. As can be seen, when only KAX was added, there was no change in the Ratio reading. This is understandable as xanthate is known to have no interaction with quartz. However, when PEO was added to a concentration of 10 mg/L, there was an abrupt increase in the Ratio reading from nearly zero to close to 13 (the much higher Ratio value was probably due to the higher particle concentration). The quartz was flocculated by the PEO. These flocs were not stable, and the Ratio reading dropped quickly after reaching the maximum. Adding KAX after PEO did not seem to have caused any difference in the Ratio reading. Therefore, it can be concluded that KAX has no effect on quartz particle flocculation by PEO.

However, as can be seen from Figure 5.7, the phenomenon was very different in the chalcopyrite single mineral system. With the addition of KAX to a concentration of 300 mg/L, there was an initial sudden increase of the Ratio reading of the 0.5 wt% chalcopyrite suspension from 1 to about 2, followed by a steady increase to about 5. The Ratio reading never decreased in the 30-min recording period – although the magnetic stirring and peristaltic pumping

continued – as have been observed in the tests with quartz-chalcopyrite mixtures or the quartz single mineral. Clearly, the KAX caused the aggregation of the chalcopyrite particles and the aggregates were more resistant to breakage than the PEO flocs.

Figure 5.7 also shows that when PEO was added, chalcopyrite particles were flocculated and the Ratio reading increased from 1 to over 5, but the flocs were not stable and broke up gradually. The breakage rate, i.e., the slope of the dropping segment of the Ratio curve, was calculated to be -0.84 min^{-1} . The Ratio reading continued the dropping trend, reaching the initial value of about 1.0 in 30 minutes, which seemed to indicate that the chalcopyrite particles were returned to the initial dispersed state.

When KAX was added 3 minutes after PEO, the breakage rate (slope) increased to a much higher value at -5.46 min^{-1} , indicating that KAX significantly sped up the breakage of the chalcopyrite flocs. However, it is interesting to note that after this initial sudden drop following KAX addition, the Ratio reading then stabilized at about 3.0 rather than dropping continuously to the original value of 1.0. It is speculated that KAX caused the breakage of the initial PEO flocs of chalcopyrite, but some of the chalcopyrite particles may have been re-flocculated by KAX, for the formed aggregates seem to be resistant to breakage, similar to the case when KAX was added alone.

When KAX was added first, followed by PEO 3 minutes later, there was an initial small and gradual increase in the Ratio reading from 1 to about 2.7, again possibly by the flocculation of the xanthate-hydrophobized chalcopyrite. This was followed by a sudden increase of the Ratio reading to above 5 after adding the PEO. The Ratio reading quickly dropped, with a slope of -1.35 min^{-1} , and finally stabilized at about 2.5.

5.3.3 Flocculation of quartz-chalcopyrite mixtures with varying amounts of chalcopyrite

The foregoing description of the PDA test results seem to point to the same trend, that the addition of KAX promotes the formation of breakage-resistant chalcopyrite flocs, and breaks PEO flocs of chalcopyrite. However, the addition of KAX does not affect quartz nor the PEO flocs of quartz. Therefore, it seems that in the PEO hetero-aggregates of quartz and chalcopyrite, the chalcopyrite particles are the “weak spots” once KAX was added. The xanthate ions are known to adsorb on the chalcopyrite particles through chemical and/or electrochemical reactions (Fuerstenau, 1982; Mielczarski et al., 1996c; Woods, 1984). Such a strong chemisorption could cause desorption of the PEO from the chalcopyrite surfaces, leading to the disintegration of the hetero-aggregates. The removed chalcopyrite particles, however, could form hydrophobic flocs due to the surface hydrophobicity induced by KAX.

This hypothesis seems to be borne out by the results shown in Figure 5.8 and Figure 5.9. Figure 5.8 shows the images of flocs of two parallel quartz-chalcopyrite flocculation tests where only the chalcopyrite content is different. Pictures were taken 3 mins after KAX addition. As can be seen, the flocs appear smaller in the 30% chalcopyrite case (Figure 5.8b) than in the 10% chalcopyrite case (Figure 5.8a). This means that the flocs broke faster with the increasing chalcopyrite content. Figure 5.9 shows PDA measurement results on quartz-chalcopyrite mixtures with different chalcopyrite contents. As can be seen, the slopes of the decreasing segment of the Ratio curves increased with increasing chalcopyrite content after adding KAX, at -5.46 min^{-1} for 100 wt%, -0.7 min^{-1} for 30 wt% and -0.15 min^{-1} for 10 wt% chalcopyrite. Also, the final Ratio readings were at about 2.5, 1.5 and 1.0 for the mixtures with 100 wt%, 30 wt% and 10 wt% chalcopyrite, respectively. In other words, after adding KAX, the more chalcopyrite the quartz-chalcopyrite mixture contains, the faster the PEO flocs break, and the higher the final Ratio reading.

5.4 Discussion

To account for the observed batch flotation and PDA flocculation and dispersion test results, it is envisaged that the following may be what happened during the flotation process: when PEO was added to the quartz–chalcopyrite mixture, it flocculated both minerals together to form hetero-aggregates. With continuous stirring, especially in a batch mechanical flotation cell, some of the flocs were broken. When KAX was added following PEO, it adsorbed on chalcopyrite surfaces and partially or completely (depending on KAX dosages) replaced the pre-adsorbed PEO, which further weakens the hetero-aggregates. As a result, chalcopyrite particles dissociated from the hetero-aggregates, causing further breakup of the flocs. This postulate is consistent with the two generally accepted flocs breakage mechanisms, i.e., large-scale fragmentation, and surface erosion (Jarvis et al., 2005; Pandya and Spielman, 1982). Fragmentation is thought to be caused by tensile stress across the entire floc, while surface erosion is attributed to the shearing stress on the floc surface. In this case, the desorption of PEO by KAX renders chalcopyrite particles on the surface less resistant to the shearing stress so that the chalcopyrite particles are stripped off from the flocs more easily (note that the chalcopyrite particles in the hetero-flocs were scattered (e.g., Figure 5.4) and hydrophobic forces would not come into play even after KAX adsorption). Even the chalcopyrite particles inside the floc are likely to dissociate from or to be less tightly connected with the surrounding quartz particles since KAX is a small molecule and can diffuse into the loose flocs. Therefore the flocs become weaker and the fragmentation worsens, which in turn exposes more chalcopyrite particles to shearing stress, eventually leading to the disintegration of the large PEO flocs and forming smaller flocs that contain quartz mostly. The individual chalcopyrite particles then associate to form hydrophobic aggregates, due to the surface hydrophobicity caused by the adsorption of xanthate.

Figure 5.10 shows two SEM images that demonstrate such an effect of KAX. Both images show samples that were taken from the quartz-chalcopyrite mixture suspensions 15 minutes after PEO was added, but in the sample shown in Figure

5.10b, KAX was added 3 minutes after PEO. The quartz-chalcopyrite mixtures contained 10 wt% chalcopyrite. Figure 5.10a and 5.10b show typical fields of view of these two samples. The most obvious difference between these two images is that large hetero-aggregates existed in the image shown in Figure 5.10a where only PEO was added. These large flocs were not observed in Figure 5.10b where both PEO and KAX were used. Another difference is the way by which chalcopyrite particles are incorporated in the flocs. In Figure 5.10a (with no KAX), chalcopyrite particles are incorporated in large and medium size flocs. In Figure 5.10b (with KAX), the small flocs are concentrated in either chalcopyrite or quartz. In other words, the large hetero-aggregates formed by the addition of PEO were broken as a result of subsequent KAX addition, to form smaller homo-aggregates of quartz and chalcopyrite. An illustration in Figure 5.11 pictures the scenario more directly. Even though the quartz flocs were broken under agitation and the action of KAX, their sizes are still larger than the single dispersed quartz particles. Therefore, the quartz flocs are less likely to be hydraulically carried over to the concentrate, and some of them may be large enough to overcome the fluid drag and drain back to the pulp from the froth layer.

It is realized that the hydrodynamic conditions in a batch mechanical flotation machine are different from a suspension that undergoes magnetic-bar stirring and peristaltic pumping. Whether the same aggregation and dispersion behavior of the quartz-chalcopyrite mixtures with the addition of PEO and xanthate as observed in the PDA tests occurred in the batch mechanical flotation machine is uncertain, especially in view of the “fragile” nature of the PEO flocs. However, the improved flotation results as shown by the grade-recovery relationship after the addition of PEO in previous chapter serve as an indication that similar aggregation or dispersion behavior may have happened in the mechanical flotation machine. In fact, our tests using a 3 L baffled container agitated at several hundred rpm showed similar aggregation behavior of xanthate and PEO on quartz and galena.

5.5 Summary

Aggregation/dispersion studies using a photometric dispersion analyzer (PDA), stereomicroscope and a scanning electron microscope (SEM), showed that during the PEO-assisted flotation, PEO flocculated quartz and chalcopyrite together, forming hetero-aggregates. Subsequent addition of a xanthate collector caused the chalcopyrite particles to break away from the PEO hetero-aggregates and leave quartz particles in homo-aggregates, due to the competitive adsorption of xanthate which probably removed PEO from the chalcopyrite surfaces. The removed chalcopyrite particles seemed to be able to form homo-aggregates as well, possibly due to the surface hydrophobicity induced by the adsorbed xanthate. Therefore, contrary to the original hypothesis, it is the xanthate not PEO that lends selectivity to the quartz/chalcopyrite flotation system. Given that xanthate is the common collector for most sulfide minerals, the combined use of polyethylene oxide and xanthate can potentially benefit the processing of polymetallic sulfide ores to reject fine and ultrafine quartz and silicate gangue.

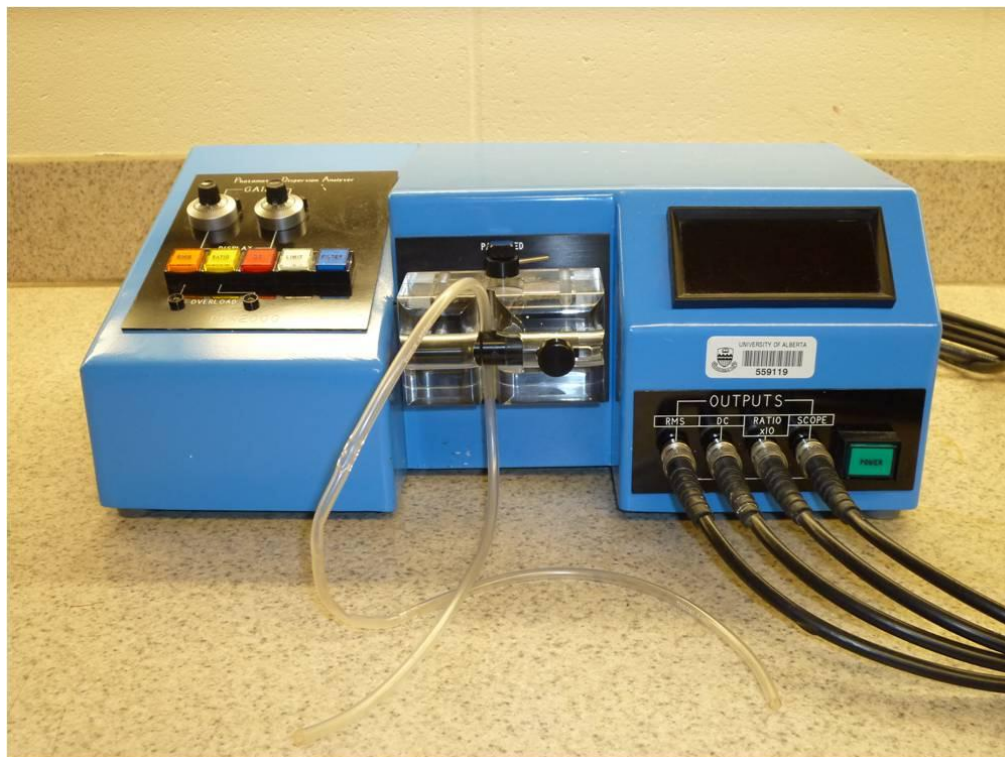


Figure 5.1 Photometric Dispersion Analyzer (PDA 2000).

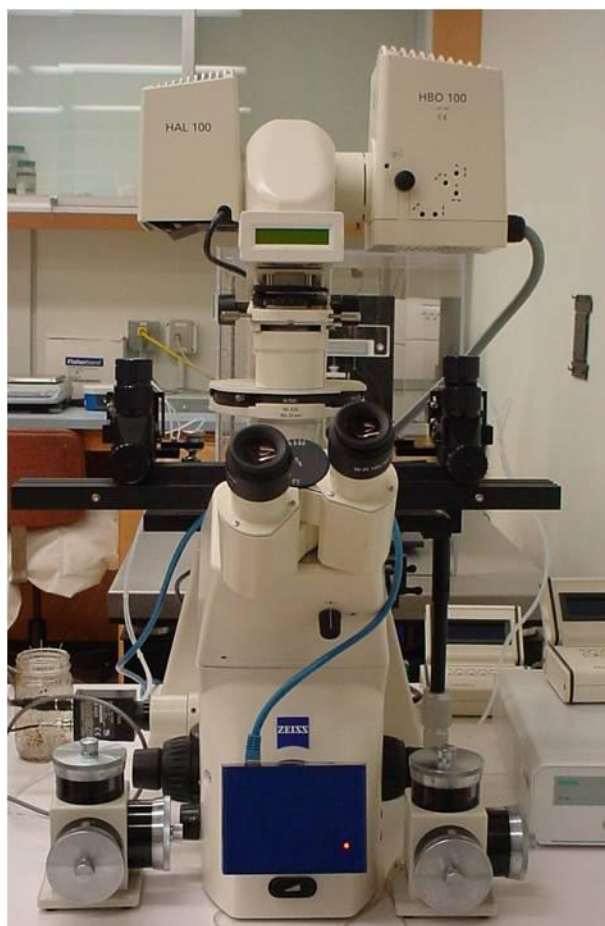


Figure 5.2 Microscope apparatus for visual observation.

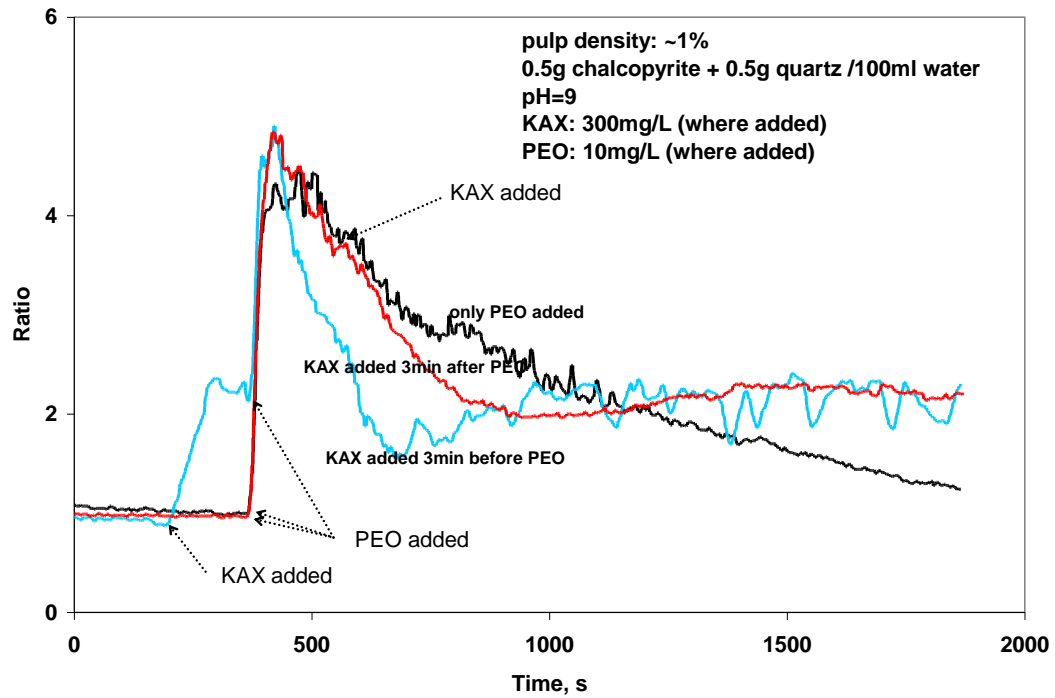


Figure 5.3 Effect of KAX and PEO on the flocculation/dispersion of 1:1 quartz-chalcopyrite mixtures.

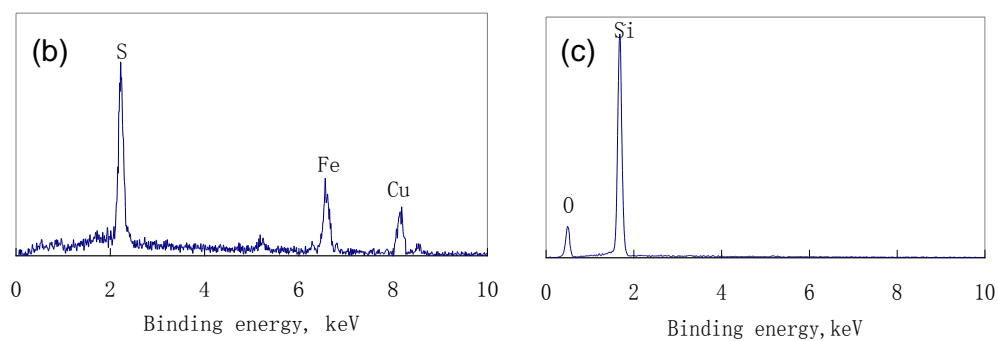
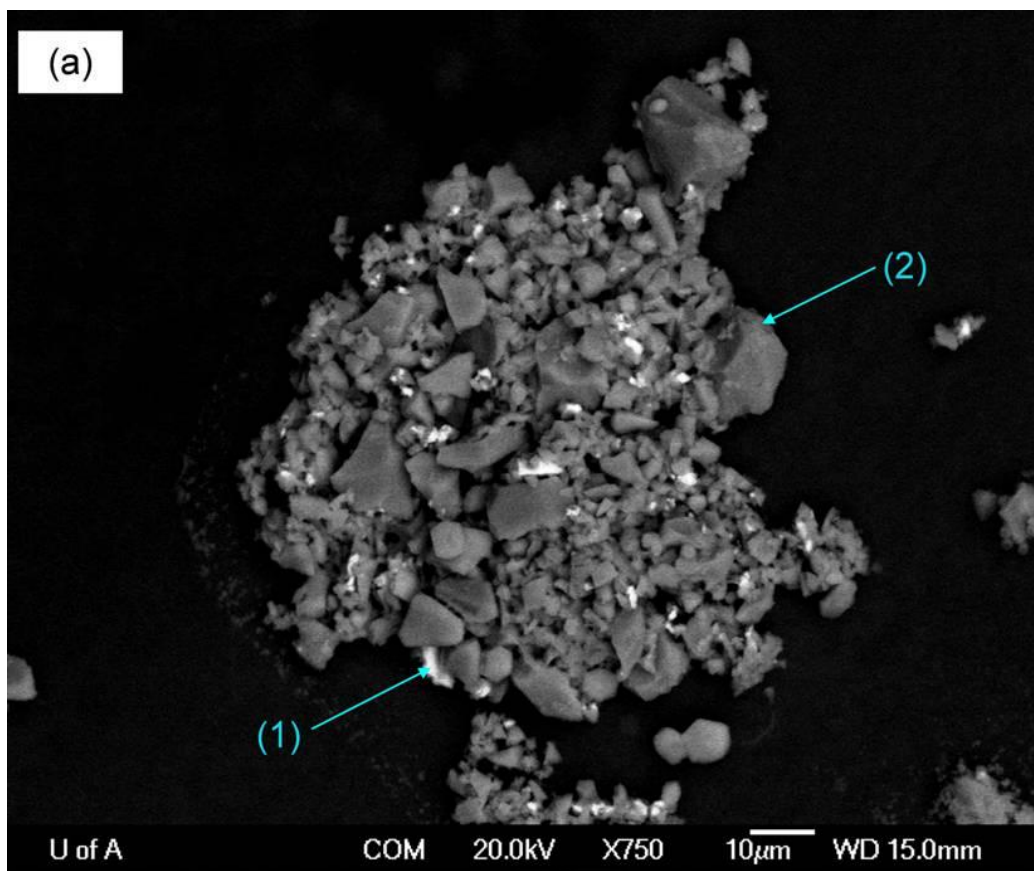


Figure 5.4 (a) SEM image of a typical PEO floc of quartz-chalcopyrite; (b) EDS spectrum of point (1): chalcopyrite; (c) EDS spectrum of point (2): quartz.

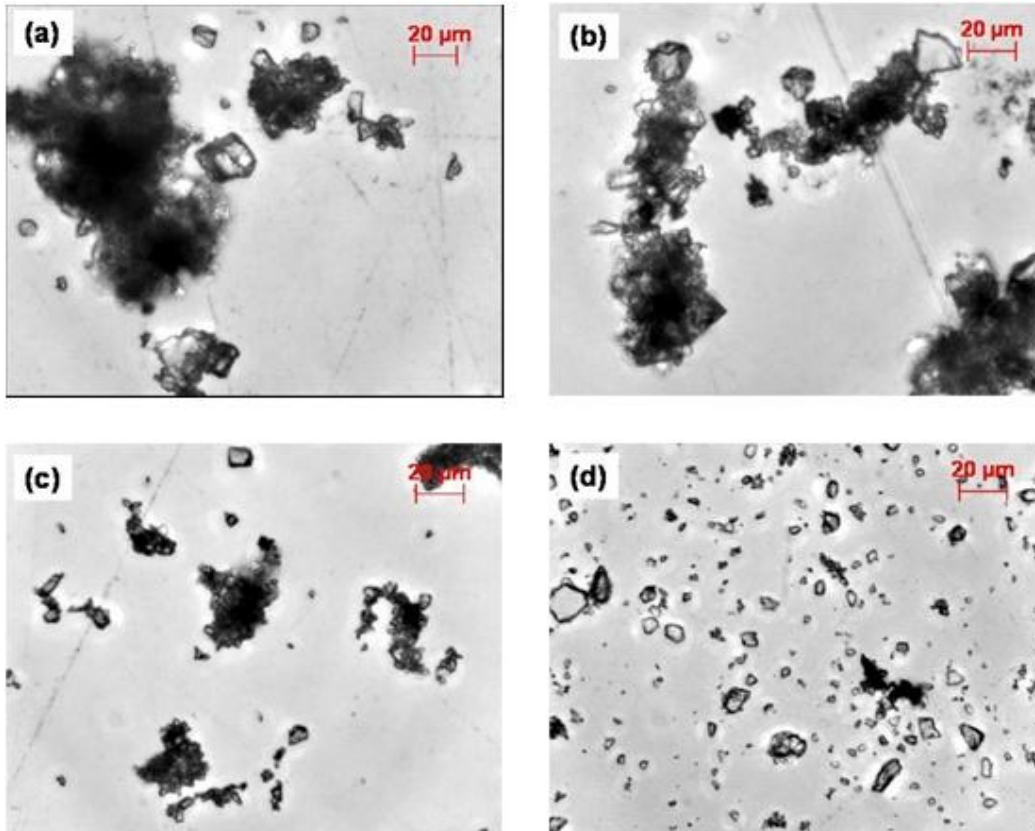


Figure 5.5 Effect of KAX on the quartz-chalcopyrite flocs induced by PEO
(a) 0 mg/L KAX; (b) 60 mg/L KAX; (c) 300 mg/L KAX; (d) 6,000 mg/L KAX.

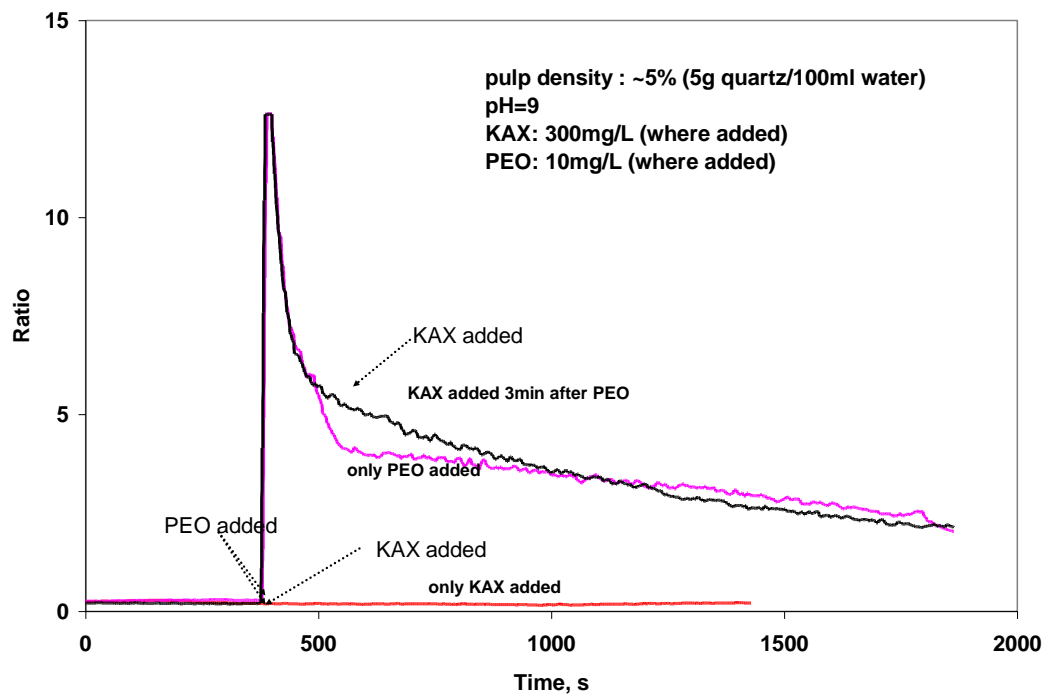


Figure 5.6 Effect of KAX and PEO on the flocculation/dispersion of quartz.

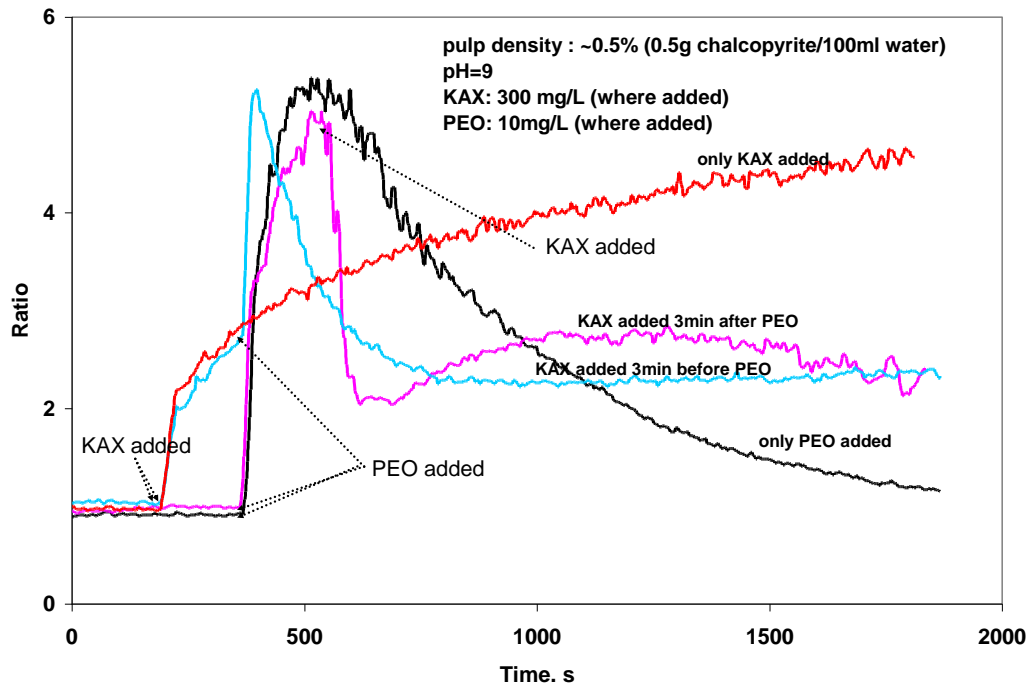


Figure 5.7 Effect of KAX and PEO on the flocculation/dispersion of chalcopyrite.

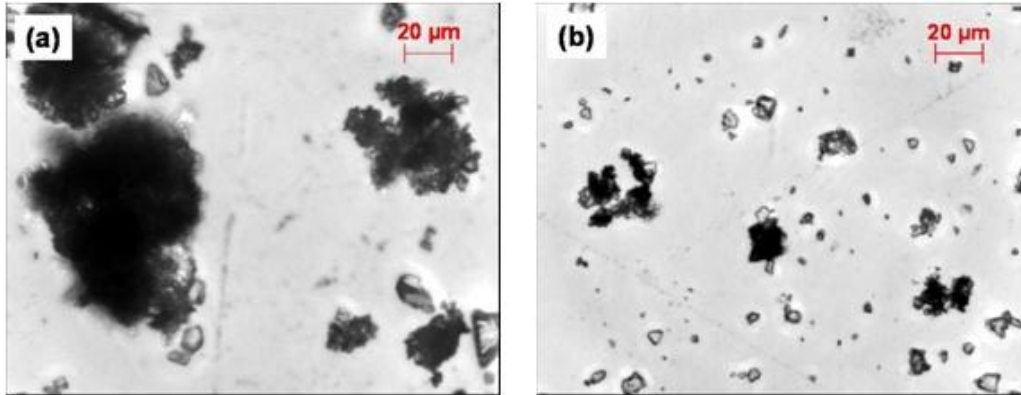


Figure 5.8 Effect of PEO and KAX on the flocculation/dispersion of quartz-chalcopyrite mixtures with different chalcopyrite content (a) 10% chalcopyrite (b) 30% chalcopyrite.

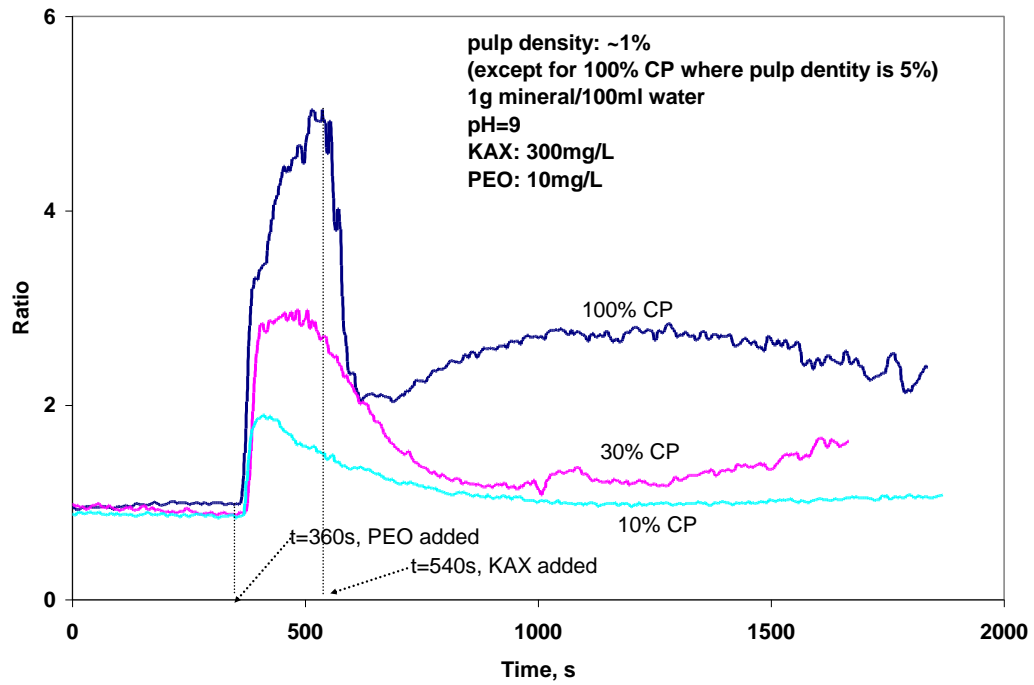


Figure 5.9 Effect of PEO and KAX on the flocculation/dispersion of quartz-chalcopyrite mixtures with different chalcopyrite contents.

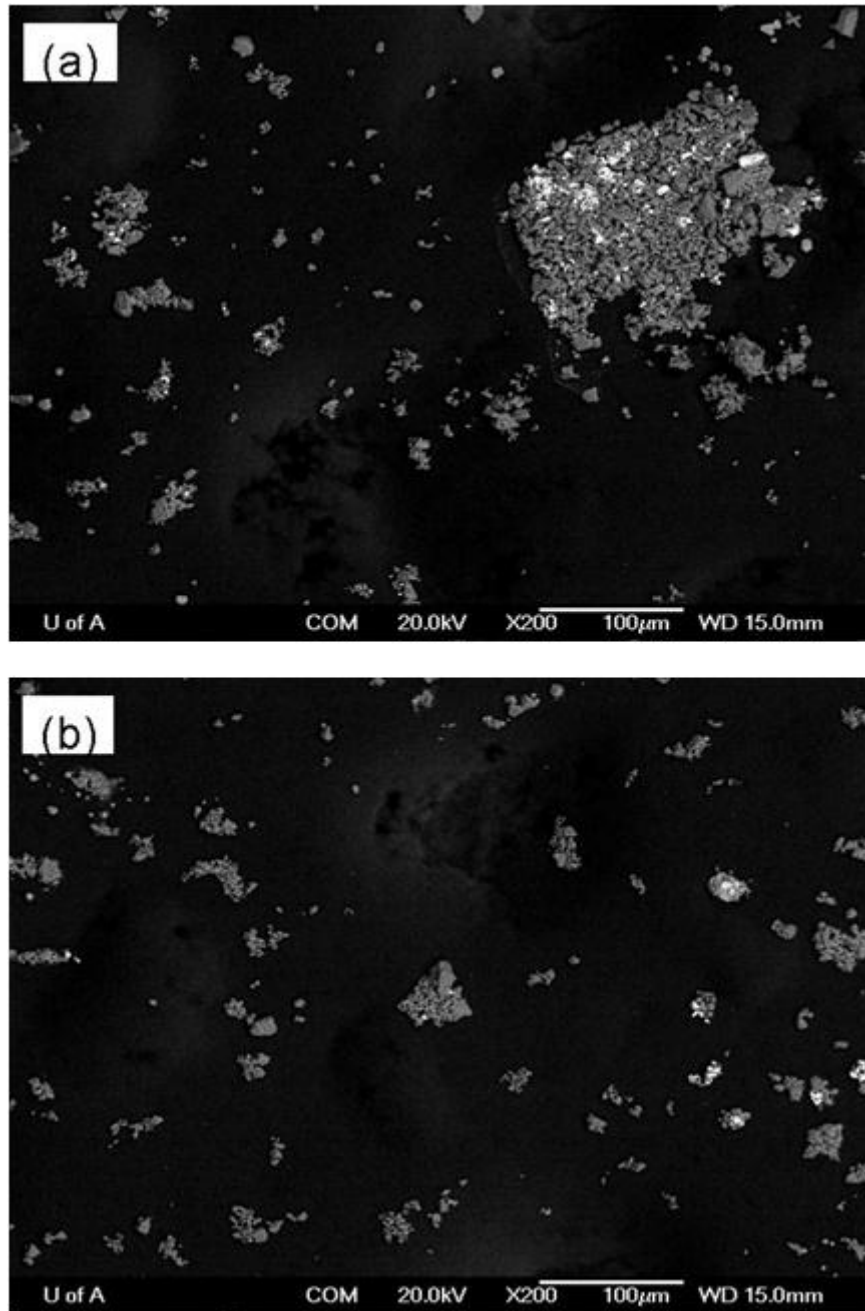


Figure 5.10 SEM images of suspension samples taken 15 minutes after the addition of PEO.

(a) without KAX; (b) KAX added 3 minutes after PEO.

Bright particles: chalcopyrite; Gray particles: quartz.

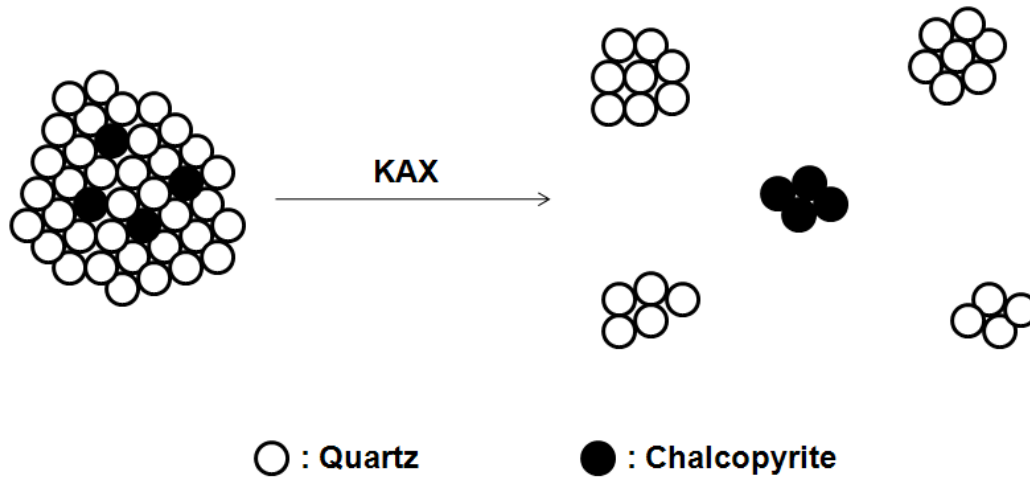


Figure 5.11 Illustration of the breakage of quartz/chalcopyrite hetero-aggregate and the formation of homo-aggregate of quartz and chalcopyrite.

Chapter VI Adsorption Mechanism of Polyethylene Oxide (PEO) and Potassium Amyl Xanthate (KAX)

6.1 Introduction

The possible adsorption mechanisms of PEO on mineral surfaces have been proposed by several researchers (section 2.7). These include hydrogen bonding (through the ether oxygen on PEO) and hydrophobic interactions (due to the ethylene groups). There is, however, very little research on the interaction between PEO and chalcopyrite, probably because PEO has rarely been applied on chalcopyrite. On the other hand, numerous work has been done on the interaction between PEO and silica. It was suggested that PEO adsorbs on silica through hydrogen bonding between the ether oxygen on PEO and the silanol groups on silica surface (Mathur and Moudgil, 1997; Rubio and Kitchener, 1976). Given that quartz surface is also covered with silanol groups, hydrogen bonding may be the main mechanism for PEO adsorption on quartz.

In this research, a novel method, cryogenic X-ray photoelectron spectroscopy (cryo-XPS), was exploited to study the interactions between the PEO and chalcopyrite as well as quartz surface. Such a study is deemed necessary to better understand the PEO-sulfide-quartz system in order to provide a robust reagent scheme for the minerals industry. The advantage of cryo-XPS is that the spectroscopic studies can be carried out *in situ*, i.e., the mineral particles, after interaction with the chemical reagents in an aqueous environment, can be frozen in place without the need to be removed from the aqueous environment and dried. The chemical states of the species, both the reagents and mineral surfaces, are therefore preserved. The XPS analysis on these frozen samples would provide direct information on the chemical states of the species and the interactions between them.

6.2 Experimental

6.2.1 Materials and chemicals

The materials and chemicals used in the adsorption mechanism study were the same as in flocculation tests (Chapter 5) and were described in section 5.2.1.

6.2.2 Zeta potential measurements

Zeta potential measurement was performed using a ZetaPALS zeta potential analyzer manufactured by Brookhaven Instruments. All solutions and reagents were prepared with stock solutions of 10^{-2} mol/L KCl to maintain a constant ionic strength. To prepare the stock suspension, one gram of the mineral (~ 20 μm) was added to a 1 L volumetric flask containing the 10^{-2} mol/L KCl solution. The flask was then sealed and inverted several times to keep the mineral particles well dispersed.

For each zeta potential measurement, 10 mL of the stock mineral slurry were withdrawn and diluted with 90 mL of 10^{-2} mol/L KCl solution, adjusted to appropriate pH, and then treated by desired reagents. A very small amount (about 2 mL) of this conditioned particle suspension was transferred to the plastic sample cell of the ZetaPALS for zeta potential measurement.

6.2.3 Adsorption tests

The adsorption density of PEO on mineral samples was determined by depletion method. PEO concentrations were determined by the molybdophosphoric acid method described by Nuysink and Koopal (Nuysink and Koopal, 1982). First, a molybdophosphoric acid solution was first prepared by dissolving 0.5 g molybdophosphoric acid, 0.5 g barium chloride dehydrated and about 1.5 mL of concentrated hydrochloric acid in 250 mL of water. Two mL of the molybdophosphoric acid solution was pipetted into a dry centrifuge tube, and mixed with 2 mL of a PEO solution with an unknown concentration. The tube was shaken gently, stored for 15 min at room temperature, and then centrifuged.

One mL of the supernatant solution was pipetted into a 50 mL standard flask and water was added to make up to volume. A small volume of the solution was transferred to a quartz cuvette and its absorbance at 218 nm was measured against distilled water in the UV/VIS spectrometer. The difference in absorbance between blank solution (water) and the test solution was found to have a linear relationship with the PEO concentration. Therefore, a calibration line was obtained by measuring a series of PEO solution with known concentrations, which is shown in Figure 6.1. The PEO concentration of the test solution was read from the calibration line after measuring its absorbance at 218 nm.

For both chalcopyrite and quartz, the adsorption kinetics was first determined by fixing mineral suspension density (3g/50mL) and PEO concentration (100 mg/L), and varying the equilibration time. In each test, 3 gram mineral was mixed with 40 mL distilled water and the solution pH was adjusted to 9. After the solid was completely wetted, 10 mL of 500 mg/L PEO solution was added. After mixing, the pH of the 50 mL suspension was checked and adjusted if necessary. The suspension was then placed in a Lab-line Orbit Environ shaker and conditioned for various period of time at 168 rpm. About 10 mL of the suspension was taken out and centrifuged for 20 min at 2300 rpm. Two mL supernatant solution was taken out to mix with 2 mL molybdophosphoric acid solution. The residual PEO concentration was found from the difference in absorbance between the blank and the test solution on the calibration line. The amount of adsorbed PEO was then calculated.

The adsorption isotherm was obtained using the same mineral suspension density (3g/50mL) but different PEO concentrations, ranging from 20 to 400 mg/L. The adsorption time was set at 3 hrs, which was almost twice as long as the equilibrium time obtained from kinetics analysis (see Figure 6.3), because higher PEO concentrations were used. Other procedure was the same as in the kinetics adsorption measurement.

6.2.4 Flocculation/dispersion measurements

The effect of pH on the flocculation of the mineral suspensions by PEO was studied using a PDA 2000 photometric dispersion analyzer. The operation procedure and the instrument have been described in detail in section 5.2.2.

6.2.5 Cryo-XPS analysis

XPS technique has been widely used to study the chemical state of an element by measuring the electron binding energy (E_B) in a specific atomic orbital of this element. The binding energy is calculated from

$$E_B = h\nu - E_K - W \quad (9)$$

Where $h\nu$ is the incident photon energy; E_K is the provoked electron escaping kinetic energy measured by the spectrometer; W is the spectrometer work function (Watts, 2003). Therefore, knowing the energy of the incident photons and the spectrometer work function, by measuring the escape kinetic energy of the ejected electrons, their binding energies E_B can be calculated. Each chemical state of the species, e.g., Cu^{2+} or Cu^+ , is characterized by a specific value of the electron binding energy. Moreover, a slight change (shift) of the electron binding energy indicates a change in the chemical environment. For instance, an increase in electron binding energy E_B means that the electron density of the atoms or ions under study has decreased, or the neighboring chemical environment has become more electropositive, and vice versa.

The XPS spectra were obtained with a Kratos AXIS-165 X-ray photoelectron spectroscopy system with a liquid- N_2 -cooled cryogenic stage. A monochromatic Al K_α X-ray source (1486.6 eV) operated at 210 W was employed. The operating pressure of the spectrometer analyzer chamber was close to 10^{-8} Pa. A two-step scanning procedure was used in these studies. A survey scan in the binding energy range of 0 eV to 1,100 eV was first recorded with an analyzer pass energy of 160

eV and a step size of 0.3 eV to identify the elements. In the second step, higher resolution spectra (20 eV pass energy and step size of 0.1 eV) were recorded around the elemental peaks of interest. The number of scans for high-resolution spectra was determined according to the spectrum intensities of the elements to be analyzed. Charge neutralization was applied to stabilize spectra during spectra collection, as the samples became insulating at very low temperatures. The spectra were fitted and deconvoluted using Casa XPS software; the background model was obtained using a Shirley algorithm and the individual peaks were fitted with Gaussian-Lorentzian line shapes.

Quartz and chalcopyrite samples were prepared at various conditions. Blank PEO and KAX solutions were also studied. A cryogenic stage was used to frozen particle suspension samples and to maintain this condition in the ultrahigh-vacuum environment. In the fast entry lock (FEL) of the spectrometer, a Cu stub (10 mm in diameter) was precooled with liquid nitrogen. A small amount of particle suspension was placed on the smooth surface of the stub, causing it to freeze. The stub and FEL were kept in flowing dry nitrogen to drive away any atmospheric moisture. Pumping inside the FEL was started after the particle suspension froze. During this process, the temperature of the stub in the FEL continuously decreased. When the pressure of the FEL was lower than 10^{-8} Pa, the temperature of the stub in the FEL was about -150°C . The frozen sample was then ready for analysis.

6.3 Results and Discussion

6.3.1 Effect of PEO and KAX on the zeta-potential of quartz and chalcopyrite

The change of zeta-potential of quartz and chalcopyrite particles submerged in PEO and KAX solutions is shown in Figure 6.2. As can be seen, PEO was able to adsorb on both quartz and chalcopyrite surfaces, driving the zeta potentials of both minerals to near zero. As PEO is a nonionic polymer, its adsorption could stretch the shear plane of the electrical double layer on the mineral surfaces far

away from the surface, lowering the magnitude of the zeta potential. On the other hand, the addition of KAX only altered the zeta potentials of chalcopyrite, making it more negatively charged as more KAX was used. It was noted that the addition of KAX did not affect the zeta potential of quartz, which confirmed that there was no interaction between quartz and KAX.

6.3.2 Adsorption of PEO on quartz and chalcopyrite

The adsorption behavior of PEO on quartz and chalcopyrite was studied by measuring the adsorption kinetics and adsorption isotherms on both minerals. The kinetic data presented in Figure 6.3 shows that both curves went up abruptly at the beginning and leveled off in 2 hours, which indicates that PEO adsorbed on both minerals very quickly. The maximum adsorption density, obtained from Figure 6.4, is 1.25 mg/m^2 on quartz and 2.2 mg/m^2 on chalcopyrite. PEO molecular chain is thought to exist as isolated coil in dilute solution and its hydrodynamic radius is about 40 nm for PEO with molecular weight of 8×10^6 (Devanand and Selser, 1990). Using these numbers, the surface coverage by adsorbed PEO was calculated to be approximately 47.3% for quartz and 83.1% for chalcopyrite at equilibrium. Chalcopyrite not only adsorbed more PEO but also adsorbed the PEO faster than quartz, indicating that chalcopyrite probably has a higher affinity to PEO.

6.3.3 Interaction of quartz with PEO

6.3.3.1 Effect of pH on quartz flocculation by PEO

As reviewed in section 2.7, the interaction between quartz and PEO is generally thought to be due to hydrogen bonding between the silanol groups on quartz surface and the ether oxygen in PEO molecular chains. Since silanol groups are sensitive to the pH value of quartz suspensions, undergoing protonation and deprotonation in acidic and basic solutions, respectively, hydrogen bonding is expected to be affected by pH value as well. Therefore, the effect of pH on the

flocculation efficiency of PEO towards quartz was measured, and the results could be used as an indication of the strength of the hydrogen bonding between quartz and PEO. The results are shown in Figure 6.5. It can be seen from this figure that the best flocculation was observed at around neutral and slightly alkaline pH, i.e., pH 6.5 and pH 9. In both cases, the value of Ratio increased sharply right after adding PEO, indicating that the quartz particles were strongly flocculated. After a short time, the value of Ratio dropped gradually, indicating the breakage of the flocs. However, after about 30 min, the value of Ratio was still higher than the original value, which meant that quartz particles were still flocculated to some degree. At acidic pH, i.e., pH 2, after PEO was added, the value of Ratio increased sharply, too, but dropped quickly and went back to the original value in less than 3 min. The results indicated flocs formed at pH 2 were very weak. The faster disintegration of the quartz flocs at pH 2 suggested that the attraction between quartz and PEO at pH 2 was probably not as strong as at pH 6.5 or pH 9. At very alkaline pH, i.e., pH 11, the flocculation of quartz was even worse than at pH 2. The value of Ratio went up only very slightly when PEO was added. This result implied that the attraction between quartz and PEO at pH 11 was very weak.

According to the current view of quartz surface speciation, there are three types of surface groups: $>\text{SiOH}_2^+$, $>\text{SiOH}$ and $>\text{SiO}^-$ (where $>$ represents the bulk quartz) (Borkovec, 1997; Morrow and Cody, 1976). Duval et al. (Duval et al., 2002) analyzed and calculated the percentage of these three species at various pH and their results are shown in Figure 6.6. Based on the surface density of the three species, the low flocculation efficiency at high pH (pH 11) could be attributed to the lower density of electron acceptor sites, i.e., $>\text{SiOH}_2^+$ and $>\text{SiOH}$. However, it can not explain the low flocculation efficiency at low pH (pH 2) because there are more $>\text{SiOH}_2^+$ and $>\text{SiOH}$ groups at the low pH. It seems that hydrogen bonding between quartz and PEO alone cannot explain the pH effect on quartz flocculation. In fact, two more types of hydrogen bonds should be present in the system: water-quartz and water-PEO hydrogen bonding. The effect of pH on quartz flocculation

was probably a manifestation of the competition among these three hydrogen bonds.

Du et al. (Du et al., 1994) reported that, at quartz-water interface, the interfacial water molecules are strongly affected by both electrostatic interaction and hydrogen bonding of the molecules with the quartz surface. Their conclusions are: (1) at low pH, hydrogen bonding forms between water molecules and quartz surface silanol group, resulting in 1 or 2 monolayer of oriented water molecules with the oxygen atoms facing the quartz surface; (2) at high pH, the strong electric field produced by quartz surface's negative charge can orient several monolayers of water molecules, with the oxygen pushed away from the surface; (3) at intermediate pH, these two interactions compete with each other and the interfacial water molecules are less ordered. In terms of hydrogen bonding, it can be understood in such a way that fewer bonds form between quartz and water at higher pH because of the stronger electrical field.

PEO may also be able to interact with quartz through electrical interaction in addition to hydrogen bonding. But unlike water molecules, no permanent dipoles exist in PEO molecular chains so the hydrogen bonds formed between PEO molecules and quartz would not be affected by the electrical field.

As for water-PEO hydrogen bond, it forms when PEO is dissolved in water. The ether oxygen of PEO competes with water as proton acceptor. It was calculated that the energies of these two hydrogen bonds are comparable and that about 70% of the ether oxygen are hydrogen bonded with water for PEO with low molecular weight at low concentration (Dormidontova, 2002). For PEO with high molecular weight, this number should be smaller as the result of steric hindrance. Therefore, the ether oxygen of PEO exists in two chemical environments: hydrogen bonded with water, and isolated. When PEO solution is added to quartz suspension, the isolated ether oxygen would

- (1) form hydrogen bonds with the isolated silanol groups;

- (2) replace water pre-bonded on silanol. This scenario is less likely because the energies of these two bonds are comparable;
- (3) indirectly attach to the silanol groups through the formation of hydrogen bonds with the water molecules bonded to the silanol groups; This scenario is also less likely because this water has already formed hydrogen bonds with surrounding water.

The water bonded ether oxygen would attach to surface silanol groups through the bonded water, which could still act as proton acceptor. But it is more likely that this water has already accepted protons from surrounding water. Therefore, it is the isolated silanol groups on quartz and isolated ether oxygen on PEO that determine the interaction between PEO and quartz in aqueous environment.

As mentioned earlier, PEO may also be able to interact with quartz through electrical interaction in addition to hydrogen bonding. But unlike water molecules, no permanent dipoles exist in PEO molecular chains so the hydrogen bonds formed between PEO molecules and quartz would not be affected by the electrical field. In fact, it might even help the formation of hydrogen bonding by bringing PEO molecules closer to the surface. The electrostatic interaction is more likely take place between $>\text{SiO}^-$ and the ethylene group $-\text{CH}_2-\text{CH}_2-$ because the electrical field would induce a dipole in the ether oxygen and push it away. Therefore, when PEO chains are adsorbed on quartz surface, the chains are likely arranged in such way that the ether oxygen attaches to $>\text{SiOH}$ and $>\text{SiOH}_2^+$, through direct or indirect hydrogen bonds, and the ethylene group attaches to $>\text{SiO}^-$ through electrostatic interaction, as depicted in Figure 6.7.

The hypothesis proposed above could now be used to explain the effect of pH on quartz flocculation. At low pH, even though there were more $>\text{SiOH}_2^+$ and $>\text{SiOH}$ groups on quartz surface, most of them probably were hydrogen bonded with water and little are left for PEO because the charge on quartz was low. The other reason was that the amount of isolated ether oxygen might decrease as well. At low pH, there are more H^+ present in quartz suspension. PEO would adsorb and

even prefer to adsorb H^+ so that less isolated ether oxygen was available to bond with the silanol groups. This argument was partly supported by the drop in pH of the PEO solution as more PEO was dissolved, as shown in Figure 6.8, which indicates that PEO adsorbed H^+ during dissolution. It is also understandable that PEO prefer H^+ to silanol as the former is a proton. Therefore, the low density of isolated silanol groups on quartz surface and the low density of isolated ether oxygen on PEO led to a weak interaction between PEO and quartz.

At intermediate pH, some hydrogen bonds between water and quartz are probably destroyed by the stronger repulsion between the negative quartz surface and the negative dipole (oxygen side) of water, so that more $>SiOH_2^+$ and $>SiOH$ groups are available for PEO despite that the total amount of $>SiOH_2^+$ and $>SiOH$ groups decreases. The stronger electrical field may also play a role in enhancing the interaction between PEO and quartz. At high pH, as mentioned above, the decrease in the amount of $>SiOH_2^+$ and $>SiOH$ groups weakens the hydrogen bonding interaction. Even though the increase of surface charge of quartz leads to a higher electrostatic interaction, it probably cannot compensate the loss in hydrogen bonding between PEO and quartz. The foregoing argument also shows that hydrogen bonding is the predominant force for PEO adsorption on quartz, while electrostatic interaction plays a secondary role.

6.3.3.2 *Cryo-XPS analysis of the interaction between quartz and PEO*

In order to find evidence for the above hypothesis, cryo-XPS was employed to detect the hydrogen bonding and electrostatic interaction between PEO and quartz because the electron binding energy of the tested element is very sensitive to the change of its chemical environment.

The following four quartz particle suspension (CP) samples were analyzed with cryo-XPS:

- 1) QZ-9. Quartz particles submerged in water at pH 9. No PEO was added

- 2) QZ-PEO-9. Quartz particles submerged in water at pH 9 in the presence of PEO
- 3) QZ-2. Quartz submerged in water at pH 2. No PEO was added
- 4) QZ-PEO-2. Quartz submerged in water at pH 2 in the presence of PEO.

The four suspension samples were prepared in similar ways, as follows: One gram of $-20\ \mu\text{m}$ quartz particles and 50 mL distilled water were mixed and agitated using a magnetic stirrer in a 100 mL beaker. The pH of the suspension was adjusted to desired value. PEO was added (when used) and the suspension was stirred for 15 min. A small amount of the settled particles were taken out using a spoon, which was tilted to drain off the water, and then placed on the copper stub of the XPS spectrometer. The dosage of PEO was 0.5 mL 0.1% PEO, i.e., 500 g/t. The XPS spectra of three orbital electrons, C 1s, O 1s, Si 2p, were recorded, which were fitted and deconvoluted using Casa XPS software.

The XPS spectra of C 1s from the four quartz particle suspensions are shown in Figure 6.9. All peaks have been calibrated, by setting the highest peak at 284.65 eV, which was thought to originate from hydrocarbon due to carbon contamination. The peak at the position of around 286 eV was attributed to carbon atoms bonded to oxygen, possibly also due to carbon contamination, as well as from PEO (where PEO was added, i.e. QZ-PEO-9 and QZ-PEO-2). The peak at the position of higher E_B , i.e., above 288 eV, appeared in all four samples and it was assigned to carbon atoms in the impurity carbonate minerals present in the quartz sample.

The Si 2p spectra are shown in Figure 6.10. If the peaks are calibrated by using C 1s 284.65 eV as standard, there is a positive chemical shift in binding energy after PEO addition at both pH values as shown in Table 6.1. Given the binding energy of Si 2p should not be affected by the addition of PEO, such shifts can be attributed to the alteration of electrical double layer at the quartz surface caused by the addition of PEO. According to Shchukarev (Shchukarev, 2010), for surface charged samples, the electrical double layer remains during fast freezing process

due to the layer of ice, and it influences the kinetic energy of the photoelectrons when they pass through the interface. The carbon layer due to contamination is on the top of the ice surface, which is neutral, and so its kinetic energy is not affected by the electrical field below. If C 1s is still used as calibration standard, for negatively charged particles, the negative electrical field accelerates the photoelectrons, increases the kinetic energy and thus the calculated binding energy is smaller. For positively charged particles, such effect is reversed and the calculated binding energy is larger. Quartz is negatively charged so the binding energy calculated here is smaller than that reported by others, which is about 103.65 eV. The larger shift at pH 9 (CS = 0.59 eV) than at pH 2 (CS = 0.4 eV) can be explained by the higher negative surface charge at pH 9 than at pH 2. Therefore, the binding energy of Si 2p should be set as the calibration standard instead of C 1s.

Table 6.1 Binding energy of Si 2p peaks in the four quartz suspension samples, using C 1s 284.65 eV as calibration standard

Si 2p (eV)	
QZ-PEO-2	103.35
QZ-2	103.25
QZ-PEO-9	103.25
QZ-9	103.06

Quartz surface is covered by $>\text{SiOH}_2^+$, $>\text{SiOH}$ and $>\text{SiO}^-$. If there is any change caused by the interaction with PEO, it would be reflected in O 1s spectra. Therefore, comparisons of O 1s spectra were made before and after the addition of PEO at pH 9 and pH 2, and the results are shown in Figure 6.11 and Figure 6.12, respectively. The deconvolution of the spectra was based on the knowledge of the various chemical environments where O atoms are present. At pH 9, major quartz surface species include $>\text{SiOH}$ and $>\text{SiO}^-$. The O atom can also be found in frozen ice and bulk quartz. Therefore, the O 1s spectra of QZ-9 was deconvoluted into four peaks. Given that the majority of the signal was from the

bulk, the largest peak was assigned to bulk oxygen (-Si-O-Si-). The second largest peak was assigned to oxygen in frozen ice (H₂O) because there was supposed to be 2-3 layer of water molecules (Shchukarev et al., 2007) and the binding energy of that peak was also supposed to be the highest. The rest two peaks were assigned to >SiOH and >SiO⁻, with the binding energy being higher in >SiOH than in >SiO⁻. For the spectra of QZ-PEO-9, there was one more peak, which was assigned to the adsorbed PEO. At pH 2, there is one more surface species, >SiOH₂⁺. So the new peak in spectra of QZ-2 and QZ-PEO-2 was assigned to >SiOH₂⁺. All peaks were calibrated using Si 2p 103.65 eV as the standard and are listed at Table 6.2 and Table 6.3.

Table 6.2 Binding energy of O 1s peaks of quartz suspension samples at pH 9

	O 1s (eV)				
	water	from PEO	SiO ₂	>SiOH	>SiO ⁻
QZ-9	533.32	–	532.83	532.68	531.19
QZ-PEO-9	533.55↑	533.45	532.86	532.35↓	531.44↑

The comparison of the two sets of peaks was made and also presented at Table 6.2 and Table 6.3. Both showed the same chemical shift trend, i.e., the binding energy of O 1s remained the same for -Si-O-Si-, went down for >SiOH and >SiOH₂⁺, and went up for H₂O and >SiO⁻. It is understandable that no shift was observed for O 1s in -Si-O-Si- as those signals were from the bulk and should not be affected. The decrease in O 1s binding energy in >SiOH and >SiOH₂⁺ are probably due to the hydrogen bonding with PEO. The electrons donated by PEO lead to a higher electron density around O atom and hence a lower binding energy. The increase of O 1s binding energy in >SiO⁻ can be attributed to the electrostatic interaction with PEO. Since >SiO⁻ is negative, such interaction would shift electrons away and result in a higher binding energy. The increase of O 1s binding energy in H₂O may also be attributed to hydrogen bonding. When PEO adsorbs on quartz surface,

it weakens its electrical fields and thus more H₂O can form hydrogen bonds with >SiOH and >SiOH₂⁺. It may also result from other factors, such as the orientation of H₂O molecules and the thickness of the ice layer. The structure and property of the ice layer is still not well understood yet.

Table 6.3 Binding energy of O 1s peaks of quartz suspension samples at pH 2.

	O 1s (eV)					
	>SiOH ₂ ⁺	water	from PEO	SiO ₂	>SiOH	>SiO ⁻
QZ-2	534.87	533.53	–	532.93	532.57	531.46
QZ-PEO-2	533.38↓	533.83↑	533.69	532.94	532.35↓	531.95↑

The chemical shift in O 1s binding energy of PEO was also calculated. The binding energy of O 1s of PEO solution at pH 9 was obtained by measuring the cryo-XPS spectrum of a PEO solution sample. The O 1s spectra was shown in Figure 6.13. It was deconvoluted into two peaks, one with lower binding energy, assigned to PEO, and the other assigned to H₂O. The binding energy was calibrated using the carbon contamination, 284.65 eV, as standard. The adjusted binding energy of O 1s is 532.29 eV. When the binding energy of O 1s of PEO in QZ-PEO-9 was also calibrated using C 1s from carbon contamination, 284.65eV as standard, a value of 533.05 eV was obtained (this is different from the value in Table 6.3 where calibration was done using Si 2p). Therefore, there was a definite increase in binding energy of O 1s of PEO after its interaction with quartz, which supports the hydrogen bonding between PEO and >SiOH.

6.3.4 Interaction of chalcopyrite with PEO, and with KAX

6.3.4.1 Effect of pH on chalcopyrite flocculation by PEO

The surface of chalcopyrite has been extensively studied and found to be covered with oxides/hydroxides and metal-deficient sulfide due to the oxidation and hydration of chalcopyrite in aqueous suspension (Buckley and Woods, 1984; Luttrell and Yoon, 1984; Zachwieja et al., 1989). Like quartz, chalcopyrite is also negatively charged. Therefore, the electrostatic interaction and hydrogen bonding could both play a role in the interaction between chalcopyrite and PEO. However, the effect of pH on chalcopyrite flocculation is different from that on quartz. As can be seen from Figure 6.14, the flocculation efficiency of PEO on chalcopyrite increased with pH. The reason might be the different origin and character of oxides/hydroxides on chalcopyrite surface. As mentioned above, the oxides/hydroxides on chalcopyrite surfaces are produced through oxidation and hydration, and are mainly comprised of iron oxides/hydroxides. At low pH, most of the oxides/hydroxides dissolve in water leaving the surface mainly covered with metal-deficient sulfide and thus not many hydroxyl groups are available for hydrogen bond formation. As pH increases, more oxides/hydroxides are present on the surface and the surface charge increases, too, which results in a stronger interaction with PEO.

Chalcopyrite is thought to be hydrophobic to some degree after oxidation. At low pH, chalcopyrite should be more hydrophobic because oxidation is more severe and because of the removal of iron hydroxides from the surface. The higher original value of Ratio output of the PDA 2000 photometric dispersion analyzer at lower pH, as shown in Figure 6.14, also indicated a more hydrophobic chalcopyrite. Rubio (1981) observed that PEO flocculated the hydrophobic particles such as talc, graphite and chalcopyrite better than the hydrophilic ones such as rutile, quartz, copper, and silica, and proposed that hydrophobic interaction was responsible for PEO adsorption. In the adsorption isotherm measurement, it was observed that chalcopyrite did adsorb more PEO than quartz.

But Figure 6.14 shows that chalcopyrite flocculation by PEO was worse at lower pH, where chalcopyrite was more hydrophobic. Therefore, hydrophobic interaction may not be a major force for chalcopyrite and PEO interaction but the hydrophobicity of chalcopyrite may play a synergistic role in PEO adsorption.

6.3.4.2 *Cryo-XPS analysis of the interaction of chalcopyrite with PEO and KAX*

Cryo-XPS tests were performed on chalcopyrite in order to find evidence for the interaction mechanism between PEO and chalcopyrite and to better understand the replacement of PEO by KAX. The following four chalcopyrite particle suspension (CP) samples were analyzed with cryo-XPS:

- 1) CP. Chalcopyrite submerged in water at pH 9. No reagent was added
- 2) CP-PEO. Chalcopyrite particles were reacted with PEO at pH 9
- 3) CP-KAX. Chalcopyrite particles were reacted with KAX at pH 9
- 4) CP-PEO&KAX. Chalcopyrite particles were reacted with PEO, then with KAX at pH 9.

The four suspension samples were prepared in the similar way as the quartz samples. One gram of -20 μm chalcopyrite particles and 50 mL distilled water were mixed and agitated using a magnetic stirrer in a 100 mL beaker. The pH of the suspension was adjusted to 9. The desired reagents, i.e., PEO or KAX, were added and the suspension was stirred for 15 min. A small amount of the settled particles were taken out using a spoon, which was tilted to drain off most of the water, and then placed on the copper stub of the XPS spectrometer. The dosages of reagents were higher than in flotation tests, i.e., 0.5 mL 0.1% PEO, 0.05 g KAX for CP-KAX and 0.1 g KAX for CP-PEO&KAX, which gave a PEO dosage of 500 g/t and a KAX dosage of 5,000 g/t or 10,000 g/t to ensure signal strength. The XPS spectra of five orbital electrons, C 1s, O 1s, Cu 2p, Fe 2p and S 2p, were recorded, which were fitted and deconvoluted using Casa XPS software. Each XPS peak was assigned to one component with reference to Mielczarski et al.'s XPS results (Mielczarski et al., 1996a; Mielczarski et al., 1996b).

The XPS spectra of C 1s from the four chalcopyrite particle suspensions are shown in Figure 6.15 and the peaks were all calibrated by setting the largest peak from hydrocarbon due to carbon contamination and the binding energy as 284.65 eV. The peak at the position of around 286 eV was attributed to carbon atoms bonded to oxygen, possibly also due to carbon contamination, as well as from PEO (where PEO was added). The peak at the position of higher E_B , i.e., above 288 eV, appeared in all four samples and it was assigned to carbon atoms in the impurity carbonate minerals present in the chalcopyrite sample. The peak at the position of lower E_B below 283 eV appeared only in CP and CP-PEO and was attributed to the surface charge of these two samples, where other elements such as O, Cu and S, also showed such low E_B peak in their spectra. In CP-KAX and CP-PEO&KAX, there was a peak at the position of around 287 eV, which was assigned to carbon atoms from KAX since the KAX solution showed a C 1s peak at similar position (Figure 6.16).

The XPS spectra of the Fe 2p electrons are shown in Figure 6.17. All the spectra were deconvoluted into two peaks, one at the position around 710 eV and the other around 707 eV. The former was considered to represent iron oxides and hydroxides ($Fe_{\text{oxide/hydr}}$). The broad band means that several types of iron oxides/hydroxides are present on the surface, such as $Fe(OH)_3$, $Fe(OH)_2$, Fe_2O_3 , Fe_3O_4 etc, due to the complex hydration of chalcopyrite (Cattarin et al., 1990; Pang and Chander, 1990). The second peak was assigned to the iron in the bulk mineral structure (Fe_{miner}).

The XPS spectra of Cu 2p are shown in Figure 6.18. Like the Fe 2p spectra, the Cu 2p spectra were also deconvoluted into two peaks, with the sharp one assigned to copper in the bulk mineral (Cu_{miner}), and the other assigned to copper oxide/hydroxides ($Cu_{\text{oxide/hydr}}$). The difference from Fe 2p spectra is that the area of oxide/hydroxides peak is much smaller than that of the peak from the bulk mineral, which means the hydration of copper is not as severe as iron.

The XPS spectra of O 1s electrons are shown in Figure 6.19. Three peaks at similar positions in all four samples were obtained, at around 530, 531 and 533 eV and were assigned to oxides, hydroxides and frozen water. These results also confirmed that the surface of chalcopyrite was covered with oxides and hydroxides. It should be noted that the full width at half maximum (fwhm) of O 1s from oxides and hydroxides was quite large, which indicated that there were different types of oxides and hydroxides. For CP-PEO and CP-PEO&KAX, a small peak close to the water peak was fitted in, corresponding to the adsorbed PEO. For CP-KAX and CP-PEO&KAX, the peak with highest binding energy, 533.92 eV for CP-KAX and 533.83 eV for CP-PEO&KAX, is due to the adsorbed KAX, because the area of that peak increased significantly in CP-PEO&KAX where the amount of KAX doubled, and was found to be characteristic of oxygen due to the adsorbed xanthate molecules (Mielczarski et al., 1983; Mielczarski et al., 1984). The lower binding energy peaks at around 528.31 eV in CP and CP-PEO are due to surface charge of these two samples.

The XPS spectra of S 2p electrons are shown in Figure 6.20. The reported spectra are the S 2p_{3/2} splitting component. Only two doublets were fitted in the spectra of CP and CP-PEO even though the peak at around 163 eV was very wide. This was because the sulfur species on the chalcopyrite surface were very complex, ranging from metal-deficient sulfide to polysulfides (Buckley and Woods, 1984; Luttrell and Yoon, 1984; Zachwieja et al., 1989). Even if a few more doublets were fitted, it would be difficult to assign particular species to them. The other doublets at around 161 eV was characteristic for sulfur in the bulk mineral structure. Therefore, this simple fitting was used, with one peak for sulfur in the bulk mineral (S_{miner}) and the other (MeS_x) representing various sulfur species. In samples CP-KAX and CP-PEO&KAX where KAX was added, a shoulder appeared in the spectra at higher electron binding energies, which were deconvoluted to one more set of doublets, to account for the sulfur from KAX.

Table 6.4 Binding energy of O 1s peaks of chalcopyrite suspension samples

	O 1s (eV)					
	from KAX	water	From PEO	hydroxide	oxide	surface charge
CP	–	532.84	–	531.42	530.14	528.51
CP-PEO	–	533.64↑	532.79	531.1↓	529.72↓	527.97
CP-KAX	534.04	532.94	–	531.65	530.72	–
CP-PEO&KAX	533.83	533.72↑	533.03	531.95↑	530.31↓	–

In order to investigate the interaction between chalcopyrite and PEO, the binding energy of O 1s should be compared as in the case of quartz. Since chalcopyrite is also negatively charged, the electrical double layer remained in the ice alters the measured binding energy of the elements buried under the ice. For chalcopyrite, the binding energy of sulfur from the bulk mineral is not supposed to change by the added reagents. Therefore, its value, 161.35 eV, was set as the calibration standard. The binding energies of O 1s peaks were then all adjusted, and they are listed in Table 6.4. When comparison was made between CP and CP-PEO, the binding energy of O 1s from oxides and hydroxides went down while that from water went up with the presence of PEO. This trend is the same as in the case of quartz, which means that the oxides and hydroxides on chalcopyrite surface formed hydrogen bonds with PEO when PEO was added. It should be pointed out that due to the variety of the oxides and hydroxides, the chemical shift of these two peaks may be caused by the change of chemical composition of these mixtures. But the positive chemical shift of O 1s from PEO, which was calculated to be 0.5 eV, with binding energy being shifted from 532.29 eV to 532.79 eV, confirmed the hydrogen bonding formation. When the binding energy of O 1s in CP-KAX was compared with that in CP-PEO&KAX, the same trend was found except that the binding energy of O 1s from hydroxides went up instead of down. The increase might be caused by the less severe hydration as a result of higher

dosage of KAX. The chemical shift of O 1s from PEO was still positive (0.14 eV), which still provided the evidence of hydrogen bonding.

The XPS analysis provided evidence for hydrogen bonding but unfortunately no information about electrostatic interaction could be derived. The reason is that the negative charge sites could not be determined. As discussed above, the chalcopyrite surface is comprised of oxides/hydroxides and metal-deficient sulfide due to oxidation and hydration. At zero point charge of chalcopyrite, which is about pH 2, the major species on chalcopyrite is metal-deficient sulfide, which means metal-deficient sulfide is not significantly charged. Therefore, the charge of chalcopyrite is probably caused by the deprotonation of hydroxyl group on hydroxides. Due to the complex composition of the hydroxides, it is difficult to accurately deconvolute the peak corresponding to the deprotonated hydroxyl as was performed in quartz case.

Table 6.5 Binding energy of S 2p peaks of chalcopyrite suspension samples

	S 2p _{3/2} (eV)			
	S _{mineral}	MeS _x	from KAX	surface charge
CP	161.35	162.6	–	159.12
CP-PEO	161.35	162.57	–	159.1
CP-KAX	161.35	163.18	162.28	–
CP-PEO&KAX	161.35	164.42	162.74	–

The peaks of S 2p for all the four samples were also calibrated using S_{mineral} 161.35 eV as standard and they are listed in Table 6.5. Comparison of binding energy of S 2p was first made between CP and CP-KAX to see the effect of KAX adsorption. S 2p binding energy went up by 0.58 eV, which means that the addition of KAX enhanced the oxidation of sulfur in chalcopyrite. The larger increase (1.82 eV) in CP-PEO&KAX, where the amount of KAX added doubled,

also suggested the positive effect of KAX on chalcopyrite oxidation. The binding energy of S 2p from KAX is 161.71 eV shown in Figure 6.16, and its chemical shift was calculated to be 0.57 eV in CP-KAX and 1.03 eV in CP-PEO&KAX. These increases indicate that the sulfur in KAX was oxidized as well. It is commonly accepted that the adsorption of xanthate on chalcopyrite produces two products: dixanthogen and copper xanthate (Ackerman et al., 1987; Leppinen et al., 1989). The oxidation of KAX might have produced dixanthogen. The more severe oxidation of chalcopyrite may be due to the change of the potential of the system caused by the addition of KAX, or due to a reaction between the metal-deficient sulfide and KAX.

The point here is to find out how KAX replaced the pre-adsorbed PEO on chalcopyrite. As discussed above, chalcopyrite can be easily oxidized. What happens during oxidation probably is that the oxidation takes place on S sites and affects the chemical environment of Cu and Fe, which are then hydrolyzed, forming hydroxides and metal-deficient sulfides. Some of the hydroxides would go through dehydration and produce oxides. Since Fe has stronger tendency to be hydrolyzed than Cu, there are more iron oxides/hydroxides. In a sense, the oxides/hydroxides and metal-deficient sulfides intergrow with each other. When PEO was added, it attached to the oxides/hydroxides mainly through hydrogen bonding. However, when KAX was added, it would adsorb on metal-deficient sulfides and produce dixanthogen, copper xanthate and other unknown xanthate product. These precipitates would cover the oxides/hydroxides and destroy the hydrogen bonding.

As discussed in Chapter 5, in chalcopyrite/quartz flotation system, the entrainment of quartz could be reduced by flocculation. But PEO could flocculate both minerals together and it was KAX that separated chalcopyrite from the hetero-flocs by destroying the flocs. If this hypothesis is right, the entrainment of quartz could be further reduced by splitting KAX addition, one portion before PEO and one portion after PEO. After KAX is added, the chalcopyrite surface

would be mainly covered with xanthate product. When PEO is then added, it would prefer quartz to chalcopyrite, so that less chalcopyrite would be trapped in the hetero-flocs. Then the rest of the KAX is added, it would liberate the trapped chalcopyrite by destroying the hetero-flocs but the degree of destruction would be less since less chalcopyrite is trapped. Therefore, more quartz particles could remain in flocs and its entrainment reduced.

6.4 Summary

Adsorption density, zeta potential, flocculation/dispersion and X-ray photoelectron spectroscopic measurements indicated that PEO adsorbs on quartz mainly through hydrogen bonds, which were formed between the “free” ether oxygen in PEO and the isolated “free” silanol groups ($>SiOH$) on quartz. Water competes with PEO for proton donor of the quartz surfaces. Electrostatic interaction also plays a minor role, by slightly attracting PEO and repelling water. The effect of pH on quartz flocculation reflected these combined interactions. At low pH, the strong adsorption of water on quartz surface probably leaves few isolated surface silanol groups to form hydrogen bonds with PEO, and the PEO molecules may also have few “free” ether oxygen site due to its strong affinity to proton (H^+), which are abundant at low pH. At high pH, the adsorption of water is inhibited by the high electrical field but the total number of surface silanol groups $>SiOH$ is less. Therefore, only neutral pH favors the hydrogen bonding between PEO and quartz, where the adsorption of water is inhibited to some degree and a fair number of “free” silanol groups are available to form hydrogen bonds with PEO. Both hydrogen bonding and electrostatic interaction between PEO and quartz were verified by cryo-XPS measurement.

Hydrogen bonding was also the major interaction mechanism between PEO and chalcopyrite, the surface of which is covered with oxides/hydroxides due to oxidation and hydration. Their origin accounts for the effect of pH on chalcopyrite flocculation. At low pH, these oxides/hydroxides dissolve in solution,

leaving little hydroxyl groups for hydrogen bonding with PEO. With the increase in pH, more oxides/hydroxides precipitate on the surface and lead to strong interaction and flocculation. The addition of KAX produces a layer of xanthate product, which covers the oxides/hydroxides layer and destroys the hydrogen bonding. This explains the destructive effect of KAX on chalcopyrite/quartz flocs formed by PEO.

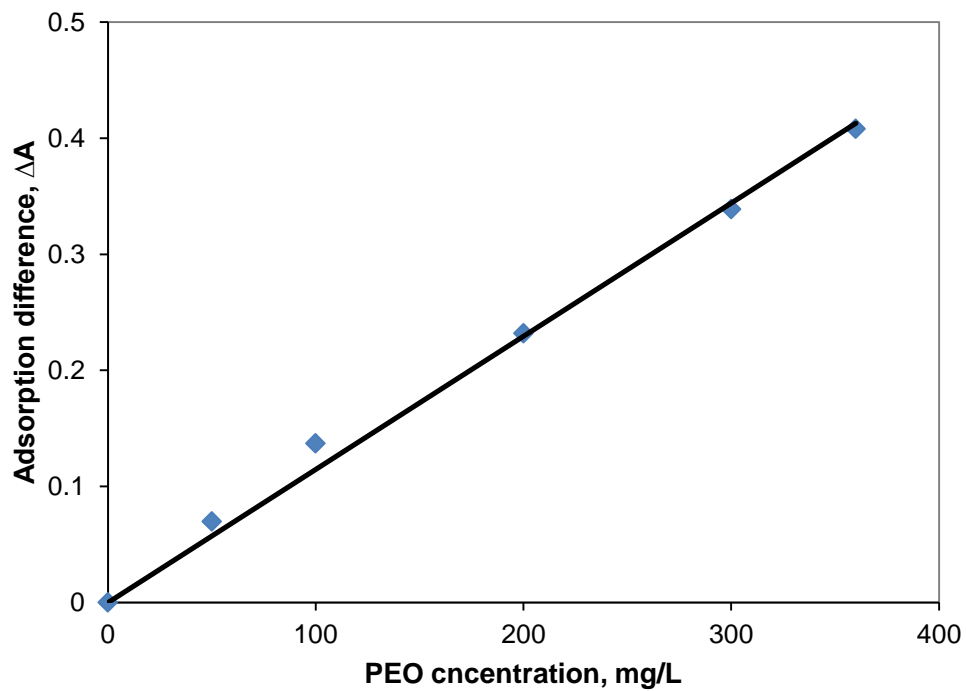


Figure 6.1 Calibration curve for PEO concentration determination

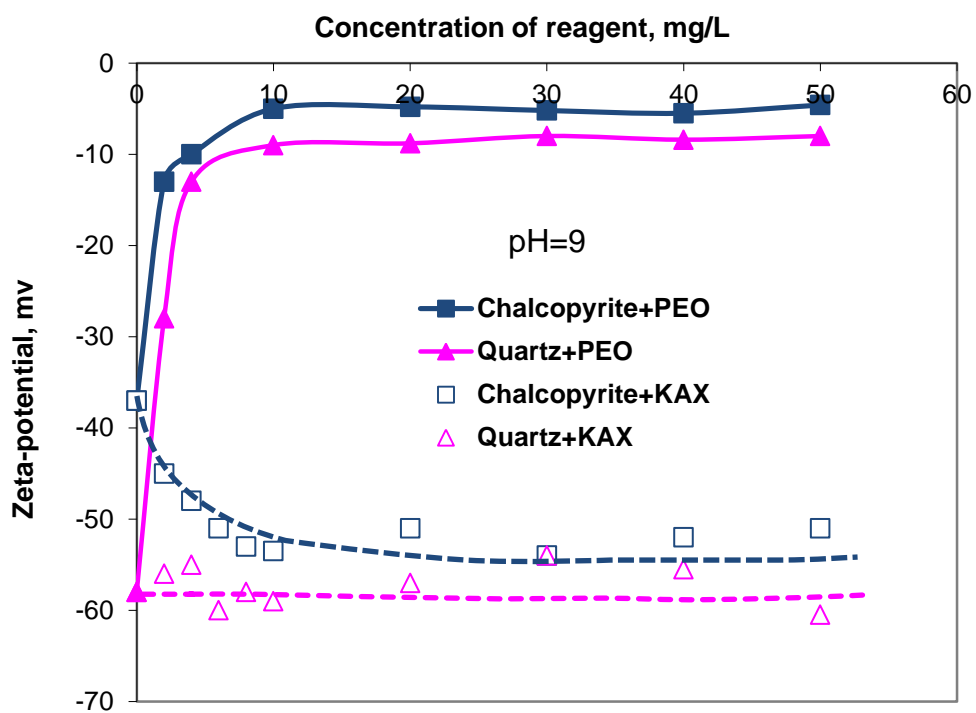


Figure 6.2 Effect of KAX and PEO on the zeta potentials of chalcopyrite and quartz.

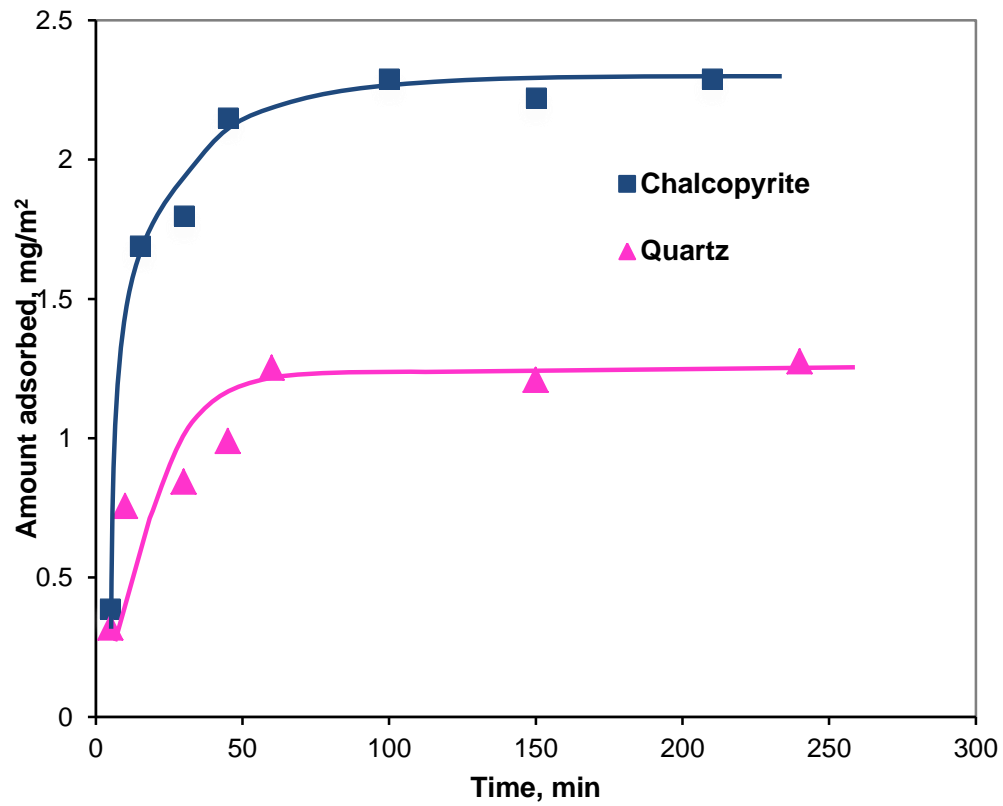


Figure 6.3 Adsorption kinetics of PEO on quartz and chalcopyrite particles

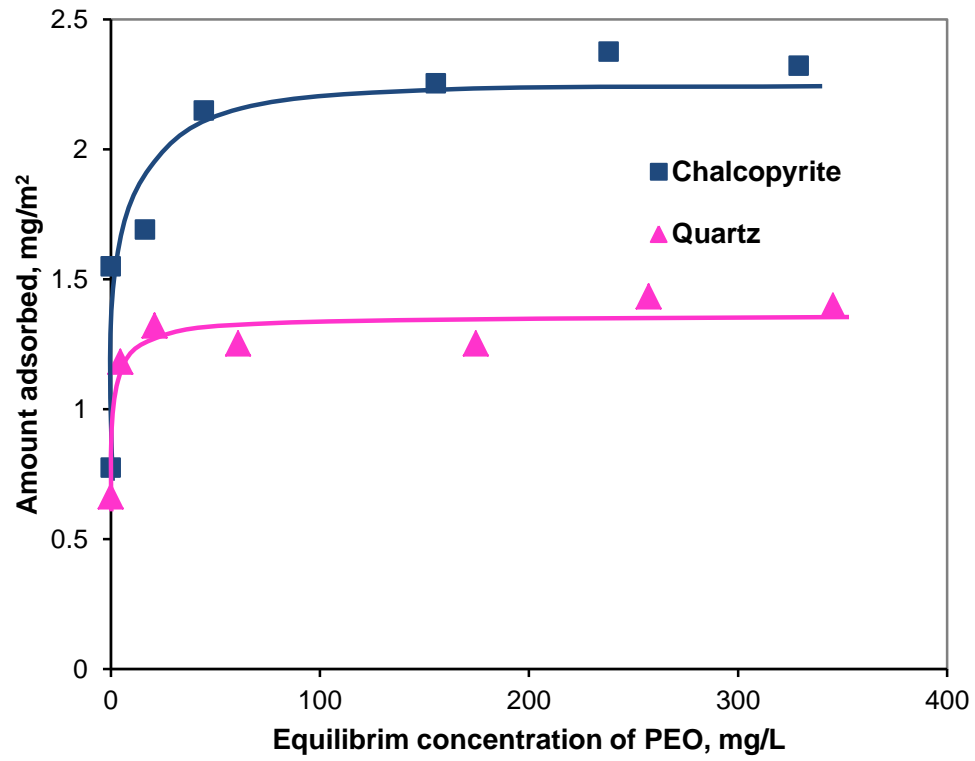


Figure 6.4 Adsorption isotherm of PEO on quartz and chalcopyrite particles

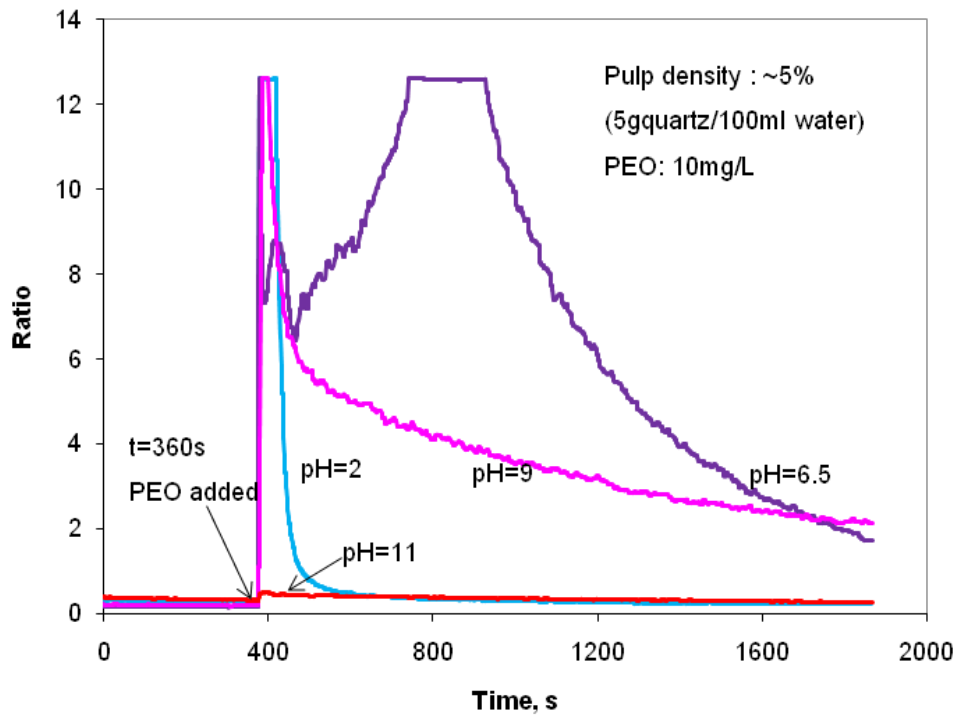


Figure 6.5 Effect of pH on quartz flocculation by PEO.

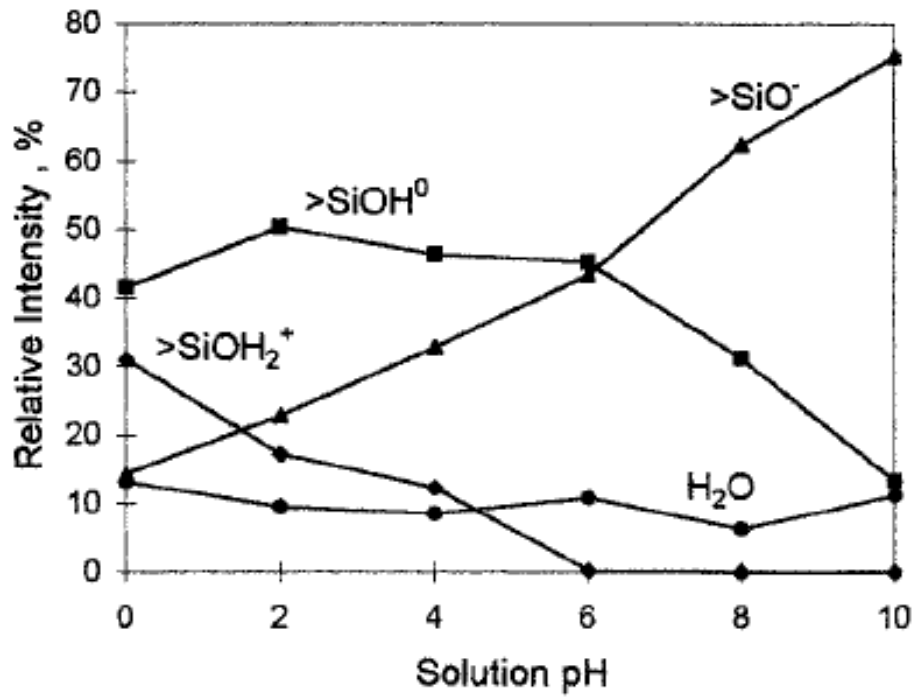


Figure 6.6 Relative surface density of three surface species on quartz surface.
(Duval et al., 2002)

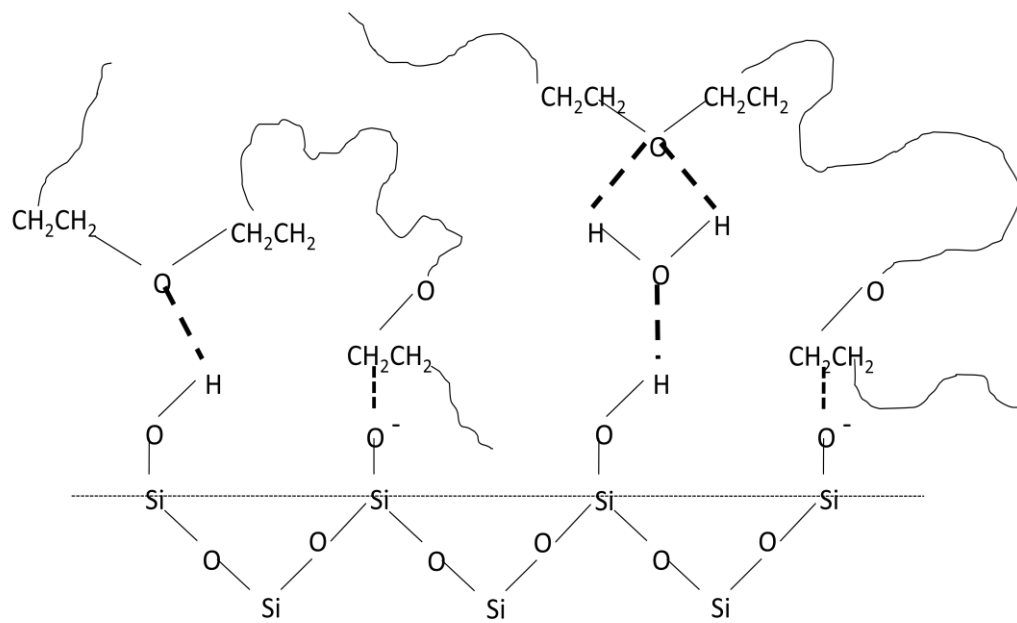


Figure 6.7 Schematic diagram of the conformation of PEO chains adsorbed on quartz surface.

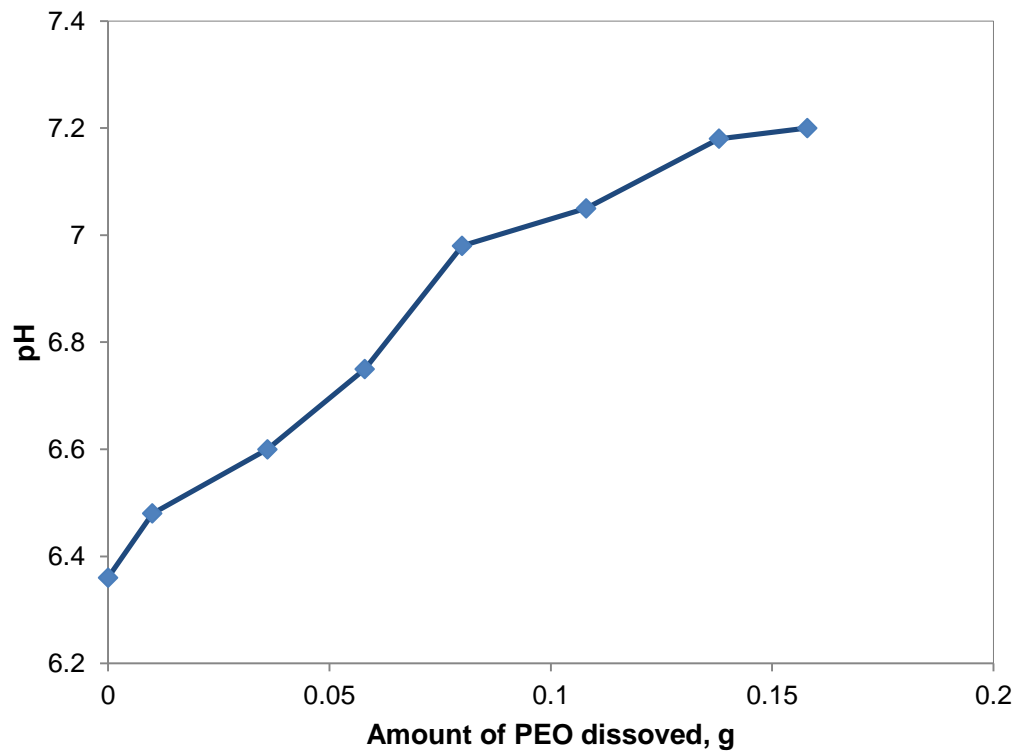


Figure 6.8 The change of pH of PEO solution as the function of the amount of PEO dissolved.

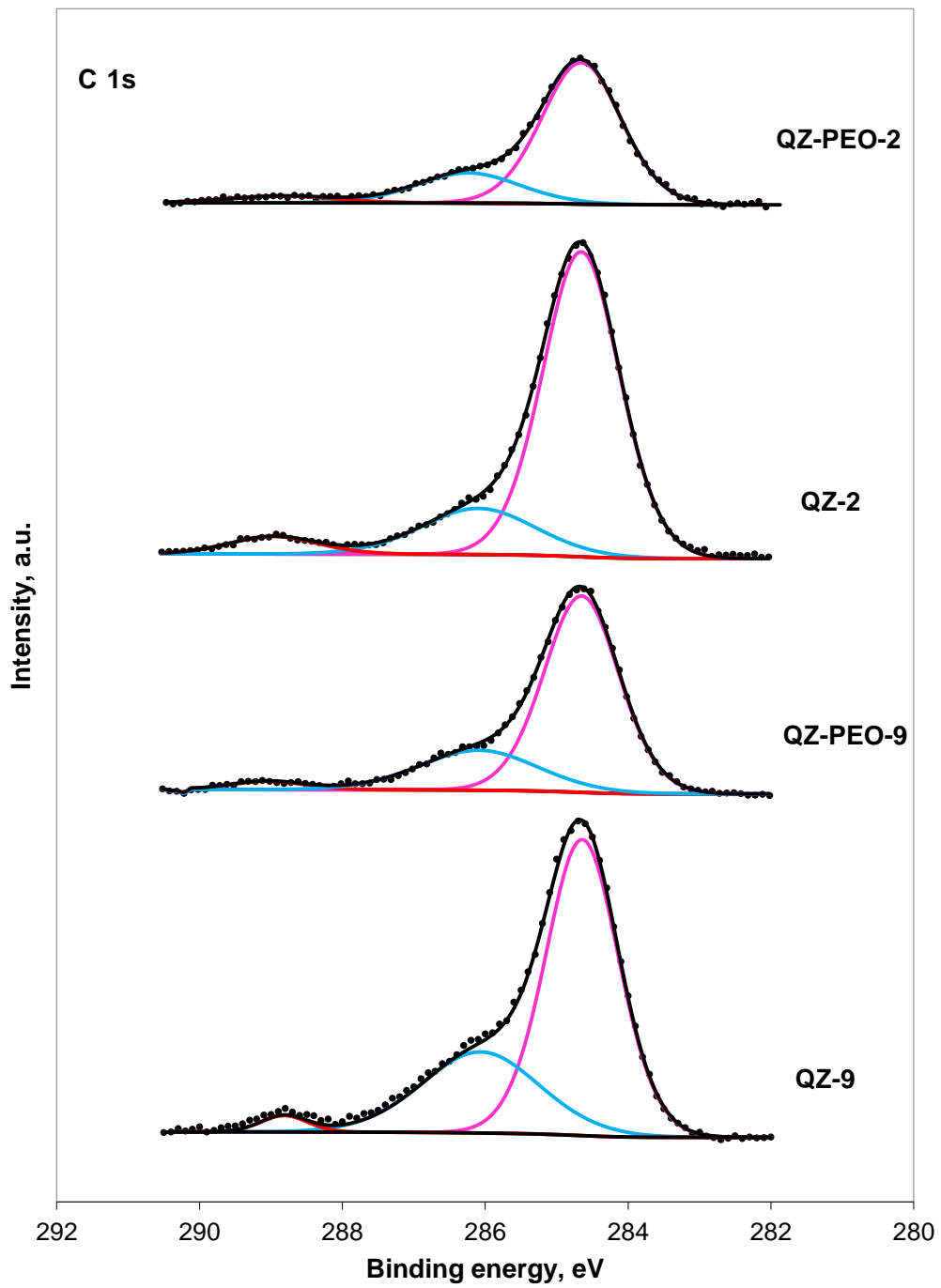


Figure 6.9 XPS spectra for C 1s region of the four quartz suspension samples.

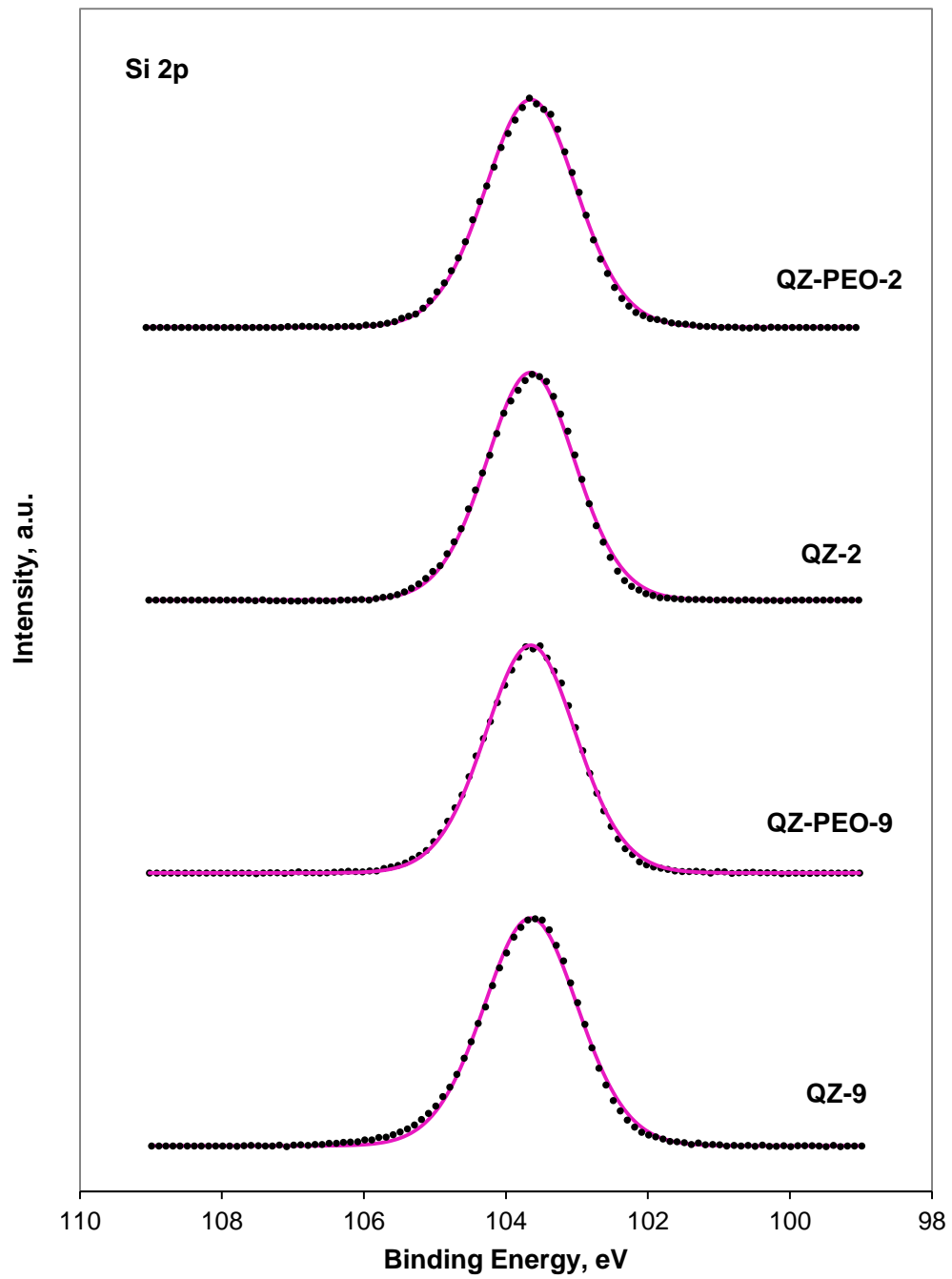


Figure 6.10 XPS spectra for Si 2p region of the four quartz suspension samples.

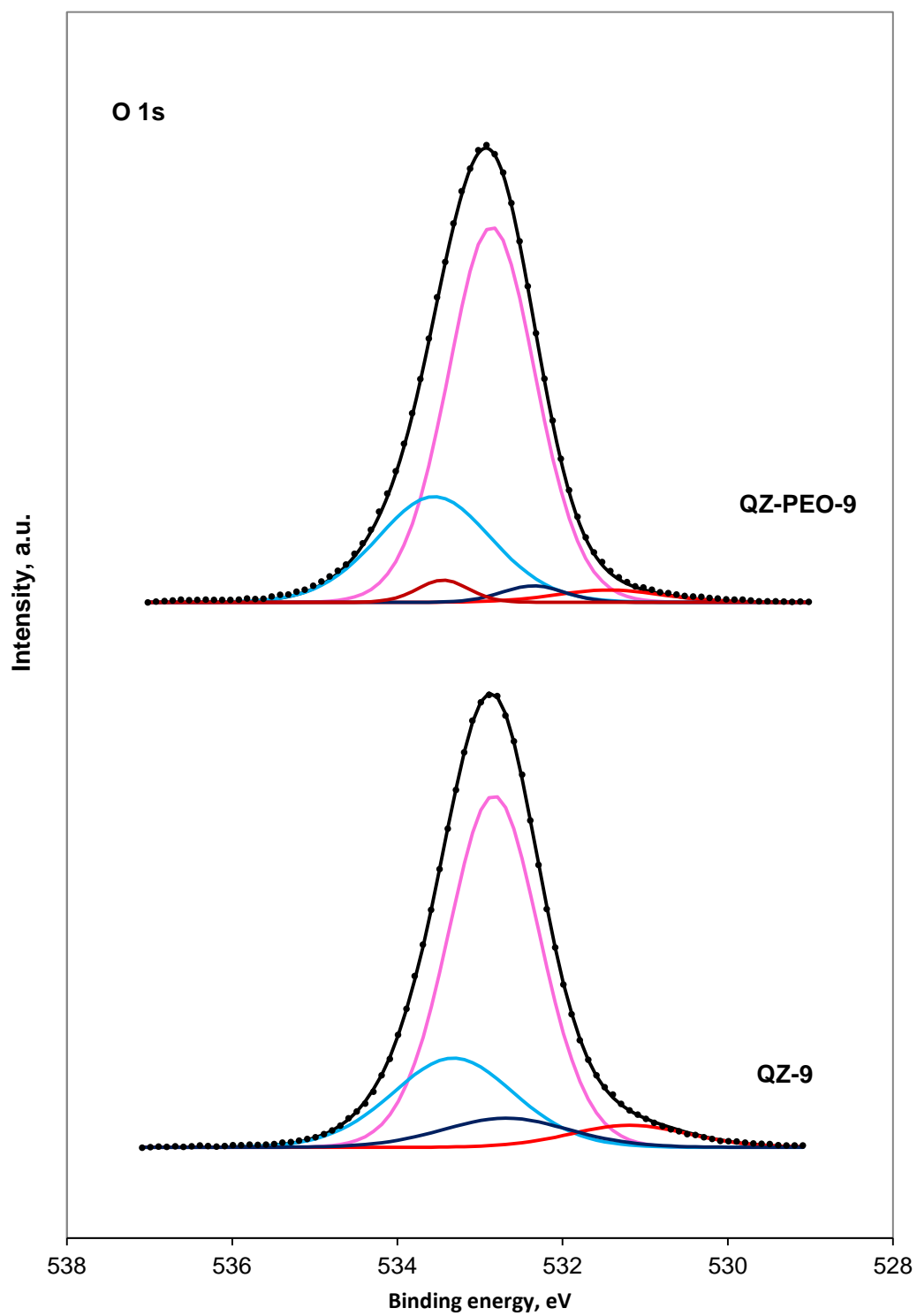


Figure 6.11 XPS spectra for O 1s region of the quartz samples at pH=9.

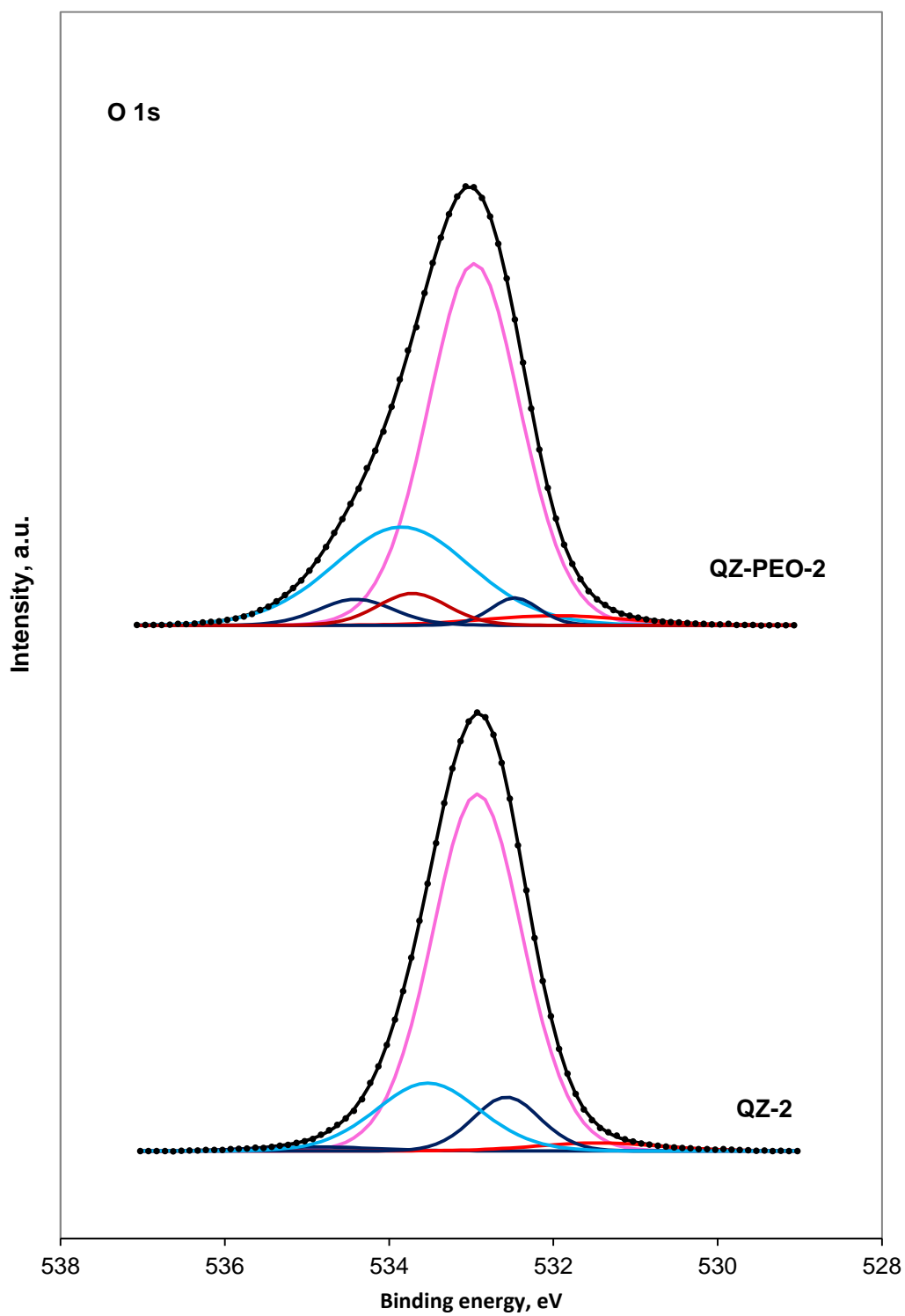


Figure 6.12 XPS spectra for O 1s region of the quartz samples at pH=2.

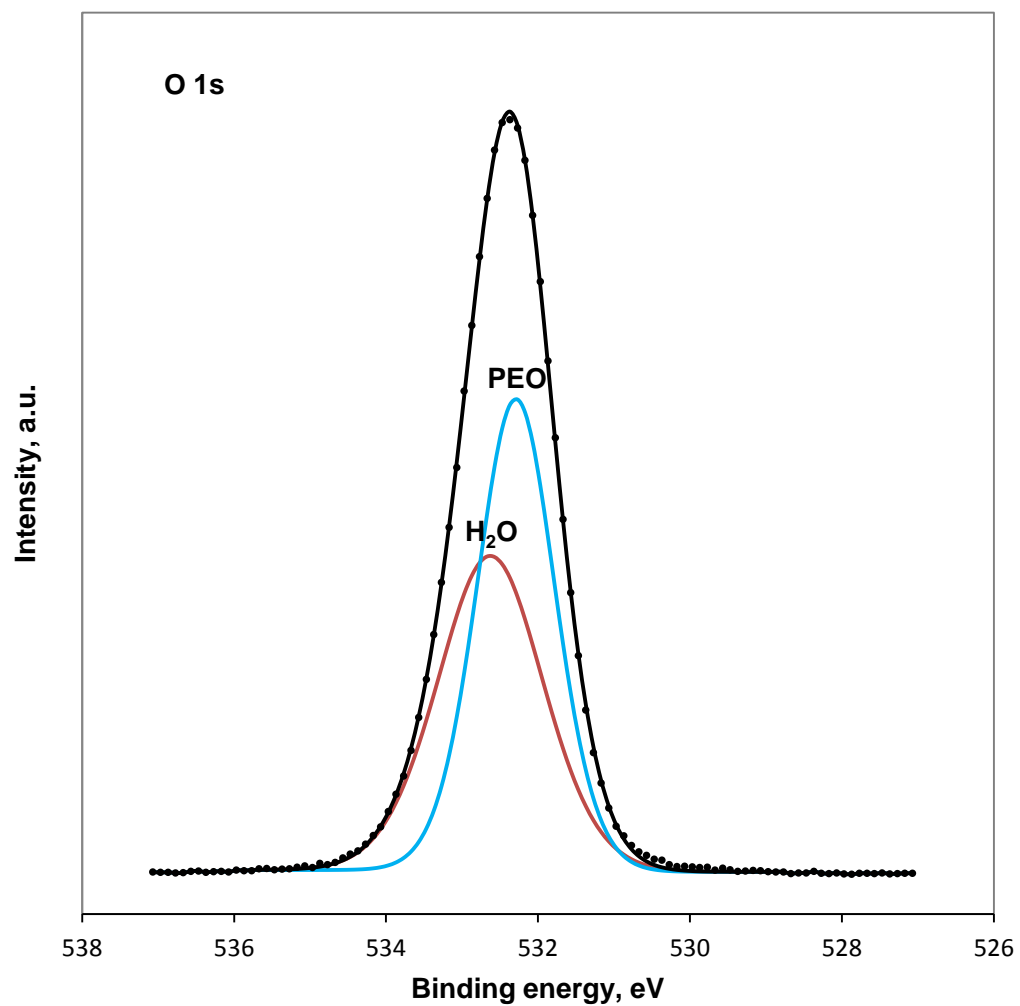


Figure 6.13 XPS spectra for O 1s region of the PEO solution at pH=9.

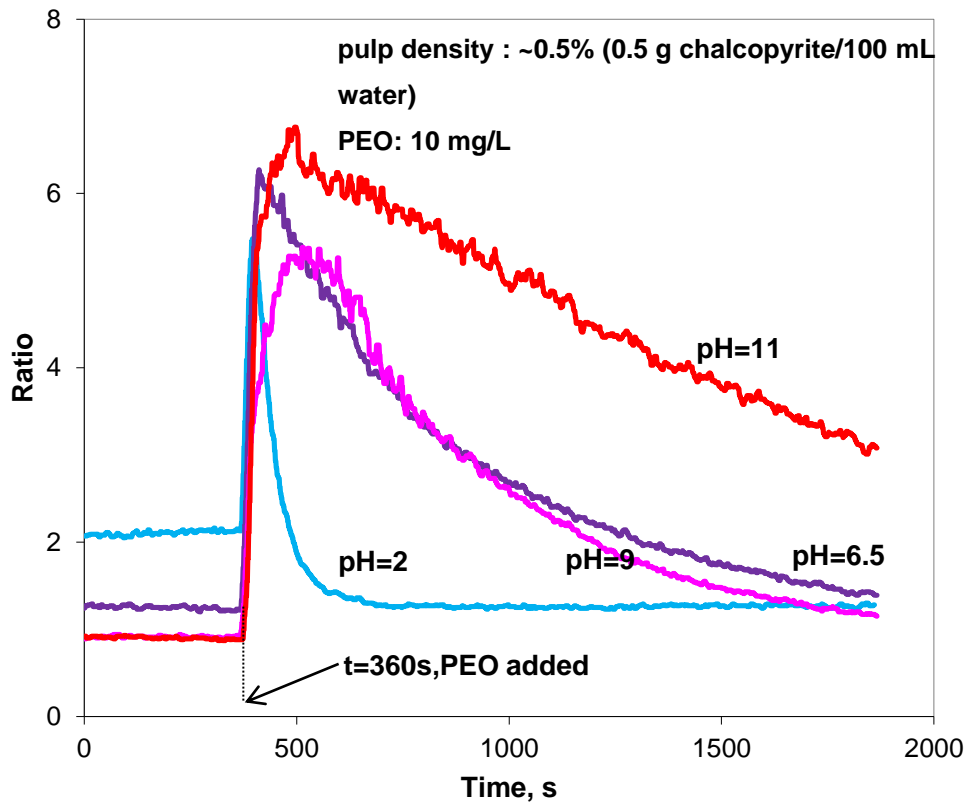


Figure 6.14 Effect of pH on chalcopyrite flocculation by PEO.

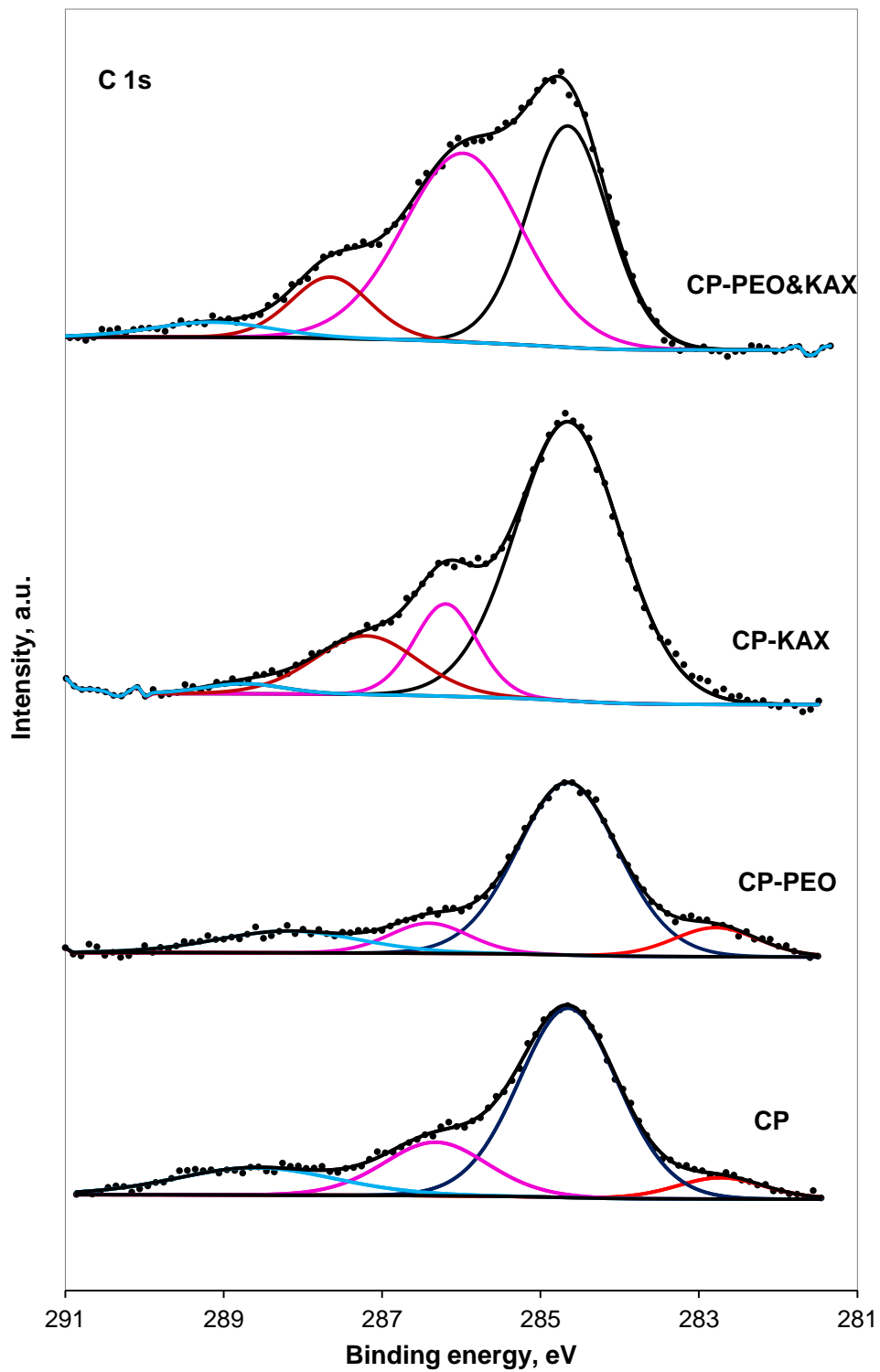


Figure 6.15 XPS spectra for C 1s region of the chalcopyrite suspension samples.

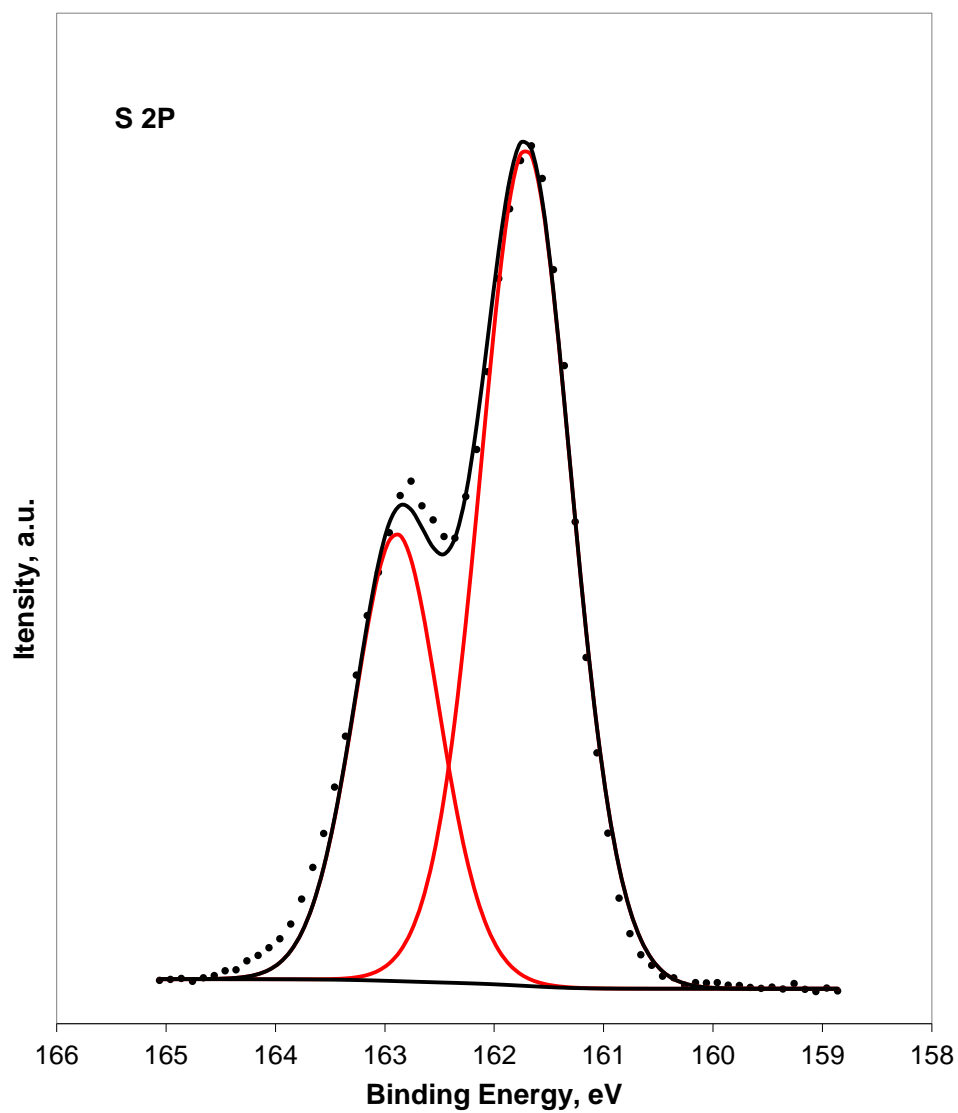


Figure 6.16 XPS spectra for S2p region of KAX solution.

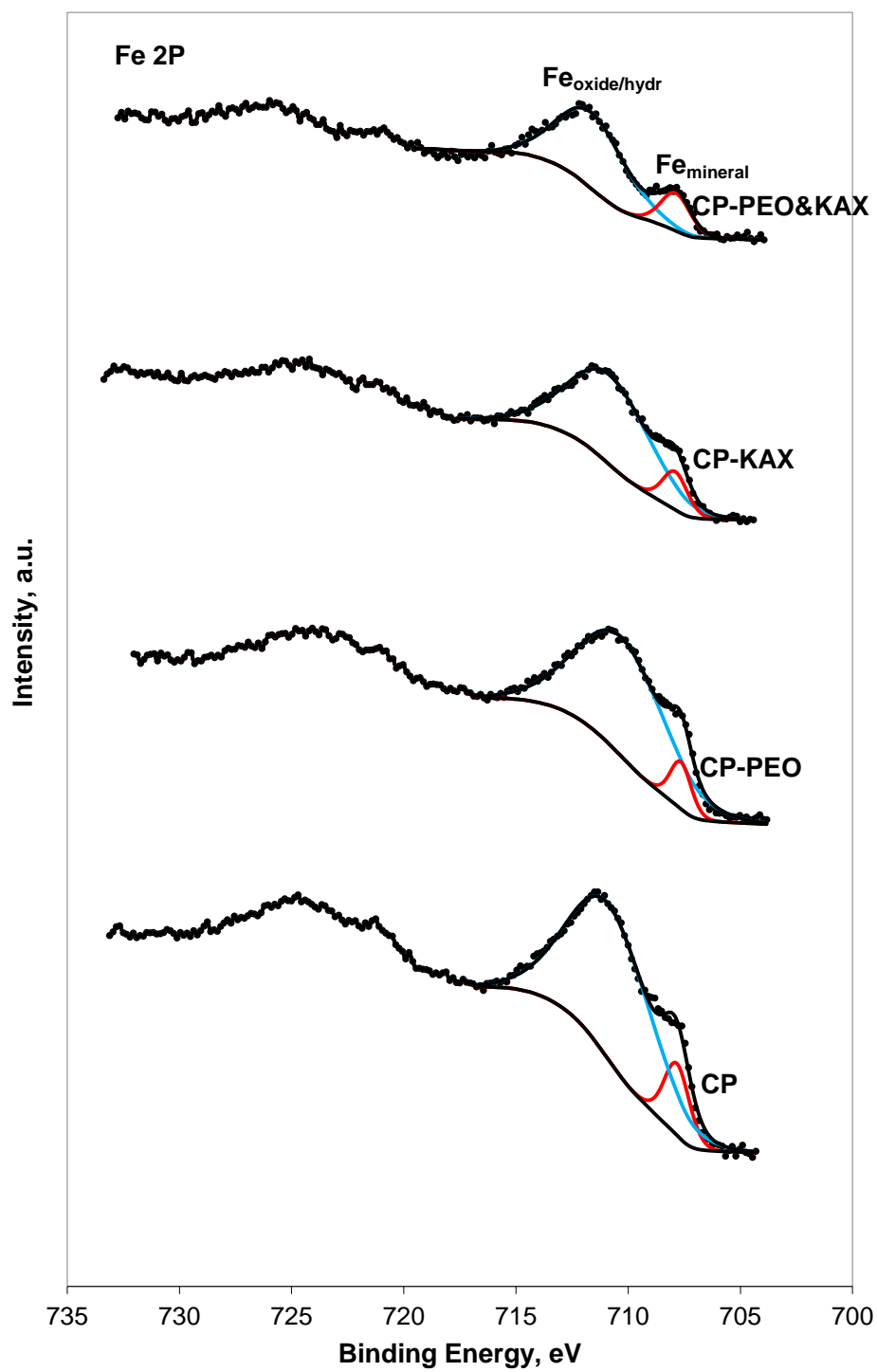


Figure 6.17 XPS spectra for Fe 2p region of the chalcopyrite suspension samples.

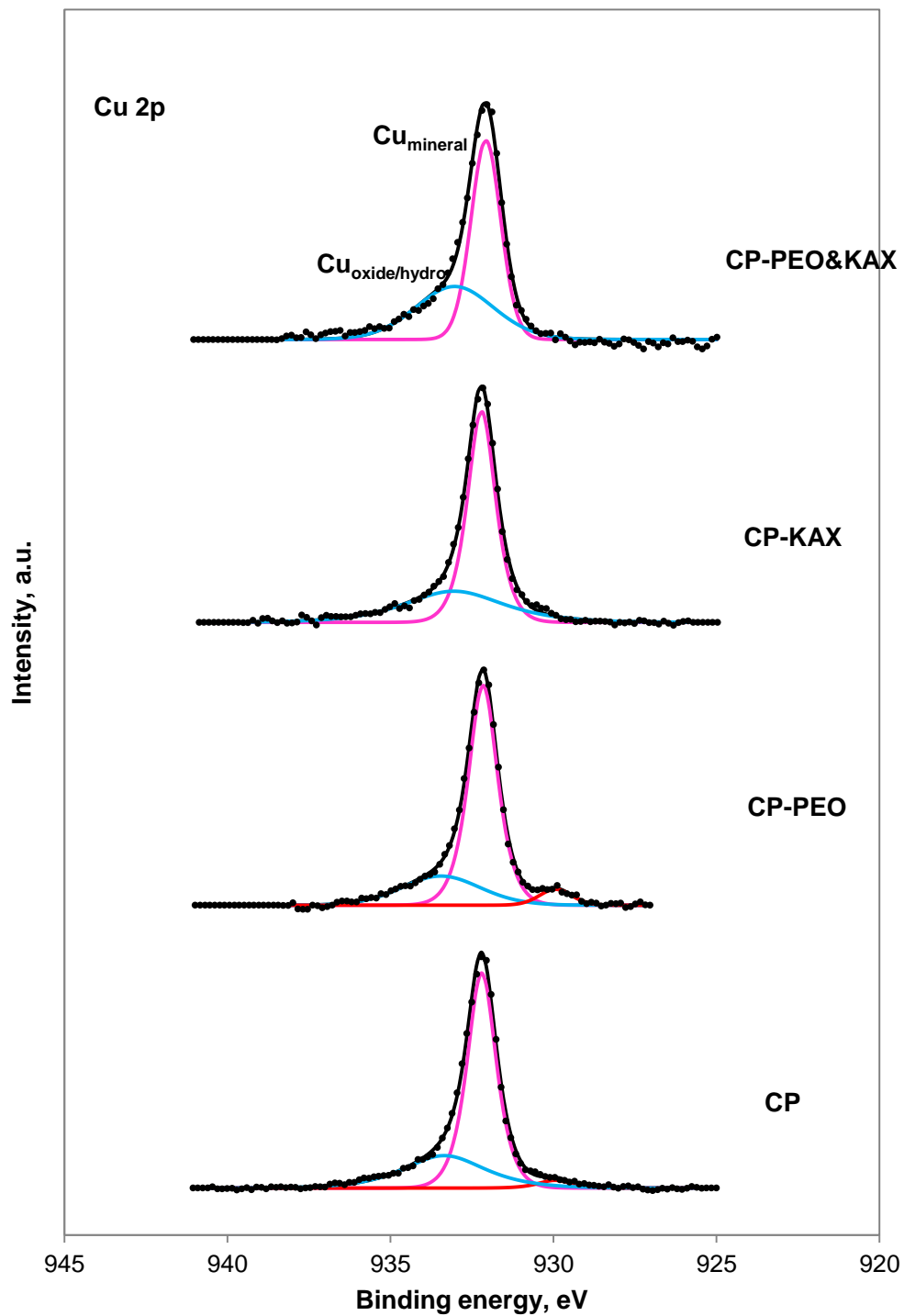


Figure 6.18 XPS spectra for Cu 2p region of the chalcopyrite suspension samples.

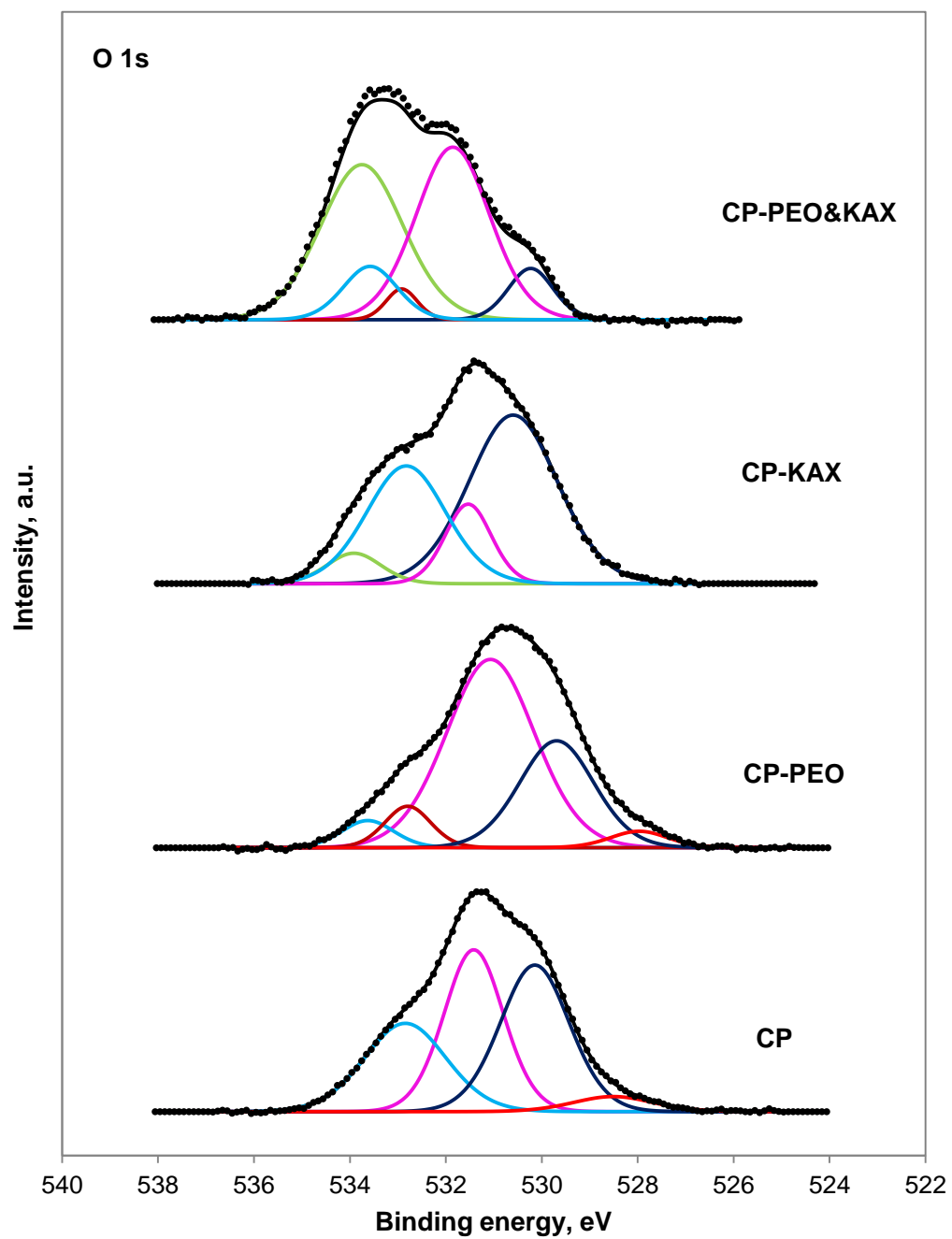


Figure 6.19 XPS spectra for O 1s region of the chalcopyrite suspension samples.

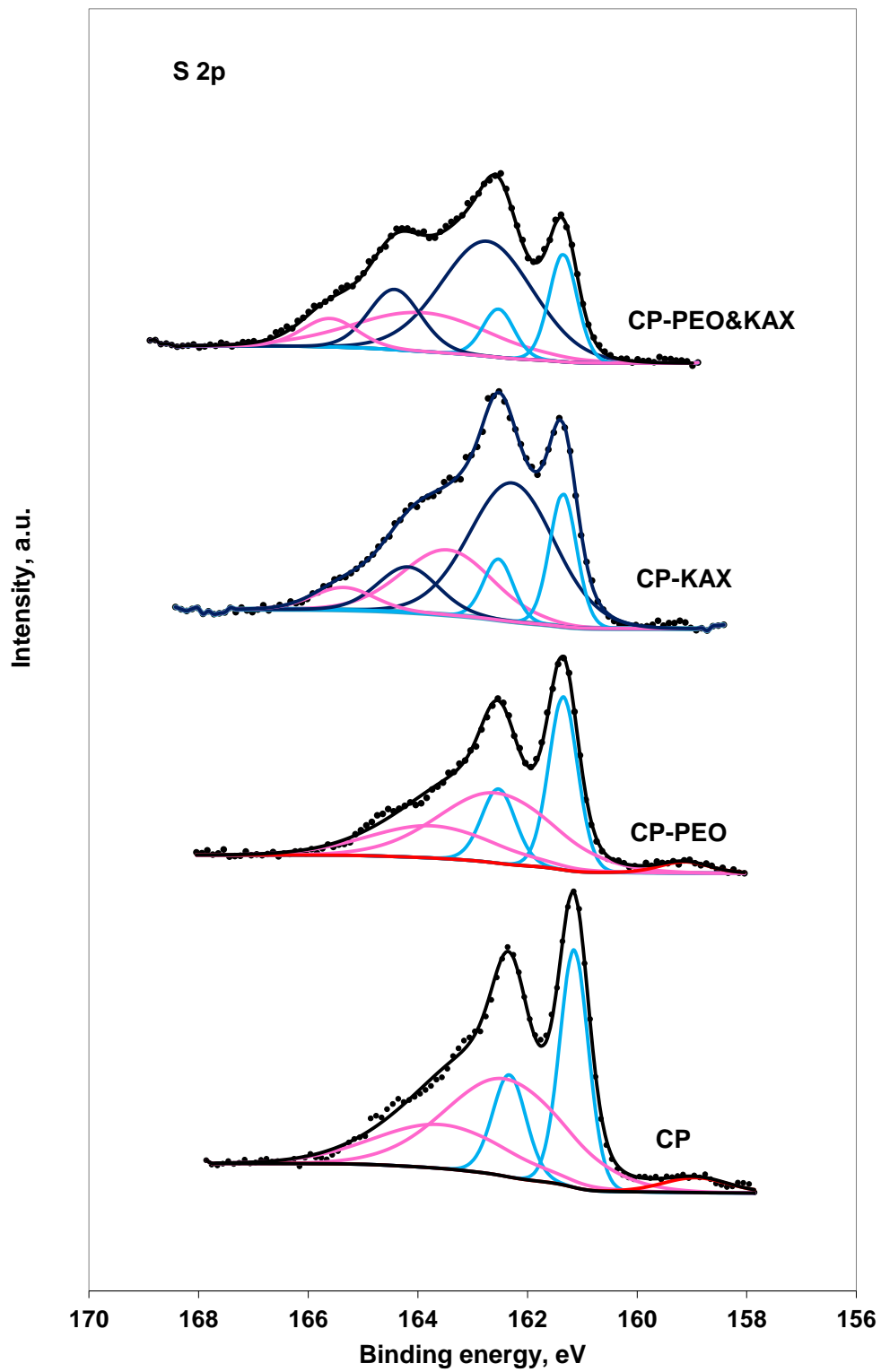


Figure 6.20 XPS spectra for S 2p region of the chalcopyrite suspension samples.

Chapter VII Effect of PEO Dissolution States on PEO-Induced Flocculation

7.1 Introduction

As discussed in previous chapters, the beneficial role of PEO to assist in the rejection of quartz gangue in the studied sulfide flotation system lies in its ability to flocculate quartz, albeit non-selectively. There are a number of factors which can affect the performance of the polymeric flocculants, such as molecular weight, polymer dosage, polymer stock solution concentration, polymer charge density, suspension pH and ionic strength, pulp density and shear, etc. With flocculation being one of many sub-procedures of the whole complex froth flotation system, it would be more desirable and practical to achieve better flocculation only through manipulating polymeric flocculant itself. As for PEO, however, its flocculation performance is difficult to control and subject to many variables, such as molecular weight, stock solution concentration, shear history, temperature, polymer solution storage time and its injection manner (Killmann et al., 1986; Brine et al., 1992a; Gibbs and Pelton, 1999; Bednar et al., 2008). In order to achieve stable results when applying PEO in the sulfide flotation system, a systematic study has been carried out to understand the mechanism behind PEO-induced flocculation.

7.2 Experimental

7.2.1 Materials and chemicals

The materials and chemicals used in sedimentation tests were the same as in PDA flocculation tests (Chapter 5) and were described in section 5.2.1.

7.2.2 Sedimentation tests

Flocculation of quartz particles by PEO was determined by sedimentation tests conducted in a 250-mL graduated cylinder. In the test, 15 grams of the quartz

particles were conditioned in 150 mL water in a 250-mL beaker at the pH of 9 for 3 min, followed by the addition of the PEO stock solution and 3 min of stirring using a magnetic stirrer. The stirring bar was 51 mm long and the stirring speed was fixed at 330 rpm. The addition rate of the PEO stock solution was fixed at 1 mL/min using a peristaltic pump as it is found that the addition speed affects PEO flocculation efficiency (van de Ven et al., 2004). The amount of PEO added was controlled by varying the flowing time.

After conditioning, the slurry was transferred to the 250-mL graduated cylinder and small amount of distilled water was added to bring the water level to 250 mL. The cylinder was then stoppered, inverted 9 times, and set still in the upright position. The slurry of the upper 200 mL was siphoned out after settling for 1 min, and the contents of solids in the bottom 50 mL were determined. A “degree of flocculation” was calculated as the percentage of solids settled into the bottom 50 mL.

7.2.3 Viscosity measurement

An Ostwald viscometer was used to measure PEO solution viscosity. To carry out the measurement, certain amount of PEO solution was added to the lower bulb, drawn into the upper bulb by suction and allowed to flow down through the capillary into the lower bulb. The time taken for the level of the solution to pass the marks was record.

7.2.4 Visual observation

Pictures of PEO suspension were taken on a Canon EOS T1i Digital SLR camera using a Canon Macro Lens EF 108 mm 1:3.5 L lens. Video clips were taken using the same microscope - video system described in section 5.2.3 and the hydraulic micromanipulator of the equipment set was utilized. The detail will be described below.

7.3 Results

7.3.1 Effect of PEO dissolution time on the sedimentation of quartz

The sedimentation behavior of the fine quartz sample in the presence of PEO was studied by conventional settling tests in 250-mL graduated cylinders. Stock PEO solutions were prepared at two concentrations, 0.05% and 0.1%, respectively. The solutions were prepared in the same way except that the stirring time was varied, and were added to the slurry directly at the rate of 1 mL/min. The dosage for all tests was the same at 33.3 g PEO/t quartz, with the addition time of 1 min for the 0.05% stock PEO solution and 0.5 min for the 0.1% stock PEO solution. The results of the sedimentation tests are shown in Figure 7.1. In this figure, the percentage of quartz settled to the bottom 50 mL sludge in the 250-mL graduated cylinder is plotted as a function of the stirring time of the stock PEO solution, i.e., the “dissolution time”. As can be seen from the figure, both the 0.05% and 0.1% stock PEO solutions showed the same trend – that flocculation efficiency of PEO reached the maximum at about 10 min dissolution time and dropped gradually at longer dissolution times. This result is contrary to conventional wisdom that better flocculation performance should be achieved by using more solubilized polymer solutions, as the polymer molecules will be more evenly distributed.

It was observed that when the PEO granules were sprinkled on a stirring water vortex, they became swollen first and it took about 40 minutes for all the swollen granules to “disappear”. Figure 7.2 shows these swollen PEO granules. As can be seen, when the PEO granules are being dissolved, water molecules penetrate into the granules, making it swollen and semi-transparent. With continuous stirring, the molecular chains detach from the swollen granules gradually. When thermodynamic equilibrium is reached, the PEO molecules become single coils or clusters. The dissolution process is schematically illustrated in Figure 7.3. When the dissolution time period is short, the swollen granules can still be seen with naked eyes, the dissolution equilibrium has not been reached, and the molecular chains are still entangled together. The swollen granules can be thought of as

undissolved aggregates of PEO molecular chains. The sizes of the undissolved aggregates increase at the beginning of dissolution due to water penetration and swelling. With continuous stirring, they reach a maximum and then decrease as the detachment of the molecular chains from the aggregates outpaces the water penetration/swelling. For the 0.1% and 0.05% stock PEO solutions, with the same dissolution time, the sizes of undissolved aggregates in both solutions are probably about the same, so are their flocculation performance. The sizes of aggregates likely reached the maximum at about 10 min because the best flocculation took place at that point.

7.3.2 Effect of storage temperature of the PEO solutions on the sedimentation of quartz

It has been reported that aging deteriorates the flocculation efficiency of the PEO solutions (Kratochvil et al., 1999). If the flocculation efficiency is indeed determined by the dissolution process of PEO, with the highest efficiency being at the maximum undissolved aggregate size, it is logical to reason that the deteriorating effects of aging a PEO solution can be slowed down using lower storage temperature since the dissolution rate would be reduced by the lower temperature.

Two 0.05% PEO solutions were prepared and after dissolving for 10 min, both solutions were kept still. One solution was placed in a water-ice mixture bath and kept in the refrigerator. The temperature of the solution was kept around 5°C and the sample was designated as PEO-5. The other solution was kept at room temperature, which happened to be 28°C (PEO-28). Both solutions were then used in the flocculation tests, and the results are shown in Figure 7.4. As can be seen, PEO-5 performed much better than PEO-28. This result is consistent with the hypothesis suggested above. At the lower temperature, the molecular chains detach more slowly from the undissolved aggregates, so that with the same aging time, the sizes of the aggregates in PEO-5 should be larger than those in PEO-28.

Since the two solutions are of the same concentration, their aggregates sizes can be compared by measuring their flowing time through a viscometer. Ostwald viscometer was used for this purpose and the results are shown in Figure 7.5. In order to eliminate the effect of temperature on viscosity, the viscometer with PEO-5 solutions was placed in a water-bath heater for 20 mins before measurement. As expected, the flowing time of PEO-5 was longer than that of PEO-28. These results confirmed that at the same dosage, the larger the PEO undissolved aggregates, the better their flocculation performance.

7.3.3 Effect of preparation method of PEO solution on the sedimentation of quartz

The aforementioned testwork confirmed that the flocculation efficiency of PEO could be reduced by aging of the PEO solution. However, (Hood et al., 1985) reported that if a PEO solution was stored at high concentrations, aging did not have any significant effect on its flocculation performance. In their experiments, a 0.25% PEO stock solution was prepared and kept in a refrigerator until needed. The reproducibility was good and no effect of aging was reported. To further study the phenomena, a high concentration PEO stock solution, 0.5%, was prepared and aged for 18 hrs and then diluted to 0.05%. The 0.5% PEO solution was treated the same way as PEO powder to prepare the 0.05% PEO solution, i.e., 10 mL 0.5% PEO solution was withdrawn and mixed with 90 mL water using a magnetic stirrer. The stirring time (dissolution time) was set at 5, 10, 25, 45 and 60 min. Similarly, PEO granules were sprinkled to a stirring water vortex with a magnetic stirrer (different stirring times) to make a 0.05% solution. The two sets of 0.05% PEO solutions were then used in the quartz flocculation tests. The results were shown in Figure 7.6. As can be seen, unlike the 0.05% stock solutions prepared with PEO granules, the 0.05% stock solution prepared by diluting the concentrated 0.5% PEO solution did not show significant drop in flocculation efficiency even though it had been aged for 18 hrs. It seems that aging indeed has no effect on PEO solutions with high concentrations.

In fact, it was observed that the concentrated 0.5% PEO solution looked quite different from the low concentration PEO solutions (0.1% or 0.05%). It was very viscous and was more like a gel than a liquid. During the preparation of the 0.5% solution, the PEO granules were swollen first and the swollen granules disappeared after stirring for about 40 min, a phenomenon similar to the low concentration (0.05%) PEO solution. However, the suspension became very viscous and gel-like within a short dissolution time when the swollen granules were still visible. Apparently, 0.5% is above the critical overlapping concentration of this PEO sample, above which the molecular chains all tangle together, form an inter-connected network and tend to be distributed evenly (Strobl, 2007), as shown schematically in Figure 7.7, the sketch in the middle.

When this thick gel-like PEO solution was diluted, the network would be broken into smaller pieces and dispersed in water, with the molecular chains gradually detaching from it due to the penetration of water molecules. The dilution process is also illustrated in Figure 7.7. From the perspective of dissolution, this interconnected PEO network is similar to PEO granules except that it is one large single piece of relatively loose aggregate while the PEO granules are made of a number of smaller dense aggregates. A picture was taken when one mass of 0.5% solution was injected into water to illustrate such difference, as shown in Figure 7.8. It is likely that it takes longer time to dissolve the large single piece of networked aggregate than the smaller granules, so that the sizes of undissolved aggregates are larger at any given stirring time for the 0.5% \rightarrow 0.05% diluted PEO solutions than the PEO solutions prepared from dry granules, which is probably why the flocculation efficiency of the 0.5% \rightarrow 0.05% diluted PEO solution is higher. The measurement of flowing time in the Ostwald viscometer also suggested that the aggregates were larger and more resistant to stirring for the 0.05% PEO solutions diluted from the 0.5% solution (Figure 7.9). However, at short stirring time, i.e., 5 min, the flocculation efficiency of this solution was quite low (Figure 7.6) even though the sizes of aggregates at that moment are expected

to be large because of the short stirring time. The reason might be because the stirring time was too short to break down the large aggregate so that the number of aggregates was too small to provide enough flocculation sites for quartz particles.

Therefore, it seems that aging only affects the flocculation efficiency of PEO solutions of low concentrations because the undissolved aggregates sizes in those solutions decrease with time. At high concentrations, since the molecular chains are well connected, aging does not affect the flocculation efficiency significantly. This phenomenon suggests a more effective way to prepare the PEO stock solutions, i.e., rather than preparing a dilute PEO solution directly from dry PEO granules, the PEO stock solutions may be prepared at a high concentration, and then diluted to the desired concentration for use. Such solutions show more stable flocculation performance than those prepared from dry PEO granules.

7.4 Discussion

The above results indicated that the flocculation efficiency of PEO depended on the sizes of undissolved aggregates. At the same dosage, the larger the aggregates sizes, the better the flocculation. Bridging is accepted as the mechanism for polymer flocculation and it is thought that the particles are linked together by polymer chains when they are adsorbed on more than one particle, as shown in Figure 2.4. However, PEO molecular chains in an aqueous solution are very flexible and tend to flatten on the particle surface after adsorption (Kawaguchi et al., 1984; Dijt et al., 1990), especially at low surface coverage, which, unfortunately, is the prerequisite for flocculation. Therefore, when single PEO chains are adsorbed on particle surface, there would not be enough dangling loops and tails for the bridging flocculation. But when the molecular chains are present in undissolved aggregates, they are much less flexible. When the PEO aggregates are adsorbed on particle surfaces, they can retain their conformation and would not flatten on the particle surfaces. When another particle collides with the

adsorbed PEO aggregate, it can be connected to the first particle by the PEO aggregate. It should be pointed out that it is still through H-bond that these PEO aggregates adsorb on quartz particle surfaces. When one aggregate adsorbs on the surface, there would be more than one H-bond formed between, which may lead to a stronger interaction and hence the better flocculation induced by the aggregates.

When the undissolved aggregates sizes are comparable to particle sizes or even larger, one aggregate can adsorb/attach to more than one particle so that the flocculation efficiency is high. In the extreme case where PEO aggregate is much larger than the mineral particles, it can adsorb many particles. In fact, when PEO granules are stirred for 10 min, there are still some swollen granules left which are as large as 2-3 mm. The quartz particles used are smaller than 20 μm , so that the PEO aggregates are at least 100 times larger than the quartz particles, and the PEO showed excellent flocculation performance under this condition. It was also observed that all the quartz particles could be flocculated together by such a PEO solution and formed a mass of paste-like material under gentle stirring. Such material was sticky, elastic and of certain degree of mechanical strength, and could be taken out from the solution as a whole. It is possible that the material was made of a network of the PEO aggregates and quartz particles. When the PEO aggregate is much smaller than the quartz particles, it can adsorb on at most two particles. Furthermore, the contact area between PEO and quartz are smaller and the attraction between them is also smaller so that more than one PEO aggregate are probably needed to bind two quartz particles. Finally, when the size of a PEO aggregate is small, after it adsorbs on one particle, the chances for it to collide with another particle are also small. All of these arguments point to reduced flocculation efficiency when PEO aggregate size is small.

In the flocculation tests, it was observed that the flocs were quite large at the beginning but were destroyed quickly as shown in Figure 5.6. After PEO was added, the Ratio output of the PDA 2000 photometric dispersion analyzer

instantly increased from about zero to as high as 12 but then dropped rapidly and eventually stabilized at around 5, indicating that the large flocs formed by PEO at the beginning were weak and quickly broke as a result of stirring. Such pattern also happened to chalcopyrite particles flocculated by PEO, as shown in Figure 5.7. The weak interaction between PEO and mineral particles, i.e., hydrogen bonding and electrostatic interaction, might be one of the reasons. But it was found that when the above mentioned paste-like material was formed and then taken out from the suspension, it could resist certain amount of tension and torsion. Stanley and Scheiner(1985) also found that in clay dewatering, PEO-induced flocs broke apart with the presence of water but grew stronger with the removal of water. These observations could not be explained only by the weak interactions between the PEO and the solids. PEO aggregates and the way they flocculate mineral particles may have played a role. The aggregates are not thermodynamically stable and dissociate with stirring. Therefore, the breakage points of the flocs can be the contact points between a PEO aggregate and a quartz particle, or the aggregate itself, as shown in Figure 7.10. When the floc is large, the tension exerted by the stirring across the floc and the aggregate is high, which probably accelerates the dissociation and the floc destruction. When the floc is taken out of the suspension, without the surrounding water, the aggregates tend to retain their conformation or even contract, which probably not only makes it harder to dissociate, but also renders the flocs stronger.

During the observation of the PEO-quartz flocs, one video clip has been taken accidentally, which partially supports the PEO aggregate-glue model. In this clip, the black lump is a chalcopyrite particle (-20 μm) floc formed by PEO and the rod is a silica tube with its end sealed by melting. One gram of chalcopyrite particles was first mixed in 200 mL water and then flocculated by adding 1 mL 0.1% PEO, which gave an overall PEO concentration of 5 mg/L. Three min after the addition of PEO, 1 mL chalcopyrite floc suspension was taken out and diluted with 20 mL distilled water with a pH of 9. The silica rod was then immersed into the diluted suspension. To make sure the silica rod was well hydrated before being immersed

in the suspension, it was soaked in chalcopyrite particle suspension for several minutes before PEO was added.

The silica rod was mounted on and controlled by hydraulic micromanipulators. The diluted suspension was placed under a microscope connected to a video system (CCD camera and a monitor). As can be seen from the video, when the silica rod was made to approach the chalcopyrite floc, a small fragment of the floc was dragged away and then sprung back. When the silica rod was made to approach the chalcopyrite floc the second time, the small fragment was detached from the floc and became attached to the silica rod. As can be seen, the silica rod was able to drag the large piece of the floc for a short distance. Both the silica and the chalcopyrite surfaces are negatively charged at pH 9 so there was no electrostatic attraction between them. The likely reason for the attraction is due to the bridging by the PEO. The retraction of the small fragment of the floc seems to suggest that the conformation of the adsorbed PEO molecules was aggregates rather than a single PEO chain. If it were a single chain, it was not likely for it to be stretched for such a long distance.

7.5 Summary

The presence of undissolved PEO aggregates is the key to good flocculation: the larger the aggregates, the better the flocculation. The sizes of the aggregates are determined by the PEO dissolution pattern. The better the dissolution, the smaller the aggregates. PEO dissolution is a thermodynamic process so that its dissolution rate can be controlled through thermodynamic parameters such as temperature, as well as other operating parameters such as stirring time and stirring intensity. On the other hand, PEO molecules can form inter-connected network at high concentrations, which behaves as a large aggregate and remains as smaller aggregates after dilution. The diluted solutions thus obtained possess excellent flocculation capability. Therefore, for PEO to act as an effective flocculant, the

PEO should only be partially dissolved, or the PEO solutions diluted from a concentrated (0.5% or higher) PEO stock solution.

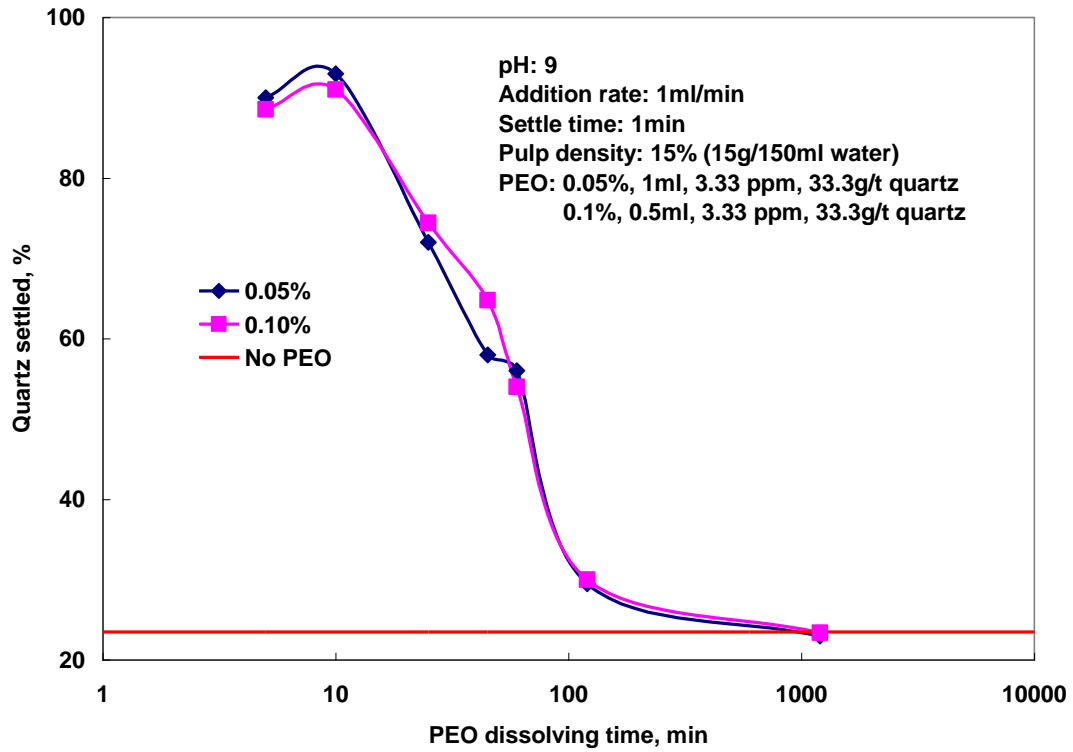


Figure 7.1 Effect of dissolution time of PEO suspension on quartz flocculation.

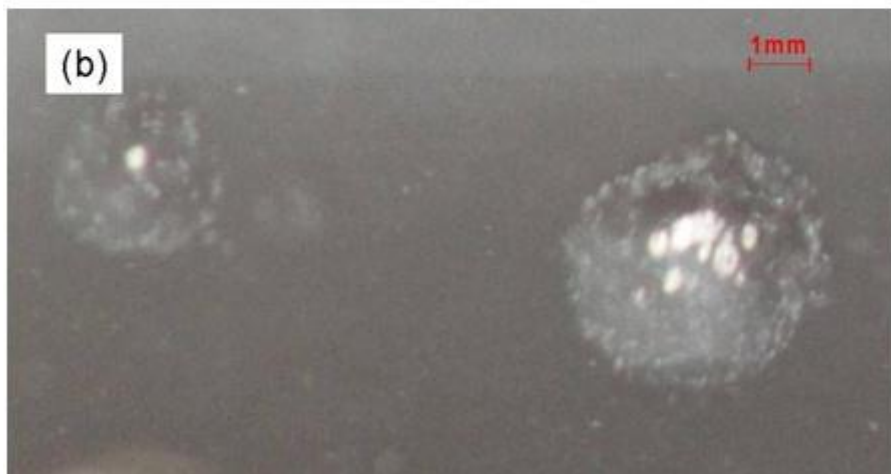
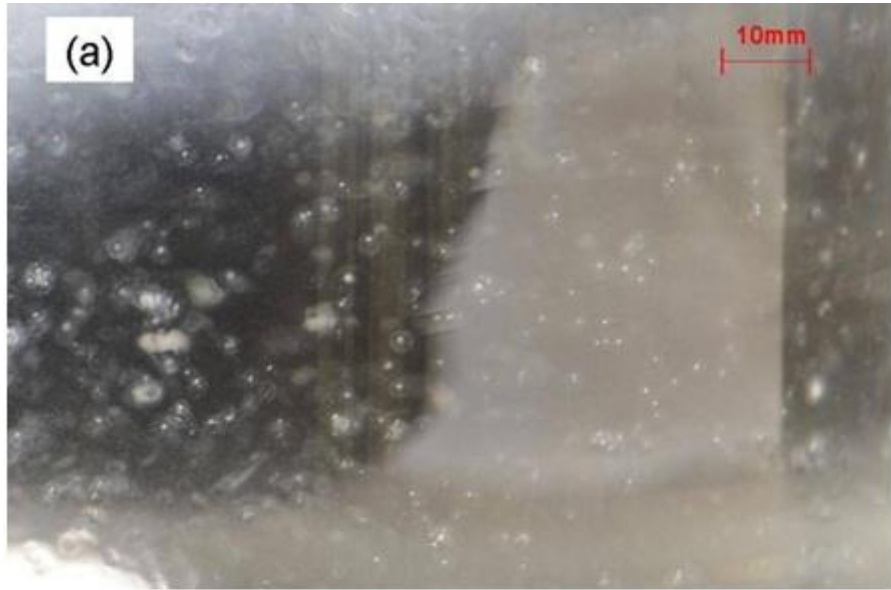


Figure 7.2 Images of swollen granules of PEO in water.

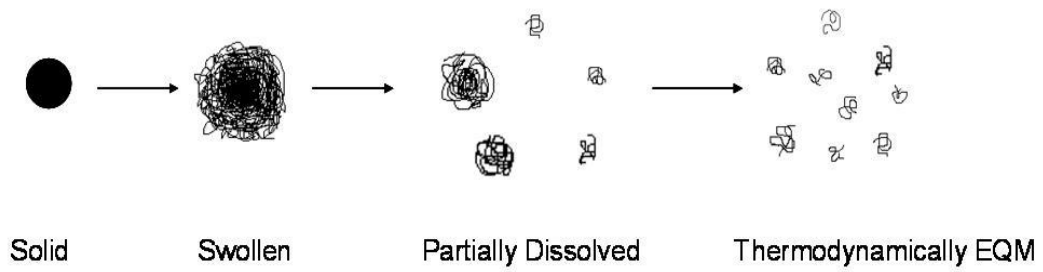


Figure 7.3 Illustration of PEO granule dissolution process at low concentrations.

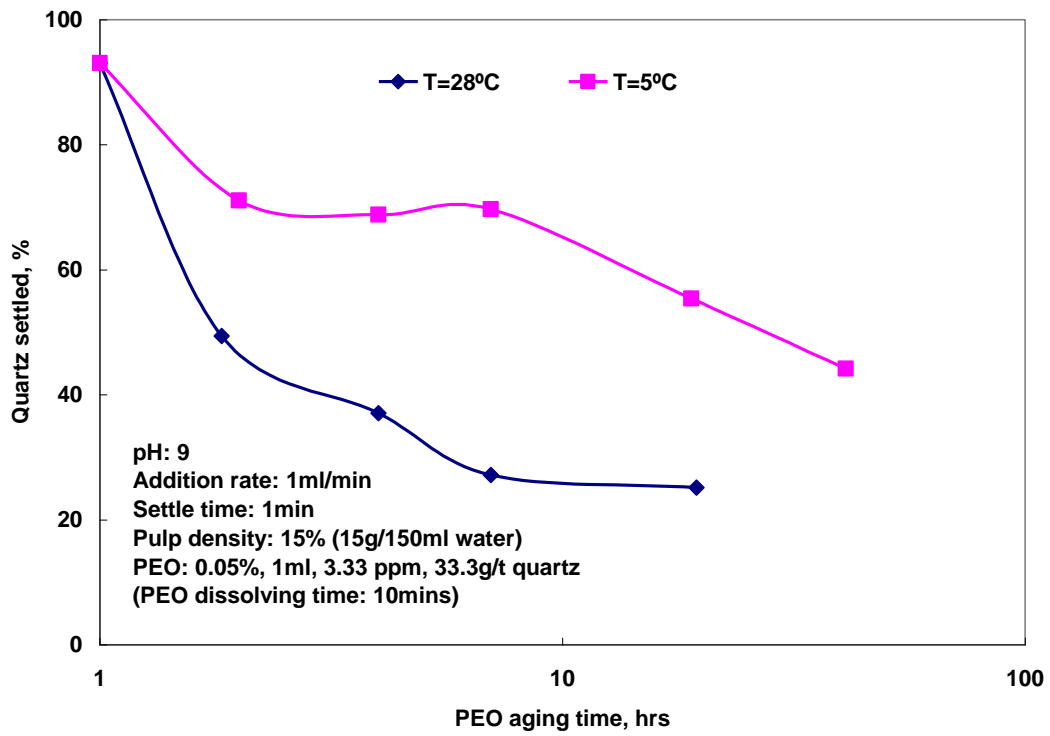


Figure 7.4 Effect of storage temperature of stock PEO solution on quartz flocculation.

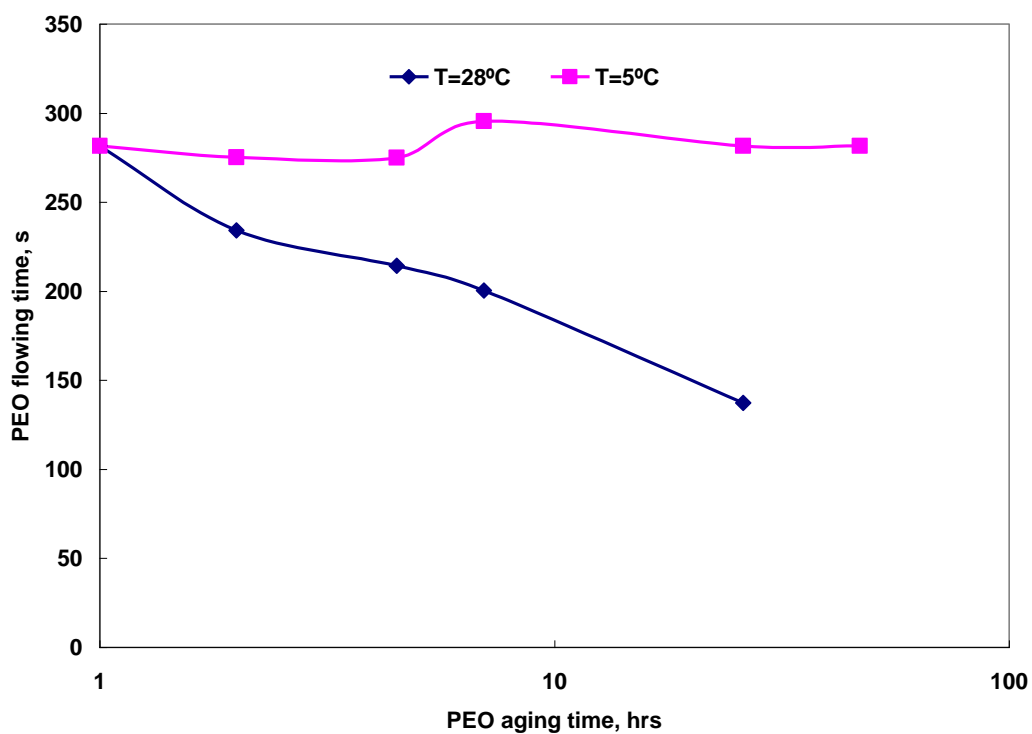


Figure 7.5 Comparison of PEO undissolved aggregates sizes using Ostwald viscometer.

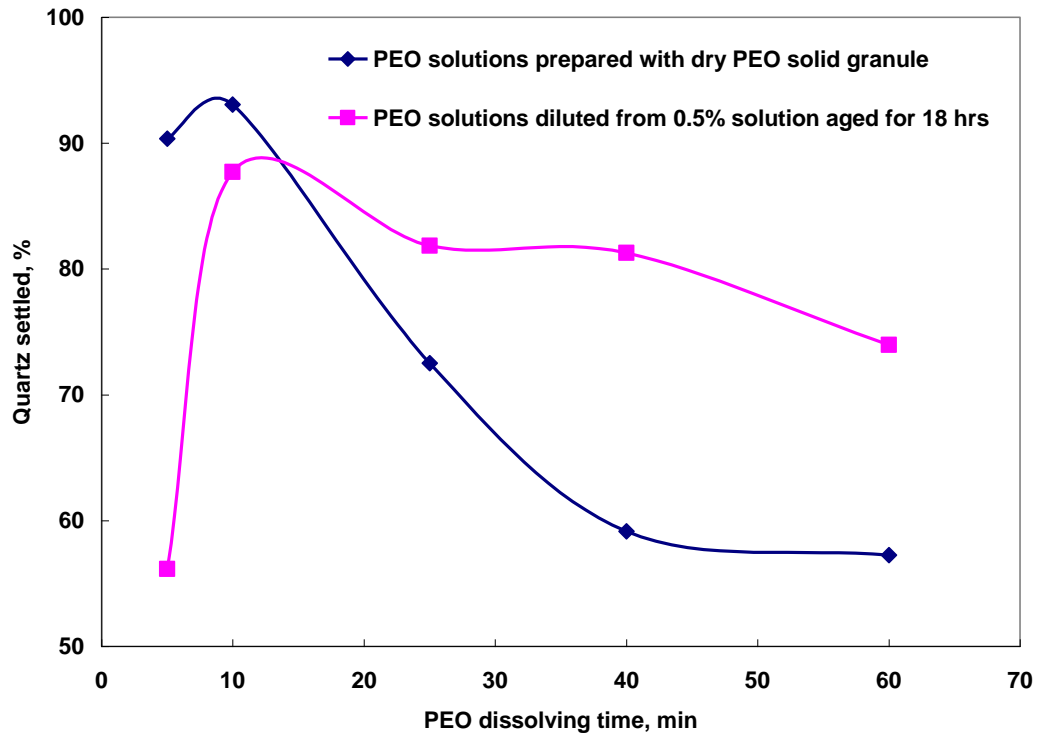


Figure 7.6 Effect of preparation method on flocculation efficiency of PEO solution.

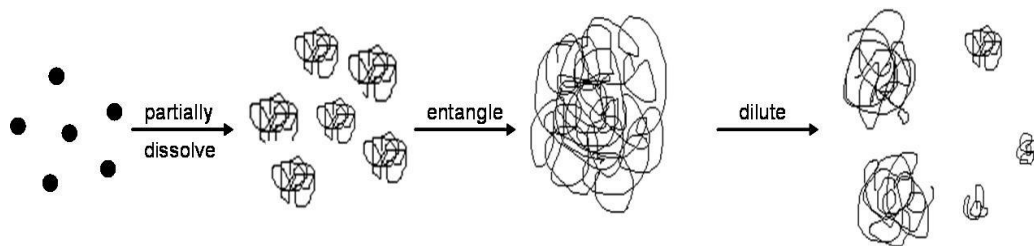


Figure 7.7 Illustration of PEO particle dissolution-dilution process at high concentrations.

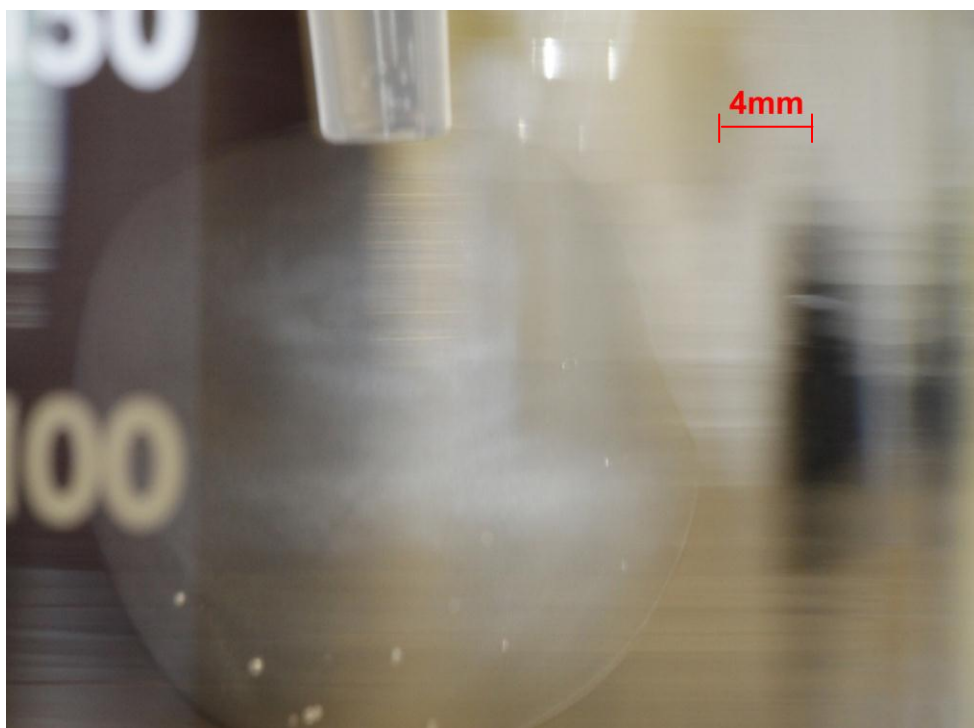


Figure 7.8 Image of a mass of 0.5% PEO solution injected in distilled water.

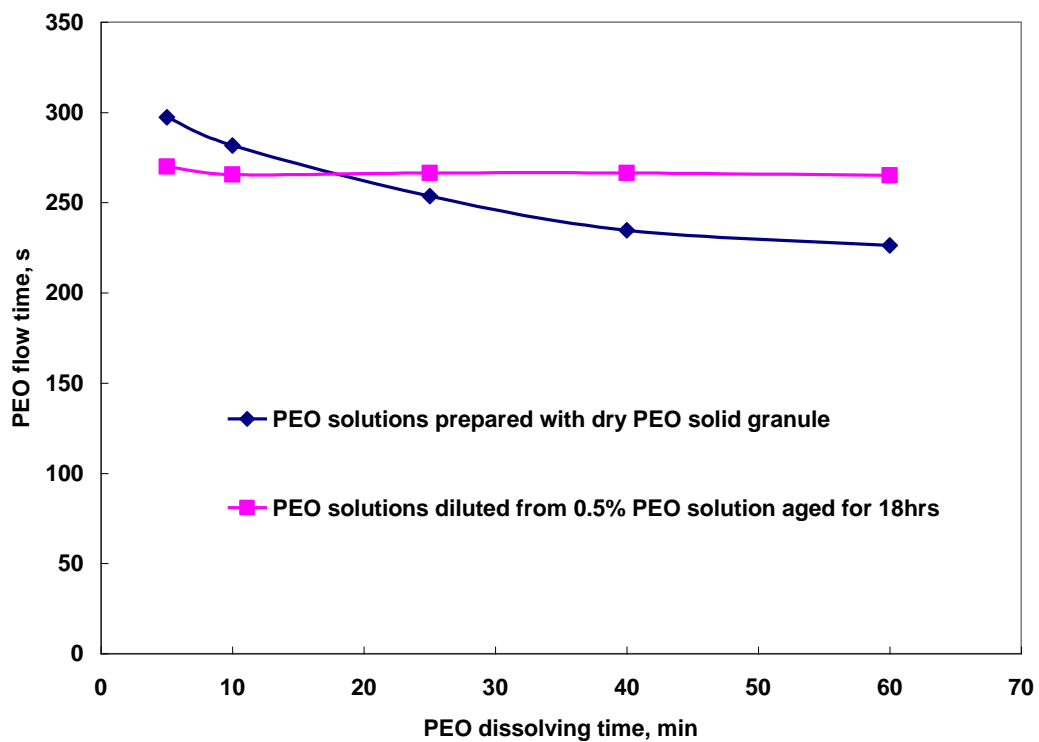


Figure 7.9 Comparison of undissolved PEO aggregates sizes prepared with different methods.

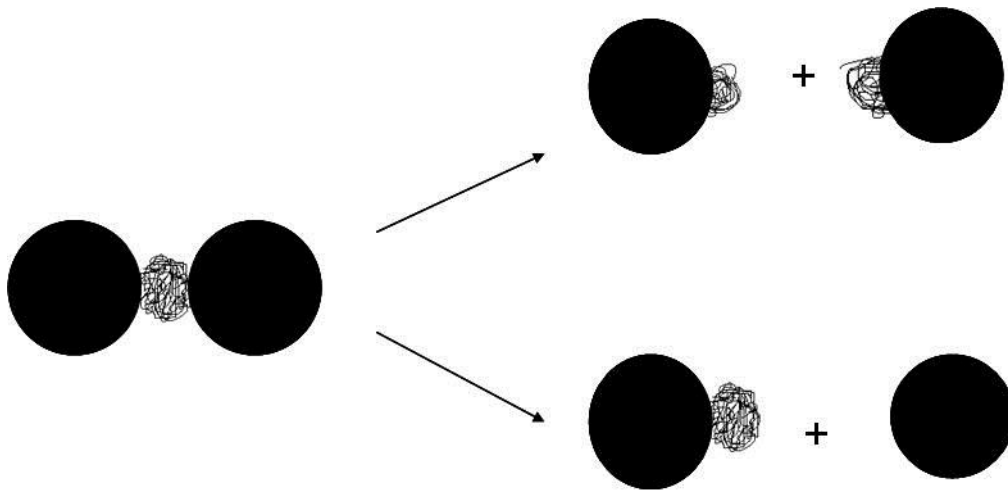


Figure 7. 10 Illustration of destruction of PEO-induced floccs.

Chapter VIII Frothing Property and Dosage Control of PEO

8.1 Introduction

Batch flotation tests showed that PEO reduced quartz entrainment only at moderate dosages. When it was overdosed, quartz entrainment became worse. It was also observed that PEO could replace F-150 as the frother in the batch flotation of the commercial Au-Cu sulfide ore sample. It was suspected that there might be some connection between these two observations. In order to prevent potential negative effect of PEO on quartz entrainment and flotation froth, and achieve the optimum performance for PEO, it is worth studying the frothing property of PEO and clarifying this connection.

8.2 Experimental

8.2.1 Materials and chemicals

The materials and chemicals used in this part work were the same as in flocculation tests (Chapter 5) and were described in section 5.2.1.,

8.2.2 Small-scale flotation test

Small-scale flotation tests were carried out in a columnar flotation tube with a diameter of 40 mm and a height of 200 mm, shown in Figure 8.1. In each test, 10 g quartz particles (-20 μm) were weighed and placed in a 250 mL beaker, and 200 mL of distilled water was added and the contents agitated on a magnetic stirrer. The pH of the solution was adjusted to about 9.3 using 0.01 M NaOH. The conditioned slurry was then transferred to the columnar flotation tube. The slurry was stirred inside the flotation tube for three minutes with a magnetic stir bar, and then a desired amount of PEO and DF 250 was added, followed by three minutes of stirring after each addition. Nitrogen gas flow was then turned on and a stable froth (about 40 mm in depth) was produced in the flotation tube. The top layer of

the froth was collected into a 250 mL beaker for a given time period and five 250 mL beakers were prepared to collect 5 froth products (concentrates). At the end of the flotation test, the contents of each beaker and tailing slurry were separately weighed and filtered, and the filter cake dried in an oven. The product weights were used to calculate the percentage of solids and water recovered into the froth product.

8.2.3 Frothing tests

The froth stability measurement was carried out in a frothing column which was 100 mm in diameter and 1 m tall, shown in Figure 8.2. The solution containing added reagents was fed gradually into the column, in 10 mL increments, through the bottom glass tube after the nitrogen gas valve was turned on. The gas flow rate was adjusted to a desired value through a Brook flowmeter. After each addition, the height of froth was recorded when the froth stabilized.

8.2.4 Dynamic pendant drop tests

A Dynamic Pendant Drop Apparatus (First Ten Ångströms), shown in Figure 8.3, was used to measure the interfacial tensions of solution in response to surface area changes. The solution being tested was formed as a drop at the tip of a stainless steel needle (0.916 mm outside diameter, 0.635 mm inside diameter; Kontes Inc., NJ) placed in air. The needle was connected to a computer-controlled syringe pump to allow precise control of the drop volume. The interfacial tension (IFT) γ was determined from the gravity-distorted drop shape, which was captured using an image analysis software. By fitting the distorted shape to the Young-Laplace equation, a very accurate value of the IFT could be determined. Both equilibrium and transient measurements of the interfacial tension were performed using the pendant drop apparatus. In the equilibrium measurement, the pendant drop volume was held constant for the intended time periods over which the interfacial tension changes were measured. In transient studies, step-strain deformations (by subjecting the air/water interface to sudden dilation or compression) were applied

to each equilibrium system and the responses of interfacial tension γ as a function of the changing interfacial area A were recorded.

8.3 Results

8.3.1 Small scale flotation tests on quartz particles

A set of froth flotation tests was carried out on a small scale in a columnar flotation tube. The experimental conditions were the same for all tests except the dosage of PEO used. Ten grams of quartz particles (-20 μm) were suspended in 200 mL distilled water, with pH adjusted to about 9.3. The dosage of frother, DF250, was 18 mg/L. No collector was used, so that the quartz recovery was considered exclusively due to entrainment. Figure 8.4 shows the relationship between quartz recovery and water recovery. As can be seen, a linear relationship was observed, which confirmed that quartz flotation was purely by entrainment. The slope of the line is calculated as the degree of entrainment, e_g . The degree of entrainment of quartz as a function of PEO dosage is shown in Figure 8.5. As can be seen, the degree of entrainment varied markedly with the dosage of PEO. A reduction of quartz entrainment was only achieved at PEO dosages below about 100 g/t, with a minimum degree of entrainment occurring at about 50 g/t. At higher PEO dosage, the degree of entrainment far exceeded the value ($e_g = 0.77$) when no PEO was used. But when PEO dosage was further increased, the degree of entrainment dropped again. The drop in the degree of entrainment at PEO low dosage can be attributed to the flocculation of quartz by PEO. The increase in entrainment at higher dosage is confusing as quartz was apparently flocculated at those dosages. Large quartz flocs were seen to be “floated” into the froth product. In this context, PEO seemed to act as a collector for the quartz particles. (In fact, PEO has been reported as quartz collector by (Doren et al., 1975). It is understandable, given PEO’s chemical structure. PEO chain is comprised of hydrophobic ethylene (-CH₂CH₂-) group and hydrophilic ether oxygen (-O-). If there are residual PEO molecules left in the pulp, they would adsorb on the water-air interface, acting as a frother. Its capability to function as a frother has been

confirmed in the batch flotation of the commercial Au-Cu sulfide ore sample, where PEO replaced F-150 as the frother. Those PEO molecules adsorbed at the air-water interface would also interact with quartz flocs, so that the latter were effectively attached to air bubbles and lifted into the froth phase.

At even higher PEO dosages, there were less adsorption sites on the quartz particle surfaces due to the excessive amount of PEO molecules so less quartz flocs are collected and the quartz recovery drops again. At very high dosages of PEO, quartz particles are probably sterically stabilized, i.e., dispersed instead of flocculated by PEO and cannot be collected either, which explained why quartz recovery went back to the value where no PEO was used.

It was also observed that the frothing behavior of the pulp was changed at high PEO dosages. The bubbles became noticeably smaller and the froth appeared more viscous. The changed froth behavior may have attributed to the increase in quartz recovery as well, which will be discussed below.

8.3.2 Frothing property of PEO in flotation

Wrobel (Wrobel, 1953) defined frothing power as the volume of froth generated in a standard machine under standard operating conditions. In this work, froth height of various frother solutions was measured in a frothing column at a fixed nitrogen gas flow rate of 2 L/min. Figure 8.6 shows froth height as a function of solution volumes used. Dowfroth 250 was present in all tests at a concentration of 18 mg/L. As can be seen, the froth height increases with increasing concentration of the PEO. Clearly, PEO acted as a frother. The increase in froth height can be interpreted as froth stabilization due to the presence of PEO.

8.3.3 Effect PEO on air/water interfacial tension

The pendant drop step-strain tests were carried out to examine the air/water interfacial tension. In the test carried on the water droplet only containing DF250

(suspended in air), it was observed that a sudden increase in the size of the pendent drop caused an increase in the interfacial tension and the interfacial tension gradually recovered with time and was restored after about 15 min (Figure 8.7). This is understandable since as the drop size increased, the air/water interfacial area was increased. Since the DF250 molecules could not diffuse fast enough to the air/water interface, the concentration of DF250 at the interfacial region was reduced, causing an increase in the interfacial tension. However, with time, the DF250 molecules diffused to the air/water interface and restored the initial equilibrium interfacial tension under this condition.

The same test was carried out with the DF 250 solution, which also contained 25 mg/L PEO, and the results are shown in Figure 8.8. As can be seen, the interfacial tension in the co-presence of DF250 and PEO was lower than when DF250 was present alone. The sudden dilation of the pendent water drop also caused an increase in the interfacial tension of air/water interface. However, the interfacial tension did not restore to the original equilibrium value within the time period tested, nor did it seem that it would. This is probably because the PEO molecules were only adsorbed on the air/water interfaces at some of the segments (“trains”) with the free segments extending on the air/water interface as “loops” and “tails”. A sudden dilation of the water droplet only stretched the loops slightly. Even with extended time, no more PEO molecules were adsorbed to the air/water interface. The slight drop in the interfacial tension following the dilation was probably caused by the migration of DF250 molecules to the air/water interface. As can be seen, this process seems slow, indicating that the presence of the PEO at the air/water interface may have sterically hindered the diffusion of the DF250 molecules.

8.4 Discussion

The frothing power tests and interfacial tension measurements show that PEO possesses strong frothing power. The conformation of the PEO adsorbed at the

air/water interfaces, i.e., trains, loops and tails, may have hindered the drainage of water from the plateau borders back to flotation pulp, which explains the higher water recovery at high PEO dosage in pure quartz batch flotation tests (Figure 4.5). In froth flotation, when the gas bubbles rise and cross the pulp-froth interface, water starts to drain back until bubbles are scraped into concentrate. When the drainage is slowed down, more water is kept among the bubbles and collected into concentrate. So the plateau border is thicker, which could retain more particles and lead to higher entrainment.

The higher froth height in the presence of PEO can also be explained from this perspective (Figure 8.6). Bubbles rupture due to film thinning (water drainage). When film thinning slows down, bubbles survive longer. When the air flow rate is fixed, bubbles with longer lifespan can stay longer in the column and lead to a larger froth volume, thus higher froth height.

8.5 Summary

Due to its surfactant property and affinity towards quartz, PEO can function as a collector for quartz during froth flotation. PEO overdosage would increase quartz entrainment, or more correctly, quartz recovery. The presence of PEO also favours the formation of stable froths and thicker plateau border among bubbles as a result of its long chain structure, which may make quartz entrainment more severe. Therefore, the dosage of PEO has to be accurately controlled to achieve the benefits and avoid the negative effects.



Figure 8.1 Small scale flotation setup using a columnar flotation tube.

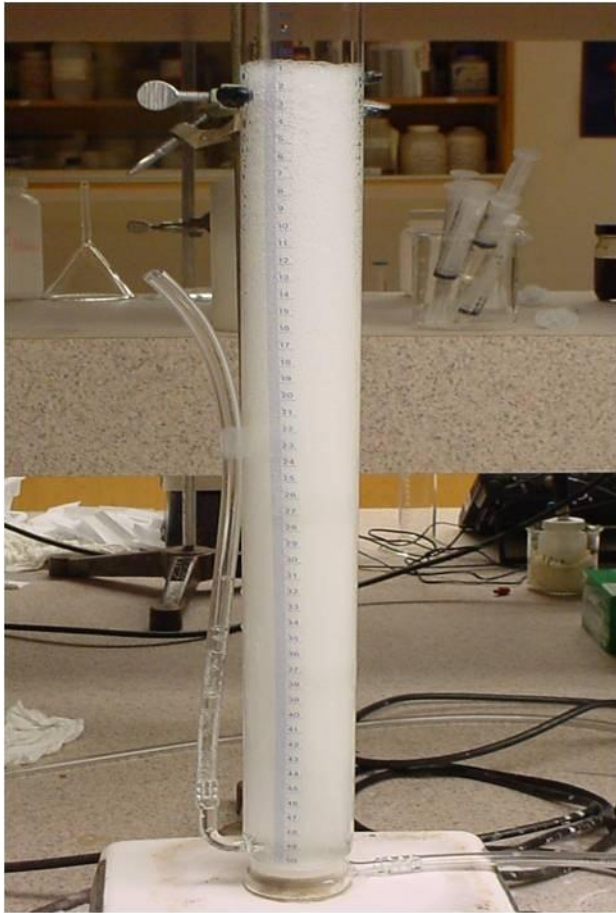


Figure 8.2 A 1-m tall frothing column for frothing property test.



Figure 8.3 Pendant drop apparatus for interfacial tension measurement.

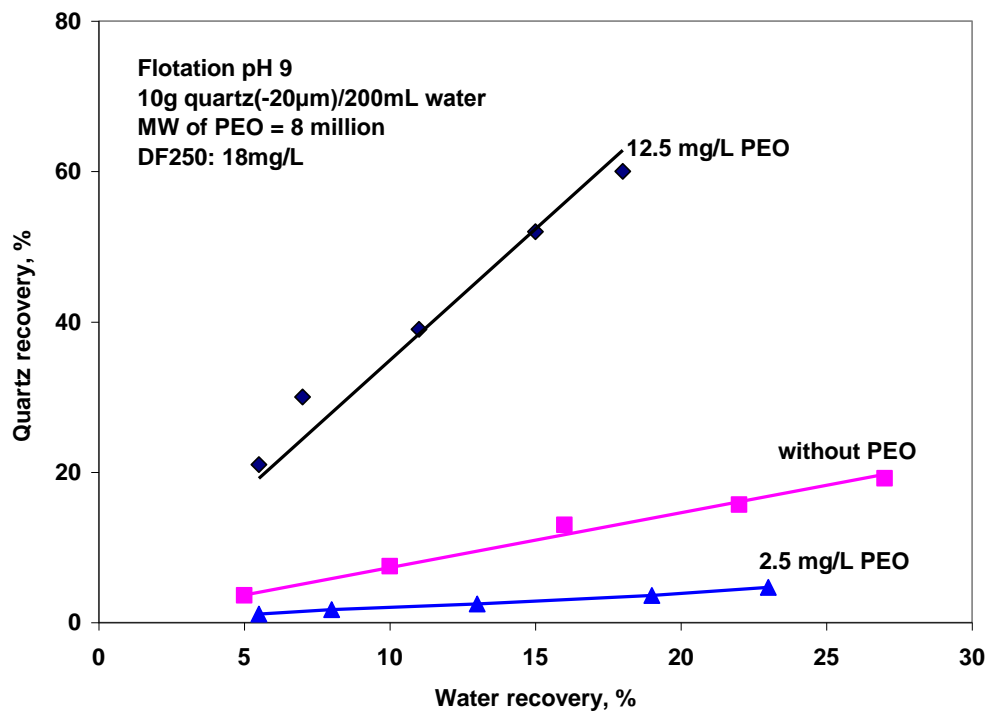


Figure 8.4 Linear relationship between quartz recovery and water recovery.

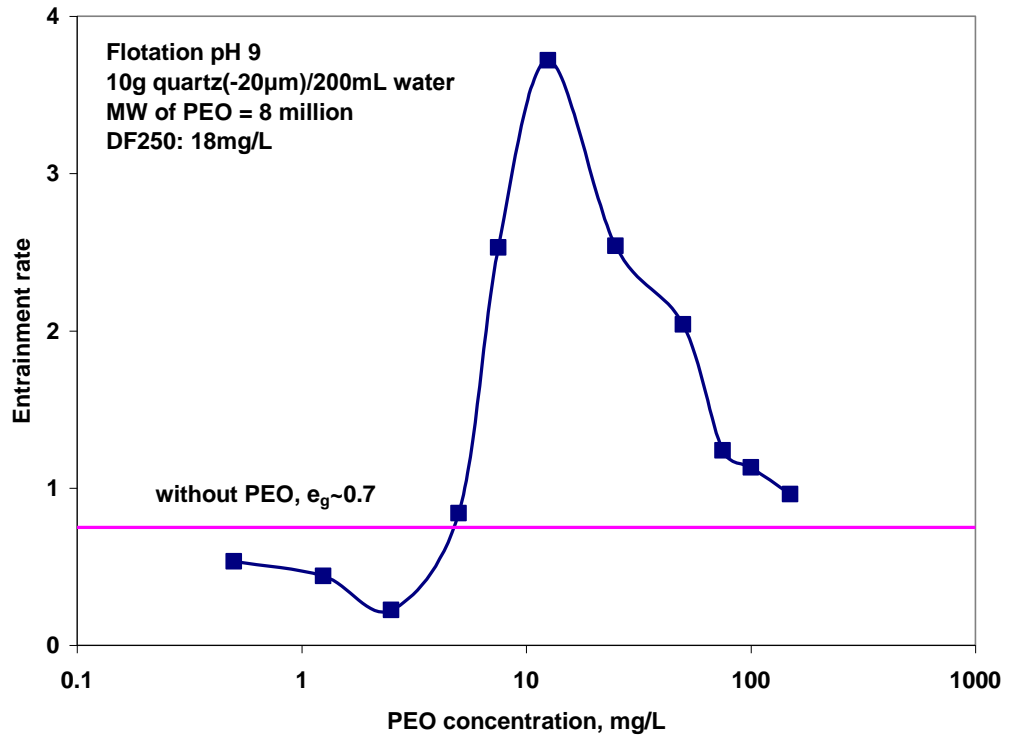


Figure 8.5 Effect of PEO dosage on the degree of entrainment of quartz.

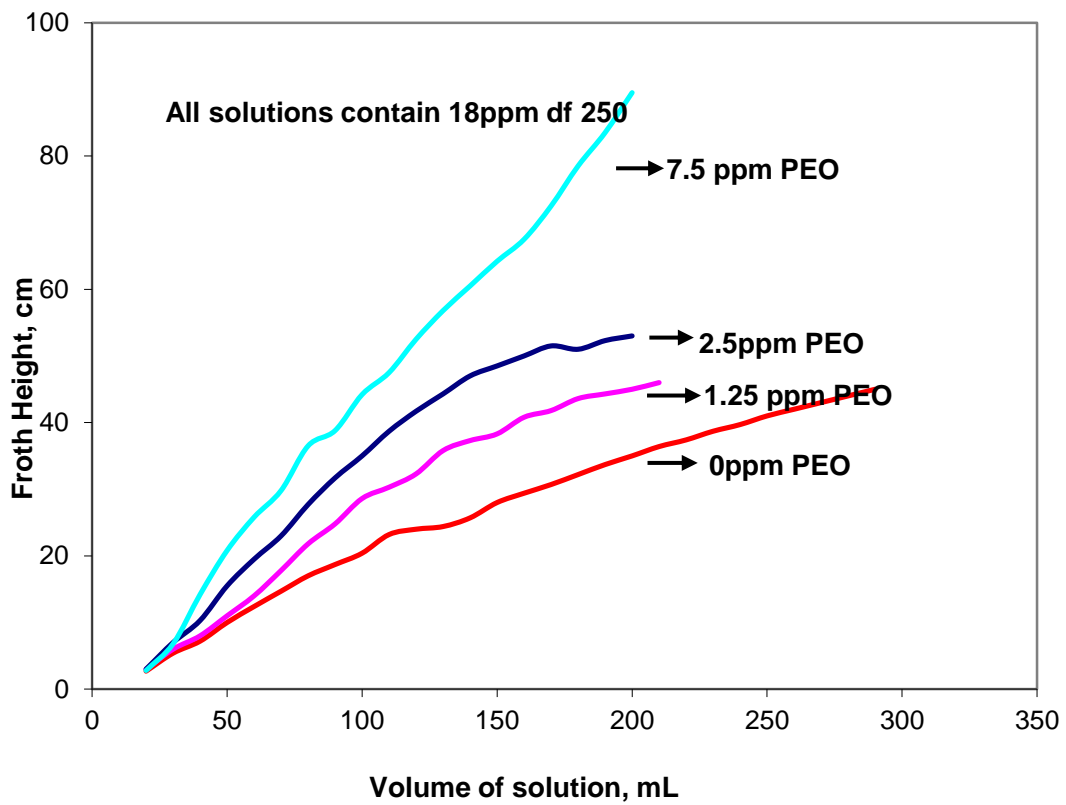


Figure 8.6 Frothing power of PEO.

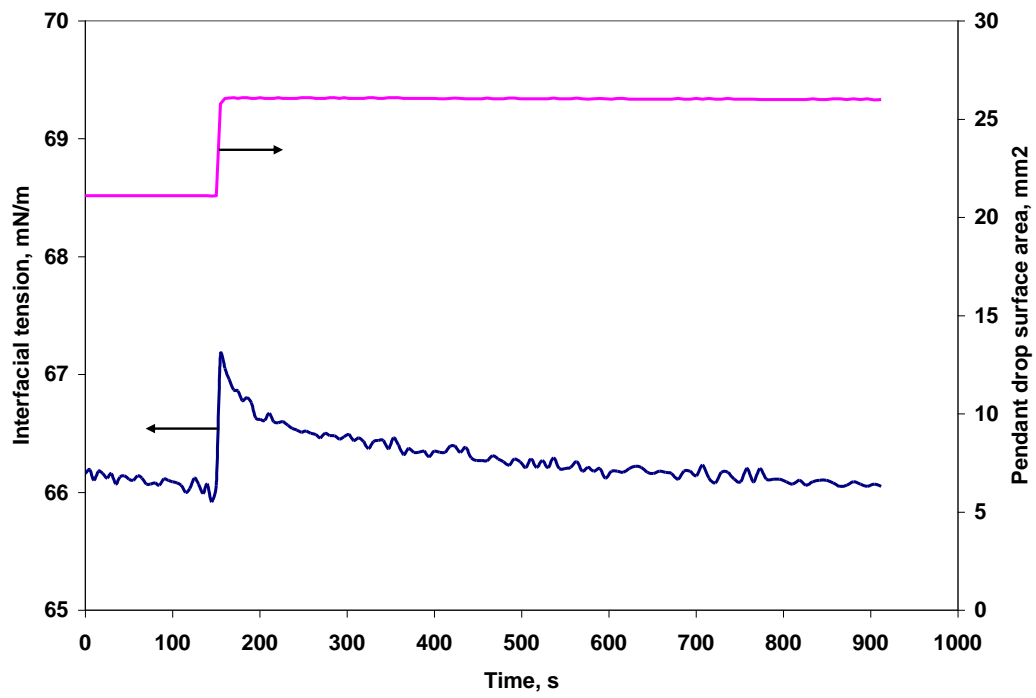


Figure 8.7 Interfacial tension vs. step-up area for a solution with 18mg/L DF250.

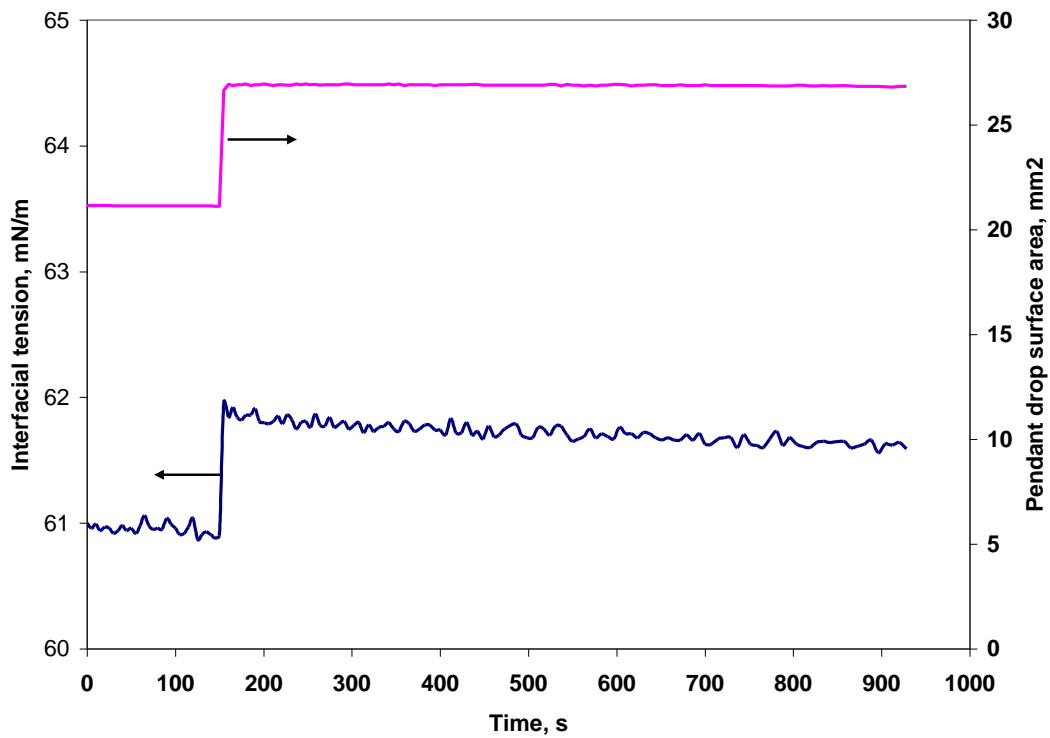


Figure 8.8 Interfacial tension vs. Step-up area for a solution with 18 mg/L DF250 and 25 mg/L PEO.

Chapter IX Conclusions and Recommendations

9.1 General findings

- 1) Results of batch flotation tests on all samples, including high purity quartz, synthetic quartz-chalcopyrite mixtures and a commercial Au-Cu sulfide ore sample, indicated that the use of polyethylene oxide (PEO) at appropriate dosages could lower quartz entrainment, improve flotation concentrate grade and separation efficiency of the froth flotation process. In the flotation of the commercial Au-Cu sulfide ore, the addition of 10 g/t PEO in the rougher and 5 g/t PEO in the cleaner significantly improved the flotation performance. At a fixed Si content in the flotation concentrate of 22%, the Cu recovery could increase from about 55% (without PEO) to about 70% (with PEO), and the Au recovery could increase from about 68% (without PEO) to about 90% (with PEO).
- 2) Aggregation/dispersion studies using a PDA 2000 photometric dispersion analyzer, stereomicroscope and a scanning electron microscope (SEM) showed that during the PEO-assisted flotation, PEO flocculated quartz and chalcopyrite together, forming hetero-aggregates. Subsequent addition of a xanthate collector caused the chalcopyrite particles to break away from the PEO hetero-aggregates, due to the competitive adsorption of xanthate which replaced PEO from the chalcopyrite surfaces. The removed chalcopyrite particles were able to form homo-aggregates, possibly due to the surface hydrophobicity induced by the adsorbed xanthate. The chalcopyrite homo-aggregates were more resistant to breakage than the PEO flocs. The combined use of PEO and xanthate could therefore potentially benefit the processing of polymetallic sulfide ores to reject fine and ultrafine quartz and silicate gangue.
- 3) Adsorption density, zeta potential, flocculation/dispersion and X-ray photoelectron spectroscopic measurements indicated that PEO adsorbed on

both quartz and chalcopyrite minerals mainly through hydrogen bonds, which were formed between the “free” ether oxygen of PEO and “free” hydroxyl groups on mineral surface. The strength of the interaction between PEO and the minerals depended on the density of these groups, which varied significantly with the pH of the suspension. For PEO, the number of “free” ether oxygen decreased with pH as it was progressively bonded to H^+ . For quartz, the number of “free” silanol groups was higher around neutral pH, as they tended to form hydrogen bonds with water at low pH and go through deprotonation at high pH. Therefore, optimum flocculation of quartz by PEO was observed at around neutral pH. On the other hand, an increase in pH caused a gradual improvement in the flocculation of chalcopyrite by PEO. This was attributed to both a smaller number of free ether oxygen on PEO and the dissolution of metal hydroxides/oxides from the (oxidized) chalcopyrite surface at low pH.

- 4) PEO-induced flocculation was difficult to control and PEO flocculation efficiency dropped rapidly when the dilute PEO solution was aged. The presence of undissolved PEO aggregates was found to be the key to good flocculation. The sizes of aggregates were dependent on PEO dissolution process. Better dissolution led to smaller aggregates and poor flocculation.
- 5) On the other hand, at high concentrations (e.g., 5 g/L), PEO molecules could form inter-connected network, which behaved as a large piece of aggregate and did not dissociate appreciably with aging. PEO solutions diluted from the concentrated stock solutions possessed excellent flocculation capability, which degraded much more slowly than a dilute PEO solution prepared directly from dry PEO granules. This observation pointed to an effective method to prevent PEO solutions from losing flocculation effectiveness.
- 6) PEO dosage was an important factor to control quartz entrainment in flotation. PEO could only reduce quartz entrainment at low and moderate dosages. At

high dosages, PEO increased quartz entrainment as a result of its function as a froth stabilizer.

9.2 Claims of originality

- 1) This research proved the concept of using high molecular weight polymers to lower gangue entrainment in froth flotation, and showed polyethylene oxide to be a potential polymer to lower quartz and silicate gangue entrainment in base metal sulphide ore flotation. Both academic researchers and the minerals industry typically use low molecular weight polymers as flotation depressants and avoid using high molecular weight polymers as the depressants, for fear that the flocs formed by the high molecular weight polymers can trap different minerals and adversely affect flotation separation. However, in this work, high molecular weight polyethylene oxide, with molecular weights of 1 million and 8 million, was successfully applied to the flotation separation of a commercial Au-Cu sulfide ore to lower the entrainment of fine quartz and significantly improved the flotation separation efficiency.

- 2) This research indicated that selective flocculation of minerals could be achieved even though the polymer flocculants may not be selectively adsorbed on the target minerals. The traditional perception is that polymers have to be selectively adsorbed on different minerals in order to achieve selective flocculation. However, it was found in this work that although the polymer, polyethylene oxide, was not selective in the chalcopyrite and quartz system – it flocculated both chalcopyrite and quartz to form hetero-flocs – selective flocculation could be achieved by the use of a selective, strongly chemisorbing collector such as potassium amyl xanthate, to one of the minerals (chalcopyrite). This finding provided a new perspective for realizing selective flocculation and reagent selection for mineral flotation systems.

- 3) This research showed the use of cryogenic X-ray photoelectron spectroscopy (cryo-XPS) as a reliable *in situ* analysis technique in the study of reagent

adsorption on mineral surfaces in aqueous suspensions. Adsorption of chemical reagents at the mineral/water interface is a very important phenomenon in flotation but its study has always been problematic as the aqueous environment makes most analysis techniques, especially the ultra high vacuum (UHV) techniques, such as XPS, irrelevant. In this research, the measurements of binding energies of O 1s and S 2s electrons in liquid-nitrogen frozen aqueous mineral suspensions allowed a very accurate and reliable chemical shift analysis of the adsorption mechanisms at the mineral-water interface.

- 4) It was found in this research that some polymers, such as polyethylene oxide, function as better flocculants when they were only partially dissolved. They lost the flocculation capability when fully dissolved. This was thought to be due to the presence of undissolved aggregates. Traditionally, polymer flocculation is considered a result of the bridging of particles by polymer molecules. This work showed that for polyethylene oxide, bridging by the larger molecular aggregates, rather than individual molecules, was the mechanism for flocculation.

9.3 Limitations of the results

- 1) The results of this work were only based on lab tests. The effectiveness of PEO on industry processing plant needs to be tested and the dosage of PEO used in bench flotation cannot be scaled up directly.
- 2) The discussion of the effect of undissolved PEO aggregates size on its flocculation efficiency was on a qualitative level. It is more of a phenomenological description than a solid scientific theory. Therefore it can only provide an approximate guideline for preparing PEO flocculant solution.

9.4 Recommendations for future research

- 1) The current work showed that it was the collector potassium amyl xanthate (KAX), not polyethylene oxide (PEO), that lends selectivity to the chalcopyrite – quartz flotation system. Since xanthate is a common collector for all sulfide minerals, the xanthate – PEO combination is expected to work in any sulfide system to reject silicate gangue. Some preliminary test work has been done in galena – quartz system with good results. PEO presents a promising reagent for sulfide ore flotation to reject non-sulfide gangue minerals.
- 2) The effect of addition sequence of PEO and KAX on flotation performance should be tested, by adding addition KAX before PEO and splitting KAX addition, with one portion before PEO and the other after PEO.
- 3) All the batch flotation showed that not only quartz entrainment was reduced, chalcopyrite recovery was also improved. It was speculated that PEO may play a role in enhancing chalcopyrite flotation since it was able to flocculate chalcopyrite. This speculation is worth investigating. If it is the case, PEO would be the perfect flocculant for sulphide ore flotation systems, reducing gangue entrainment and increasing value mineral recovery – the best solution for fine and ultrafine particle flotation.
- 4) PEO can replace regular frother even in the flotation of a commercial sulphide ore sample and generate good results. More work needs to be done on its frothing properties and its effect on flotation.
- 5) Besides polyethylene oxide, the aggregate-bridging flocculation mechanism may be true for other polymer flocculants. The effect of the degree of dissolution of different polymers on their flocculation performances should be investigated to optimize their flocculation efficiency.

Bibliography

- Ackerman, P.K., Harris, G.H., Klimpel, R.R. and Aplan, F.F., 1987. Evaluation of flotation collectors for copper sulfides and pyrite .1. common sulphydryl collectors. *International Journal of Mineral Processing*, 21(1-2): 105-127.
- Ahmed, N. and Jameson, G.J., 1985. The effect of bubble-size on the rate of flotation of fine particles. *International Journal of Mineral Processing*, 14(3): 195-215.
- Akdemir, U. and Hicyilmaz, C., 1998. Selective shear flocculation of chromite from chromite-serpentine mixtures. *Colloids and Surfaces a- Physicochemical and Engineering Aspects*, 132(1): 75-79.
- Asakura, S. and Oosawa, F., 1958. Interaction between particles suspended in solutions of macromolecules. *Journal of Polymer Science*, 33(126): 183-192.
- Attard, P., 1989. Long-range attraction between hydrophobic surfaces. *Journal of Physical Chemistry*, 93(17): 6441-6444.
- Back, D.M. and Schmitt, R.L., 2000. Ethylene oxide polymers. In: *Kirk-Othmer Encyclopedia of Chemical Technology*, 27. John Wiley & Sons, Inc., New York, pp.673-696.
- Bailey, F.E., Powell, G.M. and Smith, K.L., 1958. High molecular weight polymers of ethylene oxide-solution properties. *Industrial and Engineering Chemistry*, 50(1): 8-11.
- Bednar, F., De Oliveira, M.H., Paris, J. and De Ven, T., 2008. Transient entanglements and clusters in dilute polymer solutions. *Journal of Polymer Science Part B-Polymer Physics*, 46(3): 253-262.
- Bednar, F., Perin-Levasseur, Z., Van De Ven, T.G.M. and Paris, J., 2004. Polyethylene oxide disentanglement. *Journal of Pulp and Paper Science*, 30(2): 49-52.
- Bemer, G.G. and Zuiderweg, F.J., 1980. Growth regimes in the spherical agglomeration process. In: P. Somasundaran (Editor), *Fine Particles*

- Processing. American Institute of Mining, Metallurgical, and Petroleum Engineers, Inc., New York.
- Blueston, S., Mark, J.E. and Flory, P.J., 1974. The interpretation of viscosity-temperature coefficients for poly(oxyethylene) chains in a thermodynamically good solvent. *Macromolecules*, 7(3): 325-328.
- Borkovec, M., 1997. Origin of 1-pK and 2-pK models for ionizable water-solid interfaces. *Langmuir*, 13(10): 2608-2613.
- Braun, D.B. and Ehms, D.A., 1984. Filler and fiber retention in newsprint and groundwood specialites using poly(ethylene oxide). *Tappi Journal*, 67(9): 110-114.
- Brine, S.R., Brauer, R.M. and Wiseman, N., 1992a. Polyethylene oxide makedown procedures and their effect on paper-machine retention. *Appita Journal*, 45(2): 118-120.
- Brine, S.R., Brauer, R.M. and Wiseman, N., 1992b. Polyethylene oxide makedown procedures and their effect on paper machine retention. *Appita journal : journal of the Technical Association of the Australian and New Zealand Pulp and Paper Industry.* , 45(2): 118-120.
- Buckley, A.N. and Woods, R., 1984. An X-ray photoelectron spectroscopic study of the oxidation of chalcopyrite. *Australian Journal of Chemistry*, 37(12): 2403-2413.
- Cattarin, S., Flechter, S., Pettenkofer, C. and Tributsch, H., 1990. Interfacial reactivity and oscillating behavior of chalcopyrite cathodes during H₂O₂ reduction. 2. characterization of electrode corrosion. *Journal of the Electrochemical Society*, 137(11): 3484-3493.
- Cebeci, Y., 2003. Investigation of kinetics of agglomerate growth in oil agglomeration process. *Fuel*, 82(13): 1645-1651.
- Ching, H.-W., Tanaka, T.S. and Elimelech, M., 1994. Dynamics of coagulation of kaolin particles with ferric chloride. *Water Research*, 28(3): 559-569.
- Claesson, P.M. and Christenson, H.K., 1988. Very long range attractive forces between uncharged hydrocarbon and fluorocarbon surfaces in water. *Journal of Physical Chemistry*, 92(6): 1650-1655.

- Colombo, A.F., 1986. Concentration of iron oxides by selective flocculation-flotation. In: P. Somasundaran (Editor), *Advances in Mineral Processing*. Society of Mining Engineers, Inc., Littleton, pp. 695-713.
- Cutting, G.W., 1989. Effects of froth structure and mobility on the performance. In: J.S. Laskowski (Editor), *Frothing in Flotation*. Gordon and Breach Science Publishers, Glasgow, pp. 169-201.
- Devanand, K. and Selser, J.C., 1990. Polyethylene oxide does not necessarily aggregate in water. *Nature*, 343(6260): 739-741.
- DeWitt, C.C. and Roper, E.E., 1932. The surface relations of potassium ethyl xanthate and pine oil. I. *Journal of the American Chemical Society*, 54(2): 444-455.
- Dijt, J.C., Stuart, M.A.C., Hofman, J.E. and Fleer, G.J., 1990. Kinetics of polymer adsorption in stagnation point flow. *Colloids and Surfaces*, 51: 141-158.
- Doren, A., Vargas, D. and Goldfarb, J., 1975. Non-ionic surfactants as flotation collectors. *Transactions of the Institution of Mining and Metallurgy, Section C: Mineral Processing and Extractive Metallurgy*, 84(Compendex): c34-c37.
- Dormidontova, E.E., 2002. Role of competitive PEO-water and water-water hydrogen bonding in aqueous solution PEO behavior. *Macromolecules*, 35(3): 987-1001.
- Du, Q., Freysz, E. and Shen, Y.R., 1994. Vibrational spectra of water molecules at quartz/water interfaces. *Physical Review Letters*, 72(2): 238-241.
- Ducker, W.A., Xu, Z.G. and Israelachvili, J.N., 1994. Measurements of hydrophobic and DLVO forces in bubble-surface interactions in aqueous solutions. *Langmuir*, 10(9): 3279-3289.
- Duval, Y., Mielczarski, J.A., Pokrovsky, O.S., Mielczarski, E. and Ehrhardt, J.J., 2002. Evidence of the existence of three types of species at the quartz-aqueous solution interface at pH 0-10: XPS surface group quantification and surface complexation modeling. *Journal of Physical Chemistry B*, 106(11): 2937-2945.

- Feigin, R.I. and Napper, D.H., 1980. Stabilization of colloids by free polymer. *Journal of Colloid and Interface Science*, 74(2): 567-571.
- Fuerstenau, D.W., 1980. Fine particle flotation. In: P. Somasundaran (Editor), *Fine Particles Processing. Proc. Int. Symp. Fine Particles Processing. American Institute of Mining, Metallurgical, and Petroleum Engineers, Inc., New York*, pp. 669-705.
- Fuerstenau, M.C., 1982. Adsorption of sulphhydryl collectors. In: P. King (Editor), *Principle of Flotation. South African Institute of Mining and Metallurgy. Monograph Series 3. , Johannesburg*, pp. 91-108.
- Fuerstenau, M.C., Harper, R.W. and Miller, J.D., 1970. Hydroxamate vs. fatty acid flotation of iron oxide. *Trans. Am. Inst. Min. Metall. Eng.*, 247: 69-73.
- Fuerstenau, M.C., Miller, J.D. and Kuhn, M.C., 1985. *Chemistry of Flotation. Society of Mining Engineers of the American Institute of Mining, Metallurgical and Petroleum Engineers, Inc., New York.*
- Gibbs, A. and Pelton, R., 1999. Effect of PEO molecular weight on the flocculation and resultant floc properties of polymer-induced PCC flocs. *Journal of Pulp and Paper Science*, 25(7): 267-271.
- Gregory, D. and Carlson, K., 2003. Relationship of pH and floc formation kinetics to granular media filtration performance. *Environmental Science and Technology*, 37(7): 1398-1403.
- Gregory, J., 1973. Rates of flocculation of latex particles by cationic polymers. *Journal of Colloid and Interface Science*, 42(2): 448-456.
- Gregory, J., 1989. Fundamentals of flocculation. *Critical Reviews in Environmental Control*, 19(3): 185-230.
- Gregory, J. and Nelson, D.W., 1985. MONITORING OF AGGREGATES IN FLOWING SUSPENSIONS. *Colloids and surfaces*, 18(2-4): 175-188.
- Hamaker, H.C., 1937. The London - Van Der Waals attraction between spherical particles. *Physica*, 4: 1058-1072.
- Healy, T.W. and Jellett, V.R., 1967. Adsorption-coagulation reactions of Zn (II) hydrolyzed species at the zinc oxide—water interface. *Journal of Colloid and Interface Science*, 24(1): 41-&.

- Hemmings, C.E., 1980. An alternative viewpoint on flotation behavior of ultrafine particles. Transactions of the Institution of Mining and Metallurgy Section C-Mineral Processing and Extractive Metallurgy, 89(SEP): C113-C120.
- Hiemenz, P.C. and Rajagopalan, R., 1997. Principles of Colloid and Surface Chemistry. Marcel Dekker, Inc., New York.
- Hood, G.D., Wilemon, G.M., Stanley, D.A. and Scheiner, B.J., 1985. Dewatering of red mud. Metallurgical Soc of AIME, Fort Lauderdale, FL, USA, pp. 655-664.
- Hopkins, D.C. and Ducoste, J.J., 2003. Characterizing flocculation under heterogeneous turbulence. Journal of Colloid and Interface Science, 264(1): 184-194.
- Hunter, R.J., 2001. Foundations of Colloid Science. Oxford University Press, New York.
- Israelachvili, J.N. and Pashley, R.M., 1984. Measurement of the hydrophobic interaction between two hydrophobic surfaces in aqueous electrolyte solutions Journal of Colloid and Interface Science, 98(2): 500-514.
- Jarvis, P., Jefferson, B., Gregory, J. and Parsons, S.A., 2005. A review of floc strength and breakage. Water Research, 39(14): 3121-3137.
- Jiang, C., Wang, X. and Parekh, B.K., 2006. Ores, flotation of. In: P. Somasundaran and A. Hubbard (Editors), Encyclopedia of Surface and Colloid Science, 2nd ed. Taylor & Francis, London, pp. 4318-4335.
- Jin, P.K., Wang, X.C. and Chai, H., 2007. Evaluation of floc strength by morphological analysis and PDA online monitoring. Water Science and Technology, 56(10): 117-124.
- Jin, R.R., Hu, W.B. and Hou, X.J., 1987. Mechanism of selective flocculation of hematite from quartz with hydrolyzed polyacrylamide. Colloids and Surfaces, 26: 317-331.
- Jowett, A., 1966. Gangue mineral contamination of froth. British Chemical Engineering, 11(5): 330-333.
- Kawaguchi, M., Mikura, M. and Takahashi, A., 1984. Hydrodynamic studies on adsorption of poly(ethylene oxide) in porous-media .2. molecular-weight

- dependence of hydrodynamic thickness. *Macromolecules*, 17(10): 2063-2065.
- Killmann, E., Wild, T., Gutling, N. and Maier, H., 1986. Flocculation of pyrogenic and precipitated silica by polyethylene oxides. *Colloids and Surfaces*, 18(2-4): 241-259.
- Kjellander, R. and Florin, E., 1981. Water-structure and changes in thermal-stability of the system poly(ethylene oxide)-water. *Journal of the Chemical Society-Faraday Transactions I*, 77: 2053-2077.
- Koksal, E., Ramachandran, R., Somasundaran, P. and Maltesh, C., 1990. Flocculation of oxides using polyethylene oxide. *Powder Technology*, 62(3): 253-259.
- Kratochvil, D., Alinec, B. and van de Ven, T.G.M., 1999. Flocculation of clay particles with poorly and well-dissolved polyethylene oxide. *Journal of Pulp and Paper Science*, 25(9): 331-335.
- Krishnan, S.V. and Iwasaki, I., 1986. Heterocoagulation vs. surface precipitation in quartz-magnesium hydroxide system. *Environmental Science & Technology*, 20(12): 1224-1229.
- Laivins, G., Polverari, M. and Allen, L., 2001. Performance of poly(ethylene oxide)/cofactor retention aids in mechanical pulp finishes. *Tappi Journal*, 84(3): 57-57.
- Laskowski, J.S., 2002. Flocculation in mineral processing circuits. In: J. Ralston, J. Milller and J. Rubio (Editors), *Flotation and Flocculation: From Fundamentals to Applications*, Proceedings from Strategic Conference and Workshop, Hawaii, pp. 303-310.
- Leppinen, J.O., Basilio, C.I. and Yoon, R.H., 1989. Insitu FTIP study of ethyl xanthate adsorption on sulfide minerals under conditions of controlled potential. *International Journal of Mineral Processing*, 26(3-4): 259-274.
- Lin, I.J., Nadv, S. and Grodzian, D.J.M., 1975. Changes in the state of solids and mechano-chemical reactions in prolonged comminution processes. *Minerals Science and Engineering*, 7(4): 313-336.

- Liu, K.J. and Parsons, J.L., 1969. Solvent effects on preferred conformation of poly(ethylene glycols). *Macromolecules*, 2(5): 529-533.
- Liu, Q., Wannas, D. and Peng, Y., 2006. Exploiting the dual functions of polymer depressants in fine particle flotation. *International Journal of Mineral Processing*, 80(2-4): 244-254.
- Lu, C. and Pelton, R., 2005. Flocculation with poly(ethylene oxide)/tyrosine-rich polypeptide complexes. *Langmuir*, 21(9): 3765-3772.
- Luttrell, G.H. and Yoon, R.H., 1984. Surface studies of the collectorless flotation of chalcopyrite. *Colloids and Surfaces*, 12(3-4): 239-254.
- Lyklema, J., 1977. WATER AT INTERFACES - COLLOID-CHEMICAL APPROACH. *Journal of Colloid and Interface Science*, 58(2): 242-250.
- Mathur, S. and Moudgil, B.M., 1997. Adsorption mechanism(s) of poly(ethylene oxide) on oxide surfaces. *Journal of Colloid and Interface Science*, 196(1): 92-98.
- Mathur, S., Moudgil, B.M. and Pradip, 1996. Selective floc formation in an apatite dolomite system using polyacrylic acid. *Minerals and Metallurgical Processing*, 13(1): 1-3.
- Mathur, S., Singh, P. and Moudgil, B.M., 2000. Advances in selective flocculation technology for solid-solid separations. *International Journal of Mineral Processing*, 58(1-4): 201-222.
- Matsuura, H. and Miyazawa, T., 1968. Intrachain force field and normal vibrations of polyethylene glycol. *Bulletin of the Chemical Society of Japan*, 41(8): 1798-1808.
- Mielczarski, J.A., Cases, J.M., Alnot, M. and Ehrhardt, J.J., 1996a. XPS characterization of chalcopyrite, tetrahedrite, and tennantite surface products after different conditioning .1. Amyl xanthate solution at pH 10. *Langmuir*, 12(10): 2531-2543.
- Mielczarski, J.A., Cases, J.M., Alnot, M. and Ehrhardt, J.J., 1996b. XPS characterization of chalcopyrite, tetrahedrite, and tennantite surface products after different conditioning .2. Amyl xanthate solution at pH 10. *Langmuir*, 12(10): 2531-2543.

- Mielczarski, J.A., Mielczarski, E. and Cases, J.M., 1996c. Interaction of amyl xanthate with chalcopyrite, tetrahedrite, and tennantite at controlled potentials. Simulation and spectroelectrochemical results for two-component adsorption layers. *Langmuir*, 12(26): 6521-6529.
- Morrow, B.A. and Cody, I.A., 1976. Infrared studies of reactions on oxide surfaces. 6. active-sites on dehydroxylated silica for chemisorption of ammonia and water. *Journal of Physical Chemistry*, 80(18): 1998-2004.
- Mpofu, P., Addai-Mensah, J. and Ralston, J., 2004. Flocculation and dewatering behaviour of smectite dispersions: effect of polymer structure type. *Minerals Engineering*, 17(3): 411-423.
- Mulleneers, H.A.E., Koopal, L.K., Bruning, H. and Rulkens, W.H., 2002. Selective separation of fine particles by a new flotation approach. *Separation Science and Technology*, 37(9): 2097-2112.
- Neethling, S.J. and Cilliers, J.J., 2001. Simulation of the effect of froth washing on flotation performance, pp. 6303-6311.
- Nguyen, A.V. and Schulze, H.J., 2004. *Colloidal Science of Flotation*. Marcel Dekker, New York.
- Nuysink, J. and Koopal, L.K., 1982. The effect of polyethylene oxide molecular-weight on determination of its concentration in aqueous-solutions. *Talanta*, 29(6): 495-501.
- Packham, R.F., 1965. Some studies of the coagulation of dispersed clays with hydrolyzing salts. *Journal of Colloid Science*, 20(1): 81-&.
- Pandya, J.D. and Spielman, L.A., 1982. Flocc breakage in agitated suspensions - theory and data-processing strategy. *Journal of Colloid and Interface Science*, 90(2): 517-531.
- Pang, J. and Chander, S., 1990. Oxidation and wetting behavior of chalcopyrite in the absence and presence of xanthates. *Minerals and Metallurgical Processing*, 7(Compendex): 149-155.
- Polverari, M. and vandeVen, T.G.M., 1996. Dilute aqueous poly(ethylene oxide) solutions: Clusters and single molecules in thermodynamic equilibrium. *Journal of Physical Chemistry*, 100(32): 13687-13695.

- Pradip and Moudgil, B.M., 1991. Selective flocculation of tribasic calcium-phosphate from mixtures with quartz using polyacrylic-acid flocculant. *International Journal of Mineral Processing*, 32(3-4): 271-281.
- Pugh, R.J. and Kitchene, J.A., 1971. Theory of selective coagulation in mixed colloidal suspensions. *Journal of Colloid and Interface Science*, 35(4): 656-664.
- Rabinovich, Y.I. and Derjaguin, B.V., 1988. Interaction of hydrophobized filaments in aqueous electrolyte solutions. *Colloids and Surfaces*, 30(3-4): 243-251.
- Rabolt, J.F., Johnson, K.W. and Zitter, R.N., 1974. Infrared and raman-spectra of polyethylene oxide in low-frequency region. *Journal of Chemical Physics*, 61(2): 504-506.
- Richardson, P.F. and Connelly, L.J., 1988. Industrial coagulants and flocculants. In: P. Somasundaran and B.M. Moudgil (Editors), *Reagents in Mineral Technology*. Marcel Dekker, Inc., New York, pp. 519-558.
- Rodrigues, R.T. and Rubio, J., 2007. DAF-dissolved air flotation: Potential applications in the mining and mineral processing industry. *International Journal of Mineral Processing*, 82(1): 1-13.
- Rubio, J., 1981. The flocculation properties of poly(ethylene-oxide). *Colloids and Surfaces*, 3(1): 79-95.
- Rubio, J. and Hoberg, H., 1993. The process of separation of fine mineral particles by flotation with hydrophobic polymeric carrier. *International Journal of Mineral Processing*, 37(1-2): 109-122.
- Rubio, J. and Kitchener, J.A., 1976. The mechanism of adsorption of poly(ethylene oxide) flocculant on silica. *Journal of Colloid and Interface Science*, 57(1): 132-142.
- Ruehrwein, R.A. and Ward, D.W., 1952. Mechanism of clay aggregation by polyelectrolytes. *Soil Science*, 73(6): 485-492.
- Schubert, H., 1984. Capillary forces - modeling and application in particulate technology *Powder Technology*, 37(JAN-): 105-116.

- Shchukarev, A., 2010. Electrical double layer at the mineral-aqueous solution interface as probed by XPS with fast-frozen samples. *Journal of Electron Spectroscopy and Related Phenomena*, 176(1-3): 13-17.
- Shchukarev, A., Boily, J.F. and Felmy, A.R., 2007. XPS of fast-frozen hematite colloids in NaCl aqueous solutions: I. Evidence for the formation of multiple layers of hydrated sodium and chloride ions induced by the {001} basal plane. *Journal of Physical Chemistry C*, 111(49): 18307-18316.
- Sieglauff, C.L., 1959. Phase separation in mixed polymer solutions. *Journal of Polymer Science*, 41(138): 319-326.
- Singh, R., Rao, S.S., Manulik, S.C. and Chakravorty, N., 1997. Fine particles flotation - Recent trends. *Transactions of the Indian Institute of Metals*, 50(5): 407-419.
- Sivamohan, R., 1990. Problem of recovering very fine particles in mineral processing. A review. *International Journal of Mineral Processing*, 28(3-4): 247-288.
- Smalley, M.V., Hatharasinghe, H.L.M., Osborne, I., Swenson, J. and King, S.M., 2001. Bridging flocculation in vermiculite-PEO mixtures. *Langmuir*, 17(13): 3800-3812.
- Smelley, A.G. and Scheiner, B.J., 1980. Synergism in polyethylene oxide dewatering of phosphatic clay waste. *Report of Investigations - United States, Bureau of Mines(8436)*.
- Smith, P.G. and Warren, L.J., 1989. Entrainment of particles into flotation froths. In: J.S. Laskowski (Editor), *Frothing in Flotation*. Gordon and Breach Science Publishers, Glasgow, pp. 123-145.
- Somasundaran, P., 1980. Principles of flocculation, dispersion, and selective flocculation. In: P. Somasundaran (Editor), *Fine Particle Processing*. American Institute of Mining, Metallurgical, and Petroleum Engineers, Inc., New York, pp. 947-976.
- Somasundaran, P. and El-Shall, H., 1983. Mechanochemical effects in ultrafine grinding. In: S.G. Malghan (Editor), *Ultrafine Grinding and Separation of*

- Industrial Minerals. AIME Society of Mining Engineers, New York, pp. 21-33.
- Song, S., Lopez-Valdivieso, A., Reyes-Bahena, J.L. and Lara-Valenzuela, C., 2001. Floc flotation of galena and sphalerite fines. *Minerals Engineering*, 14(1): 87-98.
- Sonmez, I. and Cebeci, Y., 2003. Fundamental aspects of spherical oil agglomeration of calcite. *Colloids and Surfaces a-Physicochemical and Engineering Aspects*, 225(1-3): 111-118.
- Stanley, D.A. and Scheiner, B.J., 1985. Mechanically Induced Dewatering of Ion-Exchanged Attapulgite Flocculated by a High-Molecular-Weight Polymer. *Colloids and Surfaces*, 14(2): 151-159.
- Subrahmanyam, T.V. and Forssberg, K.S.E., 1990. Fine particles processing: shear-flocculation and carrier flotation - a review. *International Journal of Mineral Processing*, 30(3-4): 265-286.
- Swenson, J., Smalley, M.V. and Hatharasinghe, H.L.M., 1998. Mechanism and strength of polymer bridging flocculation. *Physical Review Letters*, 81(26): 5840-5843.
- Sworska, A., Laskowski, J.S. and Cymerman, G., 2000. Flocculation of the Syncrude fine tailings Part II. Effect of hydrodynamic conditions. *International Journal of Mineral Processing*, 60(2): 153-161.
- Szatkowski, M., 1987. Factors influencing behavior of flotation froth. *Transactions of the Institution of Mining and Metallurgy Section C-Mineral Processing and Extractive Metallurgy*, 96: C115-C122.
- Tadokoro, H., Chatani, Y., Yoshihara, T., Tahara, S. and Murahashi, S., 1964. Structural studies on polyethers, $[-(\text{CH}_2)_m\text{-O}]_n$. 2. molecular structure of polyethylene oxide. *Makromolekulare Chemie*, 73: 109-127.
- Thorne, G.C., Manlapig, E.V., Hall, J.S. and Lynch, A.J., 1976. Modelling of industry sulphide flotation circuits. In: M.C. Fuerstenau (Editor), *Flotation*, New York, pp. 725-752.
- Trahar, W.J., 1981. A rational interpretation of the role of particle-size in flotation. *International Journal of Mineral Processing*, 8(4): 289-327.

- Ven, T.G.M.V.D., Qasaimeh, M.A. and Paris, J., 2004. PEO-induced flocculation of fines: Effects of PEO dissolution conditions and shear history. *Colloids and Surfaces A: Physicochemical and Engineering Aspects*, 248(1-3): 151-156.
- Villar, J.W. and Dawe, G.A., 1975. Tilden mine - new processing technique for iron-ore. *Mining Congress Journal*, 61(10): 40-48.
- Vorchheimer, N., 1981. Synthetic polyelectrolytes. In: W.L.K. Schwoyer (Editor), *Polyelectrolytes for Water and Wastewater Treatment*. CRC Press, Boca Raton, pp. 1-47.
- Waksmundzki, A., Neczaj-Hruzewicz, J. and Planik, M., 1972. Mechanism of carryover of gangue slimes during flotation of sulphur ore. *Transactions of the Institution of Mining and Metallurgy Section C-Mineral Processing and Extractive Metallurgy*, 81: 249-251.
- Warren, L.J., 1975. Shear-flocculation of ultrafine scheelite in sodium oleate solutions. *Journal of Colloid and Interface Science*, 50(2): 307-318.
- Warren, L.J., 1985. Determination of the contributions of true flotation and entrainment in batch flotation tests. *International Journal of Mineral Processing*, 14(1): 33-44.
- Watts, J.F., 2003. *An Introduction to Surface Analysis by XPS and AES*. Wiley, New York.
- Woods, R., 1984. Electrochemistry of sulfide flotation. In: M.H. Jones and J.T. Woodcock (Editors), *Principles of Mineral Flotation, The Wark Symposium*. Australian Institute of Mining and Metallurgy, Symposia Series No. 40, Victoria, Australia, pp. 91-115.
- Wrobel, S.A., 1953. Power and stability of flotation frothers. *Mine and Quarry Engineering*, 19(10): 363-367.
- Yeung, A.K.C. and Pelton, R.H., 1996. Micromechanics: A new approach to studying the strength and breakup of flocs. *Abstracts of Papers of the American Chemical Society*, 212: 108-COLL.

- Yushchenko, V.S., Yaminsky, V.V. and Shchukin, E.D., 1983. Interaction between particles in a nonwetting liquid. *Journal of Colloid and Interface Science*, 96(2): 307-314.
- Zachwieja, J.B., McCarron, J.J., Walker, G.W. and Buckley, A.N., 1989. Correlation between the surface-composition and collectorless flotation of chalcopyrite. *Journal of Colloid and Interface Science*, 132(2): 462-468.